Coarse Graining of Electric Field Interactions with Materials

Submitted in partial fulfillment of the requirements for

the degree of

Doctor of Philosophy

in

Department of Civil & Environmental Engineering

Prashant K Jha

B.E., Mechanical Engineering, Govt. Engineering College, India

M.E., Mechanical Engineering, Indian Institute of Science, India

Carnegie Mellon University

Pittsburgh, PA

August, 2016

Acknowledgments

I am thankful to my adviser, Dr. Kaushik Dayal, for his continuous support throughout my Ph.D. Particularly, I thank him for being patient with my style of work. I have learned a great deal from him. During the discussions, I learned how to be precise and clear in conveying the ideas and thoughts. I have been benefited a lot from Dr. Dayal's paper reading class.

I would also like to thank Dr. Amit Acharya, who was always available for any question of doubt. I enjoyed his discussions during MMC seminars. I took measure theory course of Dr. Gautam Iyer. His course helped me in understanding my research work and also in dealing with the research problem. I thank Dr. Iyer for helping me in my doubts and questions.

I thank Dr. Jacobo Bielak for giving me the opportunity to be teaching assistant of his Finite Element Method course. I have learned a lot from him. I thank him for being so patient with me. I thank CEE department for their quick response and for helping me.

I would like to thank my department, Civil and Environmental Engineering, for granting me Dean's fellowship. It covered the first year of my study. I would also like to acknowledge Army Research Office for funding my research work.

I am thankful to Dr. C. S. Jog. His continuum mechanics and solid mechanics courses, at IISc, were of great use in my research. I am also grateful to him for helping me just before joining as a Ph.D. student.

I am thankful to my friends for being there at good and bad times.

Lastly, I thank my parents, and sisters, for being always there. They give strength and confidence to me. I dedicate this work to my family.

Abstract

In this work, we present our continuum limit calculations of electrical interactions in ionic crystals and dielectrics. Continuum limit calculations serve two main purposes. First, they give an idea of how the macroscopic behavior of the material is related to the interactions at the atomistic scale. Second, they help in developing a multiscale numerical method, where the goal is to model the material both at the scale of atoms and at the macroscale.

We consider two important settings for the continuum limit calculation: nanorod-like materials, where the thickness of a material in the lateral direction is of the order of the atomic spacing, and the materials, where atoms are randomly fluctuating due to the thermal energy. Our calculations, for the nanorod-like materials, show that the electrostatics energy are not long-range in continuum limit. We also consider the discrete system of dipole moments along the straight line and along the helix. We then compute the limit of the energy as the separation between the dipole moments tends to zero. The energy, in the continuum limit, is short-range in nature. This agrees with the calculations of [Gioia and James, 1997] for the magnetic thin films. We consider the system of atoms which are fluctuating due to thermal energy. We model the charge density field as random field and compute the continuum limit of the electrostatics energy.

In second part of the thesis, we present the Quasicontinuum method for the electro-mechanical deformation of the material at a finite temperature. There are two difficulties associated with this : one is the calculation of the phase average, and, second is the long-range interactions of the charged atoms. We use *max-ent* method presented in [Kulkarni et al., 2008] to formulate the problem as a minimization problem with respect to the atomic position and the atomic momenta. For the electrical interactions in the multi-scale method, we use the continuum limit of the energy for the random charge density field. We have modified the existing Quasicotninuum code, see [Marshall and Dayal, 2013], to implement the multiscale method. The code is an further extension of the code written by Jason Marshall [Marshall and Dayal, 2013].

Contents

List of Tables

List of Figures

Chapter 1

Introduction

The macroscopic behavior of the material is a result of a vast number of atoms or molecules interacting at the atomic scale. The separation of scales between the atomic spacing and the size of the material is enormous. It is not always necessary to know the details of a small-scale interaction to understand the average behavior, or behavior at the large scale, of material. But, there are cases when the small-scale interactions play a significant role in the materials response in large scale, and in such situations, the small-scale interactions can not be ignored. Consider the case of the defects in a material: we know that defects influence the material properties like elastic modulus and thermal conductivity. See [Wan et al., 1986] and [Hao et al., 2011].

In theory, the macroscopic behavior of a material can be computed by looking at the interactions of all particles or atoms at a small scale. But, this is computationally challenging and expensive, and, in some cases, it is nearly impossible to do calculations with all the atoms in a given material. Due to the vast separation, both in the time dimension and in the spatial dimension, the approximation of small-scale interactions is necessary. In [Tadmor and Miller, 2011], we get the clear idea of various length scales associated with the material. Roughly, in the spatial dimension, the small length scale is 10^{-10} meters, related to the atomic spacing and the point defects, and, the large length scale is 10^{-2} meters to 1 meters, associated with the cracks and the grain size. In the time dimension, the small length scale is 10^{-15} seconds, associated with the atomic vibration and wave propagation, and, the large length scale is of the order of 10^3 seconds, associated with the fatigue, creep, and the solidification of metals.

Therefore, we need a numerical method which can capture the small-scale interactions, wherever it is necessary and important, and approximate the small-scale interactions elsewhere. We refer to such method as a multiscale method. The multiscale method aims to combine both the atomistic model and the continuum model. Continuum limit of small-scale interactions plays a vital role in the multiscale method. To explain the continuum limit, consider the material of some fixed size. We subject the material to very slowly varying deformation (or affine deformation) and compute the volume average of energy. Continuum limit of the energy is the limit of the average energy of the material when the size of material tends to infinity.

Typically, in any multiscale method, we divide the sample into two regions: the continuum region and the atomistic region. In the continuum region, we approximate the small-scale interactions. In the atomistic region, we do the exact atomistic calculation. If the continuum region consists of a large number of atoms or particles, and the deformation is slowly varying, we can use the continuum limit of energy to approximate the interactions within continuum region. The choice of a atomistic region depends on the problem. Suppose, we want to model the nanoindentation of material. The natural choice would be to select the small region, surrounding the place where we are indenting the material, as an atomistic region. And, as we move away from the indenting zone, we can use the continuum limit of the energy. Similarly, in the case of a single point defect, we will select the small region surrounding the defect as an atomistic region, and use the continuum limit as we move away from the defect. Adaptive meshing can also be used to automate this selection. Based on the energy of the atoms, and the deformation, we select the region as an atomistic. See [Tadmor and Miller, 2011], [Mielke, 2006], [Milton, 2004] for general treatment of the multiscale method and the continuum limit.

In this work, we mainly focus on the electrical interactions in materials. We can use the work presented in this thesis in materials where electrical and magnetic interactions play a significant role. For example, ionic solids, dielectric materials, various oxides like GaN, $PbTiO_3$, ferroelectric and other magnetic materials. The electrical and magnetic interactions are different from the interatomic potentials in the sense that they are long-range in nature. In the first part of the thesis, we will present the continuum limit calculations for the nanostructures and the random media. We show that the electrical and the magnetic

interactions in the nanostructures and the thin films are different from the interactions in materials with a finite macroscopic volume. This is an interesting observation that we draw from our calculations for the nanostructures and the thin films. We find that the long-range nature of the electrical interactions is not there in the nanostructures and the thin films. We will talk more about this in section 1.4.

In next few sections, we will present the brief overview of some of the key concepts and methods that are important in this work.

1.1 Atomistic model

The atomistic models are used to solve discrete system of atoms or particles. Given the system of atoms, and the interatomic potential, the atomistic models, in the case of statics, look for the configuration of atoms such that energy is minimized, and, in the case of dynamics, compute the configuration of the system at discrete time steps. Interatomic potentials model the interaction between two or more atoms. At present, our computational capabilities allow us to deal with the material of a size in the order of 100nm^3. See [Stephensor et al., 2016]. Therefore, the use of the atomistic models is limited, as the size of the materials for engineering purposes are generally above the range of the atomistic models.

For a given system of atoms, we can have nucleus-nucleus interactions between the atoms, and nucleus-electron interactions between atoms. Also, if atoms carry charges, as in the case of ionic solids, we will also have charge-charge interactions. For a particular type of material, the nucleus-nucleus interactions can be more important. For example, in the inert gasses, the Lennard-Jonnes potential, which only models the interaction between the nucleus of atoms, gives a good result. But, the same potential is not suitable for the metals, where nucleus-electron interaction is dominant. For the metals, the <u>Embedded Atom Method</u> is more proper, which takes into account the electron distribution in a material, and the interaction of a nucleus of an atom with the electron distribution. EAM captures the behavior of metals fairly well. See [Daw and Baskes, 1984]. For oxides, like GaN and PbTiO$_3$, the core-shell method is more suitable. In the core-shell model, we model the atom with a core and a shell, with each carrying charge. See

[Sepliarsky and Cohen, 2002] and [Shimada et al., 2008] for more detail on the core-shell potential. The core-shell model is more suitable for the materials with polarization.

Once we know the correct, or say more appropriate interatomic interaction potential, we look for the configuration which minimizes the energy or which balances the forces. In the molecular statics, see [Tadmor and Miller, 2011], we do the energy minimization to get the equilibrium configuration. In the molecular dynamics, see [Rapaport, 2004], we perform the time integration of the Newton's equation of motion.

1.1.1 Molecular dynamics

Molecular dynamics, MD, is a very widely used method for the system of atoms. It differs from the molecular statics in the sense that it can handle the dynamics problem and is a force-equilibrium method. In this approach, for a given time, we compute the forces on all the atoms, and then integrate the Newton's force equation, $\boldsymbol{F} = m\boldsymbol{a}$, where $\boldsymbol{F}$ is the force vector, m is the mass matrix, and $\boldsymbol{a}$ is the acceleration vector. It is also used to fit the parameters of the interatomic potential for a particular material. For example, if we want to find the parameters of the core-shell potential, for the GaN material, we may want to use MD. See [Shimada et al., 2008], where they fit the parameters of core-shell potential for $PbTiO_3$.

MD is also used to understand the defects in a material, and, the dynamics of a defect. MD, coupled with the periodic boundary condition, is also used to simulate the big system of atoms. Periodic boundary condition approximates the situation when a material is vast, and the boundary condition at the surface of a material can be ignored. An additional advantage with MD is its suitability to finite temperature problems, for both dynamics (non-equilibrium) and equilibrium. The non-equilibrium problems are still computationally challenging using the MD method. Main reason for this is that at each time step, MD does a statistical computation, and the size of the time step is minuscule, of the order of picoseconds to nanoseconds. The size of the time step will depend on the characteristic frequency of the atomic vibration at a given temperature. This is problematic if one wants to analyze the material at one second or one millisecond. In <u>Accelerated MD</u>, they aim to accelerate the dynamics of a system, so that the event happening after the long interval, can be captured in short time. See [Voter, 1997],

[Voter et al., 2002], [Perez et al., 2009] for more details on acceleration techniques in MD method. Also see [Perez and Voter, 2008], [Voter, 2007] for the short presentation on acceleration methods.

1.2 Continuum model

Consider the typical continuum mechanics problem: the deformation of a piezoelectric cantilever beam. It consists of a large number of atoms, and in theory, the deformation of a beam and the electric field can be captured by considering the interactions of all the atoms in a beam. Once we know the position of all atoms, we can easily compute the polarization field in a material, and therefore the electrical response of a piezoelectric material to the applied load. But, considering all the possible interactions in a beam is only possible for the tiny size of the material. Instead, one may want to use the fact that the displacement field varies at macro-scale. We assume that the beam is made of a continuum material, and the field of the beam is a function of points in a material. This continuum model of a beam is then used to model the deformation and the piezoelectric effect.

We need to relate the gradient of a displacement, field in a continuum piezoelectric material, to the lattice deformation associated to the material point. And, as the atoms displace, they cause the change in the polarization. And, therefore, we would need to relate the change in polarization at the small-scale to the electric field at the large-scale. The result would be coupling between the deformation field and the electric field at the large-scale.

The details of the atomic-level interaction is not completely ignored in a continuum model. The constitutive relations, which relate the force to the kinematic quantities, have constants, and these constants depend on the interactions at the atomic level. [Blanc et al., 2002] gives insight into the continuum limit and how continuum limit is computed from molecular/atomic interactions. Book [Tadmor and Miller, 2011] talks about the multiscale and the continuum limit in great detail. See [Blanc et al., 2003], [Blanc et al., 2007b], [Blanc et al., 2007a] where they find the continuum limit when the position of atoms are random functions. In [James and Müller, 1994], the continuum limit

of the magnetostatics energy is computed.

1.3   Combining atomistic and continuum model

To deal with situations, where the interactions at small-scale play a major role in the large-scale behavior, and when, we have a very large system, and the region of interest is of very small size, we need the method that combines both the atomistic modeling and the continuum modeling. There are many numerical methods which combine the atomistic models and the continuum models. Quasicontinuum method is one such method.

1.3.1   Quasicontinuum method

Quasicontinuum, in short QC, is a multi-scale method. Tadmor, Ortiz, and Phillips first proposed this method, in 1996. See [Tadmor et al., 1996], [Tadmor and Miller,], [Tadmor et al., 1999], [Dobson et al., 2007].

In QC method, we divide the material in two regions: the atomistic region and the continuum region. In the atomistic region, we solve for the position, and the momenta (if the temperature is not assumed to be zero), of all the atoms. In the continuum region, we select few representative atom. The value of unknowns, like the displacement, the electric field, at the remaining atoms of continuum region, is computed by interpolation. This is similar to the finite element method, where the deformation of an element is dependent on how the element's nodes move.

The region, where the deformation is significant, or the energy is high, is chosen as an atomistic region. Also, we can use an adaptive method which can update the meshing depending on the energetics of the system. The criteria for defining the region as the atomistic region depends on the displacement gradient.

Multiscale method, like Quasicontinuum method, can be characterized based on many factors: the temperature of a system, long-range/short-range interactions. See [Miller and Tadmor, 2009] for reviews of many different versions of a QC, and its comparative analysis.

Finite-temperature and zero-temperature QC

QC, which can model the material at a finite temperature, will have to deal with the thermal fluctuations of atoms. In the case of finite constant temperature, we have a set of many configurations which satisfy the constraint of fixed temperature, fixed number of atoms, and, the QC has to compute the phase average (ensemble average) of a quantity of interest over these many possible configurations. See [Andersen, 1980], where the author discusses the molecular dynamics method for a system of atoms at the constant temperature or constant pressure.

Further, we can have a <u>constant</u> finite temperature (equilibrium problem), or a finite temperature <u>non-equilibrium</u> problems. See [Shenoy et al., 1999], [Dupuy et al., 2005], [Tadmor et al., 2013], [Kulkarni et al., 2008] for more on QC for finite temperature equilibrium process. See [Kim et al., 2014], [Venturini et al., 2014] for details of QC for non-equilibrium finite temperature processes.

Short-range and long-range interaction in QC

The interatomic potentials are considered short range as the energy at one atom depends on the position of few neighboring atoms. The electrical interactions are long range because the energy and the field of one atom depend on the position of charges far away. This is due to the Coulomb kernel which has a $1/r$ scaling. $1/r$ decays very slowly as we move away from one atom to other. Therefore, the contribution of far away atoms is significant. We will talk more on this in next section.

1.4 Electrical and magnetic interactions

We focus on the ionic solids, oxides like GaN, $PbTiO_3$, and the ferroelectric materials, where electrostatics interaction plays a dominant role. They find application in varieties of the field. For example, ionic crystals are used in ionic batteries, where the motion of the charged defects produces current. Solid state devices, which are used to store the digital data, use the fact that the crystal structure of material, reorients itself when it is subjected to the magnetic or the electric field. See [Atkinson et al., 2003]. Piezoelectric

materials use the fact that there is a change in the electric field if it is subjected to the deformation, and, it deforms if it is subjected to an external electric field.

1.4.1 Electrostatic interactions are long range

We can understand this better by following simple theoretical experiment. For more detail see [Marshall and Dayal, 2013].

1 Consider an infinite three dimensional lattice with a net positive charge in each unit cell. We can estimate the energy density of this system as follows:

$$W \approx \sum_{r=1}^{\infty} [\text{field at distance } r \text{ from origin}] \times [\text{total number of charges}]$$
$$= \sum_{r=1}^{\infty} 1/r \times r^2 = \sum_{r=1}^{\infty} r$$

Thus, the energy density of such a system is unbounded, and it is why we do not find any material which only consists of either the positively charged atoms or negatively charged atoms.

2 Now, assume that each unit cell has net dipole moment. Note that the net charge would be zero in each unit cell. We can estimate the energy density as follows:

$$W \approx \sum_{r=1}^{\infty} 1/r^3 \times r^2 = \sum_{r=1}^{\infty} 1/r$$

This is a divergent sum. But, field due to dipole also has some symmetry associated with it. If we take into account the symmetry and also the cancellation due to the positive and the negative charges, we find that the sum is conditionally convergent. It means that the energy density is non-local.

3 Now, we consider the case when we have a net quadrupole moment, with net dipole moment and net charge being zero, at all unit cell. Energy density is:

$$W \approx \sum_{r=1}^{\infty} 1/r^5 \times r^2 = \sum_{r=1}^{\infty} 1/r^3$$

This is absolutely convergent. For this system, to compute the energy density at one point we can consider the interaction within some cut-off radius, and outside the cut-off radius, we can ignore the contribution.

One of the interesting research topics is handling of a long-range interaction efficiently for a very large system. In [Marshall and Dayal, 2013], they use the coarse-grained (continuum limit) expression of electrostatic energy to approximate the electrical interactions.

1.4.2   Electrical and magnetic interactions in nanostructures

We will show, with the help of our calculations, that the electrical and magnetic interactions are different in the nanostructures as compared to the materials with a finite macroscopic volume. Interactions in the nanostructures, in the continuum limit, are short range. We explain this with the dipole field kernel. For the nanostructures and thin film, the $1/r^3$ scaling, of a dipole field kernel, is strong and decays fast. Therefore, there is no long-range interaction in the continuum limit. See section 2.6 for more detailed explanation.

1.5   Goal of this work

Goals of this work are as follows

1. To examine the electrical and magnetic interactions in the nanostructures. We are interested in computing the continuum limit of electrical interactions in the nanostructures.

2. To examine the electrical interactions when the charge density field is a random field. For the periodic crystal, we assume the charge density field to be periodic. We model the charge density field of a thermally fluctuating system of atoms as a random field. This calculation is important for our next goal.

3. To model the charged point defects in ionic solids when the system is at finite temperature. We use the existing framework *max-ent* [Kulkarni et al., 2008] and extend it to the multi-lattice system.

Chapter 2 contains the continuum limit calculations. In Chapter 3, we present the QC framework. In Chapter 4, the results are presented. In Chapter 5, we present the discussions about this work and also state the future projects.

1.6 C++ implementation

We use the C++ code of Jason Marshall [Marshall and Dayal, 2013]. This is a modification of previous code developed in [Knapp and Ortiz, 2001]. We have rewritten the code to make it object oriented. Adding more capabilities to this code is relatively easy now as one only has to write another class function for the new task.

Chapter 2

Continuum limit: Nanostructures and random media

In this chapter, we will talk about the continuum limit calculations for geometrically-complex atomic nanostructures and random media. We are interested in understanding how the electrical and magnetic interactions take place in a nanostructure, where the length of material is very large compared to the atomic spacing while the cross-section is few atoms thick. These results generalize the techniques developed by R. D. James, S. Müller, and their co-workers, for the crystal with electromagnetic interactions, to the nanostructures. See [James and Müller, 1994], [Geymonat et al., 1993], [Dayal and James, 2010].

The geometries of interest are nanorod and the objective nanorod. These calculations are another step in developing a multiscale method for the nanostructures. Our results also highlight the fact that the electrical and magnetic interactions in nanostructures are different compared to the macroscopically finite volume material. We use the objective structure framework developed by R. D. James to model the objective nanorod. See [Dumitrica and James, 2007], [James, 2006]. Figure 2.0.1 shows the difference between a thin material and thick material. In the figure, we are looking at the cross-section of a rod. In case 1, the size of a cross-section is of the order of the macroscopic length, and in case 2, the size of a cross-section is of the order of the atomic spacing.

We also consider the material which is at the finite temperature. We model the charge density field as a random field. As expected, the results for the random charge density field

is similar to what we see for the periodic crystals. We will also show that the case of the periodic crystal is a special case of our random charge density framework. Therefore, this calculation is more general. For continuum limit calculations of a short-range interactions, in the random media, see [Blanc et al., 2003], [Blanc et al., 2007b], [Blanc et al., 2007a], and [Blanc et al., 20].
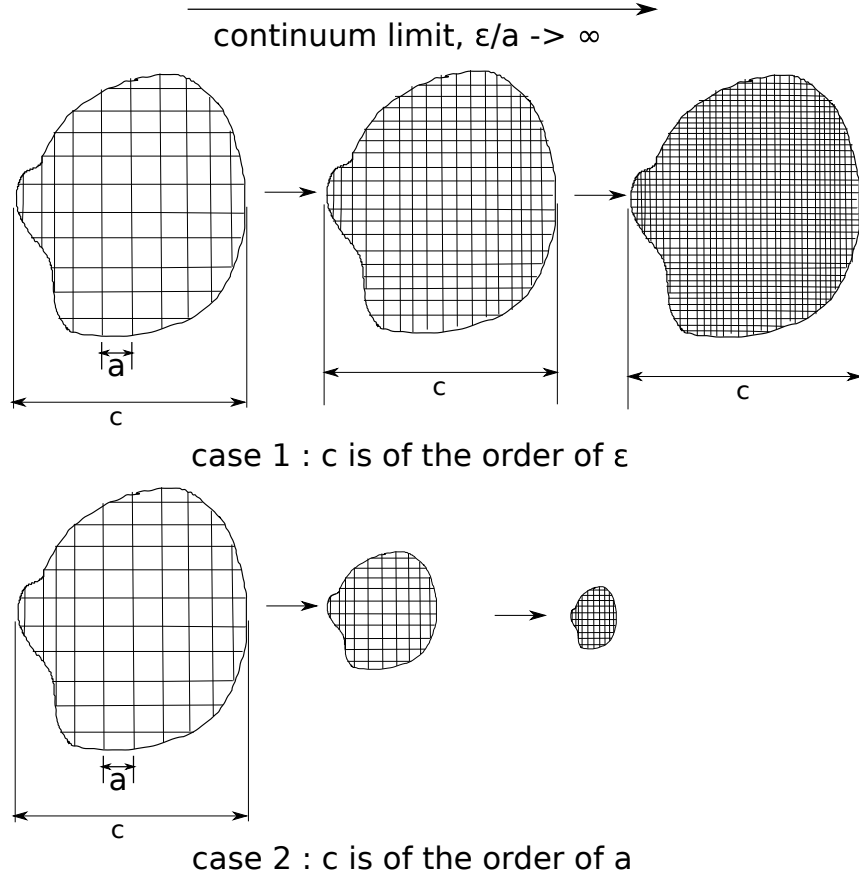
Figure 2.0.1: Cross-section of macroscopically thick rod and thin rod

This chapter is organized as follows: In section 2.1 we present the notations for rest of the chapter. In section 2.2, we briefly talk about basic concepts of length scales, electrostatics energy and continuum limit for periodic crystal. In section 2.3, we present our calculations for nanorod and objective nanorod. In section 2.4, we present our calculations for random media. In section 2.5, we present our continuum limit calculations of a system dipoles on the straight line and the helix.

13

2.1 Notations

We use conventional method to denote vector and tensors as bold faced small and capital letters. Scalar and parameters are denoted by small letters. Below is the list of some important symbols and letters :

- ρ : charge density of a material

- $\mathbb{R}, \mathbb{Z}$: real space and integer space

- $\mathcal{D}$: probability space

- Ω : material domain, depending on the problem, it can be subset of $\mathbb{R}$, $\mathbb{R}^2$, or $\mathbb{R}^3$

- $A \subset \mathbb{R}^2$: area domain

- $B_\epsilon(\boldsymbol{x})$: sphere, center at point $\boldsymbol{x}$, and of radius ϵ

- $|\Omega|$: measure of domain Ω

- $\operatorname{diam} A$: diameter of domain

- $C_0^\infty(X, Y)$: space of test function from space X to Y

- $L^2(X, Y)$: space of square integrable function from X to Y

- D' : space of continuous linear functionals on $C_0^\infty(\mathbb{R}^3, \mathbb{R})$, i.e. space of distributions

- ψ : test function in $C_0^\infty(\mathbb{R}^3, \mathbb{R})$

- T : distribution in D'

- l : atomic length-scale

- ϵ : material length-scale or distance between two material points in object

- L : continuum length-scale

- λ : denotes the size of unit cell

- $\mathcal{L}_\lambda$: collection of indexes of each atom in a atomic arrangement

- $\boldsymbol{d}_\lambda$: dipole field from $\mathcal{L}_\lambda$ to $\mathbb{R}^3$

- $\boldsymbol{m}$: dipole field

- $\boldsymbol{K}$: dipole field kernel

- $\boldsymbol{e}_1, \boldsymbol{e}_2, \boldsymbol{e}_3$: orthonormal basis in space $\mathbb{R}^3$

- U_1^l, U_2^l, U_3^l : unit cell, in 1-D, 2-D and 3-D, of measure l

- $dl_y, dA_{\boldsymbol{y}}, dV_{\boldsymbol{y}}$: length, area and volume measure

- $\boldsymbol{x}_p$: usually to denote the vector in given plane

- s : element of parametric space

- $\boldsymbol{x}(s)$: mapping of parametric space to $\mathbb{R}^3$

- $\boldsymbol{Q}$: orthogonal rotational tensor in $\mathbb{R}^3$

- $\boldsymbol{Q}^a$: orthogonal tensor with rotation of amount a

- ω : the event in probability space

2.2 Length scales, electrostatic energy and results for periodic media

First, we explain the length scales involved in our calculations.

2.2.1 Length scales

As we mentioned in the introduction, the macroscopic fields like electric field, deformation gradient vary at the scale much greater than atomic spacing. In our material model, we have three relevant length scales, and they are as follows

Continuum length scale: This is the length scale associated with the size of the material.

Separation between material points: We denote this as ϵ. We assume that macroscopic fields vary at the scale ϵ/L. This is the size of the material point.

Atomic spacing: This is the length scale associated with separation between the atoms.

In Figure 2.2.1, we can see how these three scales appear in a material.
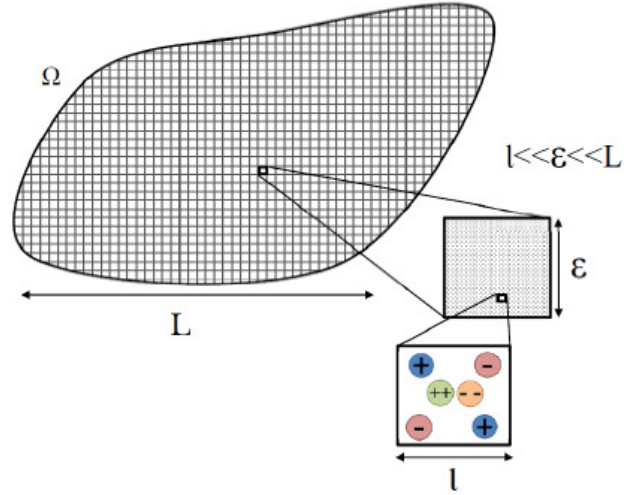
Figure 2.2.1: Length scales in a material ([Marshall and Dayal, 2013])

2.2.2   Charge density field as a two-scale function

Let $\rho : \Omega \rightarrow \mathbb{R}$ be the charge density field of material. Consider a material point $\boldsymbol{x} \in \Omega$ and assume that atoms are arranged periodically. The charge density will also depend on the small scale variable of material as in the case of the periodic arrangement, the charge density would also be periodic, on small scale variable. We assume that the variation of ρ is slow from one material point to other, i.e. at the macroscopic scale, and the variation of ρ is large as we move from one unit cell within the material point to another unit cell in the same material point. We describe ρ as $\rho(\boldsymbol{x}, \boldsymbol{y})$, where $\boldsymbol{y} = \boldsymbol{x}/l$ is the variable associated to small scale. Here $\boldsymbol{x}$ represents a material point, and $\boldsymbol{y}$ is the point within a material point. See [Allaire, 1992] for more on two scale fields.

2.2.3   Electrostatic energy

Electrostatics energy is given by

$$E = \int_{\boldsymbol{x},\boldsymbol{x}'\in\Omega} \frac{\rho(\boldsymbol{x})\rho(\boldsymbol{x}')}{|\boldsymbol{x}-\boldsymbol{x}'|} dV_{\boldsymbol{x}} dV_{\boldsymbol{x}'} \tag{2.2.1}$$

For given ϵ, let $\Omega_\epsilon = \Omega \cap (\epsilon\mathbb{Z})^3$ be set of material points. Then, we can write energy as

$$E = \sum_{\substack{\boldsymbol{x}\in\Omega_\epsilon \\ \boldsymbol{x}'\in\Omega}} \int_{\substack{\boldsymbol{z}\in B_\epsilon(\boldsymbol{x}), \\ \boldsymbol{z}'\in B_\epsilon(\boldsymbol{x}')}} \frac{\rho(\boldsymbol{x},\frac{\boldsymbol{z}}{l})\rho(\boldsymbol{x}',\frac{\boldsymbol{z}'}{l})}{|\boldsymbol{x}+\boldsymbol{z}-\boldsymbol{x}'-\boldsymbol{z}'|} dV_{\boldsymbol{z}} dV_{\boldsymbol{z}'} \tag{2.2.2}$$

where $B_\epsilon(\boldsymbol{x}) := \{\boldsymbol{z} \in \mathbb{R}^3 : |\boldsymbol{x}-\boldsymbol{z}| \le \epsilon\}$.

We can divide the summation appearing in 2.2.2 in two energies, local energy and non-local energy. They are as follows :

$$E_{local} = \sum_{\boldsymbol{x}\in\Omega_\epsilon} \int_{\boldsymbol{z},\boldsymbol{z}'\in B_\epsilon(\boldsymbol{x})} \frac{\rho(\boldsymbol{x},\frac{\boldsymbol{z}}{l})\rho(\boldsymbol{x},\frac{\boldsymbol{z}'}{l})}{|\boldsymbol{z}-\boldsymbol{z}'|} dV_{\boldsymbol{z}} dV_{\boldsymbol{z}'} \tag{2.2.3}$$

$$E_{nonlocal} = \sum_{\substack{\boldsymbol{x},\boldsymbol{x}'\in\Omega_\epsilon, \\ \boldsymbol{x}\ne\boldsymbol{x}'}} \int_{\substack{\boldsymbol{z}\in B_\epsilon(\boldsymbol{x}), \\ \boldsymbol{z}'\in B_\epsilon(\boldsymbol{x}')}} \frac{\rho(\boldsymbol{x},\frac{\boldsymbol{z}}{l})\rho(\boldsymbol{x}',\frac{\boldsymbol{z}'}{l})}{|\boldsymbol{x}+\boldsymbol{z}-\boldsymbol{x}'-\boldsymbol{z}'|} dV_{\boldsymbol{z}} dV_{\boldsymbol{z}'} \tag{2.2.4}$$

In next section, we will analyze these two energies for the thin rod and the objective structure. First, we present the continuum limit of energy when material remains three-dimensional in limit (unlike thin films or thin rod).

2.2.4 Results for the periodic charge density field

In [Marshall and Dayal, 2013], they compute the continuum limit of the electrostatic energy for the periodic charge density field. We present their result in this section so that we can compare this with our calculations for the nanostructures and the random media. Let $\Omega \subset \mathbb{R}^3$ be the material domain. Let ρ satisfy the following assumption of periodicity

$$\rho(\boldsymbol{x},\boldsymbol{y}+\boldsymbol{z}) = \rho(\boldsymbol{x},\boldsymbol{y}) \qquad \forall \boldsymbol{z}\in\mathbb{Z}^3, \forall \boldsymbol{x}\in\Omega, \forall \boldsymbol{y}\in\mathbb{R}^3 \tag{2.2.5}$$

Local and non-local energy at the material point is as follows :

$$E_{local}(\boldsymbol{x}) = \lim_{r \to \infty} \int_{\boldsymbol{y} \in U_0^3} \int_{\boldsymbol{y}' \in B(\boldsymbol{x},r)} \frac{\tilde{\rho}(\boldsymbol{X},\boldsymbol{y})\tilde{\rho}(\boldsymbol{X},\boldsymbol{y}')}{|\boldsymbol{y}-\boldsymbol{y}'|} dV_{\boldsymbol{y}'} dV_{\boldsymbol{y}} \tag{2.2.6}$$

$$E_{nonlocal}(\boldsymbol{x},\boldsymbol{x}') = \boldsymbol{K}(\boldsymbol{x}-\boldsymbol{x}') : \left(\int_{\boldsymbol{y} \in \bar{U}_0^3} \tilde{\rho}(\boldsymbol{X},\boldsymbol{y})\boldsymbol{y} dV_{\boldsymbol{y}} \right)$$

$$\otimes \left(\int_{\boldsymbol{y}' \in U_0^3} \tilde{\rho}(\boldsymbol{X}',\boldsymbol{y}')\boldsymbol{y}' dV_{\boldsymbol{y}'} \right) \quad \forall \boldsymbol{x} \neq \boldsymbol{x}' \tag{2.2.7}$$

Where U_0^3 and $\bar{U}_0^3$ are the three-dimensional unit cell with unit volume inside the material point $\boldsymbol{x}$ and $\boldsymbol{x}'$. And, $\boldsymbol{X} = l\boldsymbol{x}$. Total energy is

$$E_{local} = \int_{\boldsymbol{x} \in \Omega} E_{local}(\boldsymbol{x}) dV_{\boldsymbol{x}} \tag{2.2.8}$$

$$E_{nonlocal} = \int_{\substack{\boldsymbol{x},\boldsymbol{x}' \in \Omega, \\ \boldsymbol{x} \neq \boldsymbol{x}'}} E_{nonlocal}(\boldsymbol{x},\boldsymbol{x}') dV_{\boldsymbol{x}} dV_{\boldsymbol{x}'} \tag{2.2.9}$$

We also get the following scaling on the charge density field

$$\rho(\boldsymbol{x},\boldsymbol{y}) = \frac{\tilde{\rho}(\boldsymbol{X},\boldsymbol{y})}{l}, \qquad \boldsymbol{X} = l\boldsymbol{x} \tag{2.2.10}$$

moreover, $\tilde{\rho}$ satisfies the charge neutrality condition as given below

$$\int_{\boldsymbol{y} \in U_0^3} \tilde{\rho}(\boldsymbol{X},\boldsymbol{y}) dV_{\boldsymbol{y}} = 0 \tag{2.2.11}$$

The scaling of $1/l$ is due to the condition that the continuum limit of local energy neither go to zero or infinity trivially. The condition that the continuum limit of non-local energy is not infinity requires the charge density field to satisfy the charge neutrality condition.

We observe from the expression of energy that the local energy is entirely due to the charge-charge interaction within each material point. Hence, in Cauchy-Born rule the local energy can be incorporated along with the interatomic potential, to compute the energy at a material point. Expression of the non-local energy also agrees with our understanding that if the point of interest, where we want to calculate the electric field, is far away from some charge distribution, the electric field will be mainly due to the first moment of charge distribution. This completes the basics of the Electrostatics calculation.
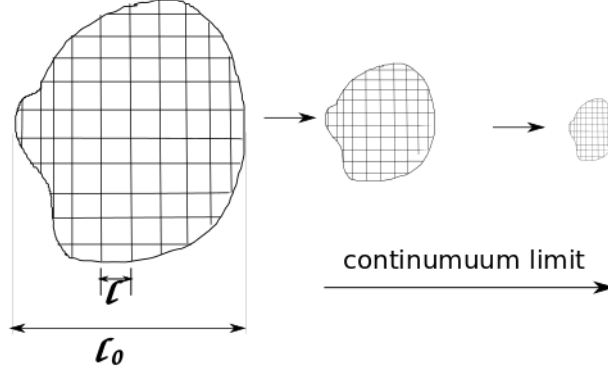
Figure 2.3.1: Cross-section of thin rod

2.3 Electrostatics calculations for nanostructures

In this section, we analyze the electrostatic energy for thin materials. This calculation extends the method in [Marshall and Dayal, 2013] to the nanostructures. Figure 2.3.1 shows the cross-section of rod, which is only few atomic spacing thick, in the continuum limit.

We use the Objective structure description of nanostrcture. This description of nanostructures includes the periodic nanorod and also nanotube with rotational symmetry.

2.3.1 Objective nanorod

Materials which can be described using Objective framework are more general than crystal lattices. They have rotational and translational symmetry. According to [James, 2006], the objective structure is the one where each atom sees the same kind of environment.

Brief introduction of the objective structure

Consider $K = \{\boldsymbol{x}_{0,j} \in \mathbb{R}^3 : j = 1, 2, ..., M\}$, set of locations of M particles/species. Objective structure is described by the repetition of K using rotational and translation transformation. Repetitions, here, are not simply translations, as in the case of multi-lattice, but a rotations and a translation. Objective structure, with N number of unit cells, and M number of species, will be as follows

$$\mathcal{L} = \left\{ \boldsymbol{x}_{n,j} \in \mathbb{R}^3 : \boldsymbol{x}_{n,j} = \boldsymbol{Q}_{n,j} \boldsymbol{x}_{0,j} + n\boldsymbol{c}, j = 1, 2, .., M, n = 0, 1, 2, .., N \right\} \qquad (2.3.1)$$

19

Where, $\boldsymbol{Q}_{n,j}$ is a rotation of the atom in the nth unit cell of species j. $\boldsymbol{c}$ is a translation vector. M species can be of the same atom or can be of different atoms with positive or negative charges. Locations of all species in n^{th} unit cell is $\{n\boldsymbol{c}+\boldsymbol{Q}_{n,j}\boldsymbol{x}_{0,j} : j = 1, 2, .., M\}$.

Simple objective structure   For simplicity, we will only consider the case when $\boldsymbol{Q}_{n,j}(\boldsymbol{x}) = \boldsymbol{Q}^n(\boldsymbol{x})$ and $\boldsymbol{c} = \boldsymbol{e}_1$. Physically, this assumption means, the action of $\boldsymbol{Q}_{n,j}$ on any vector results in n times rotation of that vector by an orthogonal second order tensor $\boldsymbol{Q}$. Also, the rotations are independent of species. In Figure 2.3.2, we show this transformation in steps. We take a unit cell and place it along the axis, and then perform the rotation on each unit cell, depending on the location of unit cell from the reference unit cell. Now, imagine some fixed number of species attached to the reference unit cell. As we perform the rotation and translation, these species also translate and rotate along with the unit cell.
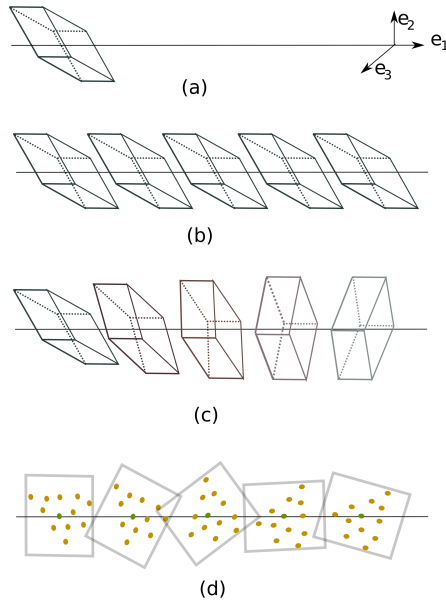
Figure 2.3.2: (a.) Unit cell (b.) Placing unit cell along the axis of objective nanorod (c.) Applying the rotation (d.) Showing the transformation of atoms, fixed to a unit cell, in the plane $(\boldsymbol{e}_2, \boldsymbol{e}_3)$, when unit cell is rotated.

Periodic nanorod

If we set $\boldsymbol{Q} = \boldsymbol{I}$, where $\boldsymbol{I}$ is the identity second order tensor, in the objective description of material, we will describe the nanorod which is periodic along its axis.

2.3.2 Material domain and the charge density field

Let $\Omega^s \subset \mathbb{R}$, and $N_{\epsilon,l}$ be the integer closest to ϵ/l, i.e. $N_{\epsilon,l} = \lfloor \epsilon/l \rfloor$. We define the domain, where atoms are arranged, for a material point $x \in \Omega_s$ as follows

$$M_\epsilon(x) := x\boldsymbol{e}_1 + \bigcup_{i=0}^{N_{\epsilon,l}} g_l^i([0,l]^3) \tag{2.3.2}$$

where, we define transformation g_l^i, for $0 \leq i \leq N_{\epsilon,l}$ as follows

$$g_l^i(A) = \left\{ \boldsymbol{Q}^i \boldsymbol{y} + il\boldsymbol{e}_1 : \boldsymbol{y} \in A \right\} \tag{2.3.3}$$

$g_l^i(A)$ rotates each vector of a set A by an amount $\boldsymbol{Q}^i$ and translates it into an amount il in the direction $\boldsymbol{e}_1$.

We can now define rescaled domain as

$$M_{\epsilon,l}(x) = x\boldsymbol{e}_1 + \bigcup_{i=0}^{N_{\epsilon,l}} g_1^i([0,1]^3) \tag{2.3.4}$$

Charge density field We assume that charge density field ρ has the symmetry of material, i.e.

$$\rho(x, \boldsymbol{y}) = \rho(x, \boldsymbol{Q}^k \boldsymbol{y} + k\boldsymbol{e}_1), \forall k \in \mathbb{Z}, \forall \boldsymbol{y} \in [0,1]^3 \tag{2.3.5}$$

2.3.3 Local energy

In 2.2.3, we do change of variable $\boldsymbol{y} = \boldsymbol{z}/l$. We get

E_{local}

$$= \sum_{x \in \Omega^s \cap (\epsilon \mathbb{Z})} \int_{\boldsymbol{y}, \boldsymbol{y'} \in M_{\epsilon,l}(x)} \frac{\rho(x, \boldsymbol{y})\rho(x, \boldsymbol{y'})}{l\, |\boldsymbol{y} - \boldsymbol{y'}|} l^3 dV_{\boldsymbol{y}} l^3 dV_{\boldsymbol{y'}}$$

$$= \sum_{x \in \Omega^s \cap (\epsilon \mathbb{Z})} \sum_{i=0}^{N_{\epsilon,l}} \sum_{j=0}^{N_{\epsilon,l}} l^5 \int_{\substack{\boldsymbol{y} \in x\boldsymbol{e}_1 + g_1^i([0,1]^3), \\ \boldsymbol{y'} \in x\boldsymbol{e}_1 + g_1^j([0,1]^3)}} \frac{\rho(x, \boldsymbol{y})\rho(x, \boldsymbol{y'})}{|\boldsymbol{y} - \boldsymbol{y'}|} dV_{\boldsymbol{y}} dV_{\boldsymbol{y'}}$$

$$= \sum_{x \in \Omega^s \cap (\epsilon \mathbb{Z})} \sum_{i=0}^{N_{\epsilon,l}} \sum_{j=0}^{N_{\epsilon,l}} l^5 \int_{\substack{\boldsymbol{y} \in x\boldsymbol{e}_1 + [0,1]^3, \\ \boldsymbol{y'} \in x\boldsymbol{e}_1 + [0,1]^3}}$$

$$\frac{\rho(x, \boldsymbol{Q}^i \boldsymbol{y} + i\boldsymbol{e}_1)\rho(x, \boldsymbol{Q}^j \boldsymbol{y'} + j\boldsymbol{e}_1)}{|\boldsymbol{Q}^i \boldsymbol{y} + i\boldsymbol{e}_1 - \boldsymbol{Q}^j \boldsymbol{y'} - j\boldsymbol{e}_1|} dV_{\boldsymbol{Q}^i \boldsymbol{y} + i\boldsymbol{e}_1} dV_{\boldsymbol{Q}^j \boldsymbol{y'} + j\boldsymbol{e}_1}$$

$$= \sum_{x \in \Omega^s \cap (\epsilon \mathbb{Z})} l^5 \int_{\substack{\boldsymbol{y} \in x\boldsymbol{e}_1 + [0,1]^3, \\ \boldsymbol{y'} \in x\boldsymbol{e}_1 + [0,1]^3}} \left[\sum_{i=0}^{N_{\epsilon,l}} \left(\sum_{j \geq i}^{N_{\epsilon,l}} \frac{\rho(x, \boldsymbol{y})\rho(x, \boldsymbol{y'})}{|\boldsymbol{Q}^i \left(\boldsymbol{y} - \boldsymbol{Q}^{j-i}\boldsymbol{y'} - (j-i)\boldsymbol{e}_1\right)|} \right. \right.$$

$$\left. \left. + \sum_{j=0}^{i-1} \frac{\rho(x, \boldsymbol{y})\rho(x, \boldsymbol{y'})}{|\boldsymbol{Q}^j \left(\boldsymbol{Q}^{i-j}\boldsymbol{y} + (i-j)\boldsymbol{e}_1 - \boldsymbol{y'}\right)|} \right) \right] dV_{\boldsymbol{y}} dV_{\boldsymbol{y'}} \tag{2.3.6}$$

Where, in second last step, we substituted the definition of g_1^i, and in last step we used the symmetry of ρ, and invariance property of volume measure with respect to the rotation and translation. We also divided the summation over j in two parts in the last equation above. Further, with change of variable and renaming of $\boldsymbol{y}$ and $\boldsymbol{y'}$ in summation over j in second part inside the bracket, and also using the definition of g_1^i, we get

E_{local}

$$= \sum_{x \in \Omega^s \cap (\epsilon \mathbb{Z})} l^5 \sum_{i=0}^{N_{\epsilon,l}} \left(\sum_{j \geq i}^{N_{\epsilon,l}} \int_{\substack{\boldsymbol{y} \in x\boldsymbol{e}_1 + [0,1]^3, \\ \boldsymbol{w} \in x\boldsymbol{e}_1 + g^{j-i}([0,1]^3)}} \right.$$

$$\frac{\rho(x, \boldsymbol{y})\rho(x, \boldsymbol{Q}^{i-j}\boldsymbol{w} + (i-j)\boldsymbol{e}_1)}{|\boldsymbol{y} - \boldsymbol{w}|} dV_{\boldsymbol{y}} dV_{\boldsymbol{Q}^{i-j}\boldsymbol{w} + (i-j)\boldsymbol{e}_1}$$

$$\left. + \sum_{j=0}^{i-1} \int_{\substack{\boldsymbol{y} \in x\boldsymbol{e}_1 + [0,1]^3, \\ \boldsymbol{w} \in x\boldsymbol{e}_1 + g^{i-j}([0,1]^3)}} \frac{\rho(x, \boldsymbol{y})\rho(x, \boldsymbol{Q}^{j-i}\boldsymbol{w} + (j-i)\boldsymbol{e}_1)}{|\boldsymbol{y} - \boldsymbol{w}|} dV_{\boldsymbol{y}} dV_{\boldsymbol{Q}^{j-i}\boldsymbol{w} + (j-i)\boldsymbol{e}_1} \right) \tag{2.3.7}$$

$$
= \sum_{x \in \Omega^s \cap (\epsilon \mathbb{Z})} l^5 \sum_{i=0}^{N_{\epsilon,l}} \left(\sum_{j \geq i}^{N_{\epsilon,l}} \int_{\substack{\boldsymbol{y} \in x\boldsymbol{e}_1 + [0,1]^3, \\ \boldsymbol{w} \in x\boldsymbol{e}_1 + g^{j-i}([0,1]^3)}} \frac{\rho(x, \boldsymbol{y})\rho(x, \boldsymbol{w})}{|\boldsymbol{y} - \boldsymbol{w}|} dV_{\boldsymbol{y}} dV_{\boldsymbol{w}} \right.
$$

$$
\left. + \sum_{j=0}^{i-1} \int_{\substack{\boldsymbol{y} \in x\boldsymbol{e}_1 + [0,1]^3, \\ \boldsymbol{w} \in x\boldsymbol{e}_1 + g^{i-j}([0,1]^3)}} \frac{\rho(x, \boldsymbol{y})\rho(x, \boldsymbol{w})}{|\boldsymbol{y} - \boldsymbol{w}|} dV_{\boldsymbol{y}} dV_{\boldsymbol{w}} \right) \tag{2.3.8}
$$

The last equation, where we have two different terms depending on $j \geq i$ or $j < i$, can be combined as below

$$
E_{local}
$$

$$
= \sum_{x \in \Omega^s \cap (\epsilon \mathbb{Z})} l^5 \sum_{i=0}^{N_{\epsilon,l}} \left(\sum_{j=0}^{N_{\epsilon,l}} \int_{\substack{\boldsymbol{y} \in x\boldsymbol{e}_1 + [0,1]^3, \\ \boldsymbol{w} \in x\boldsymbol{e}_1 + g^{|j-i|}([0,1]^3)}} \frac{\rho(x, \boldsymbol{y})\rho(x, \boldsymbol{w})}{|\boldsymbol{y} - \boldsymbol{w}|} dV_{\boldsymbol{y}} dV_{\boldsymbol{w}} \right) \tag{2.3.9}
$$

Note that we have $|j - i|$ as the superscript on g. As $\epsilon/l \to \infty$ we have $N_{\epsilon,l} \to \infty$. The measure of set $K_i := \{|j - i| : j = 0, ..., N_{\epsilon,l}\}$, for each integer i less than or equal to $N_{\epsilon,l}$, will tend to $N_{\epsilon,l}$ as $\epsilon/l \to \infty$. Also, in the limit $\epsilon/l \to \infty$, the set K_i will be equal to the set $[0, N_{\epsilon,l}] \cap \mathbb{Z}$. Therefore, in the limit $\epsilon/l \to \infty$, we have

$$
E_{local}
$$

$$
= \sum_{x \in \Omega^s \cap (\epsilon \mathbb{Z})} l^5 N_{\epsilon,l} \left(\sum_{j=0}^{N_{\epsilon,l}} \int_{\substack{\boldsymbol{y} \in x\boldsymbol{e}_1 + [0,1]^3, \\ \boldsymbol{w} \in x\boldsymbol{e}_1 + g^j([0,1]^3)}} \frac{\rho(x, \boldsymbol{y})\rho(x, \boldsymbol{w})}{|\boldsymbol{y} - \boldsymbol{w}|} dV_{\boldsymbol{y}} dV_{\boldsymbol{w}} \right)
$$

$$
= \sum_{x \in \Omega^s \cap (\epsilon \mathbb{Z})} \epsilon l^4 \frac{N_{\epsilon,l}}{\epsilon/l} \left(\sum_{j=0}^{N_{\epsilon,l}} \int_{\substack{\boldsymbol{y} \in x\boldsymbol{e}_1 + [0,1]^3, \\ \boldsymbol{w} \in x\boldsymbol{e}_1 + g^j([0,1]^3)}} \frac{\rho(x, \boldsymbol{y})\rho(x, \boldsymbol{w})}{|\boldsymbol{y} - \boldsymbol{w}|} dV_{\boldsymbol{y}} dV_{\boldsymbol{w}} \right) \tag{2.3.10}
$$

$$
\tag{2.3.11}
$$

Note that $N_{\epsilon,l}/(\epsilon/l)$ is 1 in the limit $\epsilon/l \to \infty$. Thus, in the limit, we have

$$
E_{local}
$$

$$
= \sum_{x \in \Omega^s \cap (\epsilon \mathbb{Z})} \epsilon l^4 \left(\sum_{j=0}^{N_{\epsilon,l}} \int_{\substack{\boldsymbol{y} \in x\boldsymbol{e}_1 + [0,1]^3, \\ \boldsymbol{w} \in x\boldsymbol{e}_1 + g^j([0,1]^3)}} \frac{\rho(x, \boldsymbol{y})\rho(x, \boldsymbol{w})}{|\boldsymbol{y} - \boldsymbol{w}|} dV_{\boldsymbol{y}} dV_{\boldsymbol{w}} \right) \tag{2.3.12}
$$

Scaling on the charge density field

We argue that the term inside bracket is electrostatic energy of the material point x. If this energy is not trivially zero, or infinity, in the limit, then there must exist $\tilde{\rho}$ such that

$$\rho(x, \boldsymbol{y}) = \frac{\tilde{\rho}(x, \boldsymbol{y})}{l^2} \tag{2.3.13}$$

In the limit, we have

$$E_{local} = \int_{\Omega^s} \left[\lim_{N \to \infty} \int_{\substack{\boldsymbol{u} \in x\boldsymbol{e}_1 + [0,1]^3, \\ \boldsymbol{u}' \in x\boldsymbol{e}_1 + \bigcup_{i=0}^{N}(g_1^i([0,1]^3))}} \frac{\tilde{\rho}(x, \boldsymbol{u})\tilde{\rho}(x, \boldsymbol{u}')}{|\boldsymbol{u} - \boldsymbol{u}'|} dV_{\boldsymbol{u}} dV_{\boldsymbol{u}'} \right] dl_x \tag{2.3.14}$$

2.3.4 Non-local energy

After change of variable in Equation 2.2.4, we get

$$E_{nonlocal} = \sum_{\substack{x,x' \in \Omega^s \cap (\epsilon\mathbb{Z}), \\ x \neq x'}} l^6 \sum_{i=0}^{N_{\epsilon,l}} \sum_{j=0}^{N_{\epsilon,l}} \int_{\substack{\boldsymbol{u} \in x\boldsymbol{e}_1 + [0,1]^3, \\ \boldsymbol{u}' \in x'\boldsymbol{e}_1 + [0,1]^3}}$$

$$\frac{\rho(x, \boldsymbol{Q}^i\boldsymbol{u} + i\boldsymbol{e}_1)\rho(x', \boldsymbol{Q}^j\boldsymbol{u}' + j\boldsymbol{e}_1)}{\left| x\boldsymbol{e}_1 + l\left(\boldsymbol{Q}^i\boldsymbol{u} + i\boldsymbol{e}_1\right) - x'\boldsymbol{e}_1 - l\left(\boldsymbol{Q}^j\boldsymbol{u}' + j\boldsymbol{e}_1\right) \right|} dV_{\boldsymbol{u}} dV_{\boldsymbol{u}'}$$

$$= \sum_{\substack{x,x' \in \Omega^s \cap (\epsilon\mathbb{Z}), \\ x \neq x'}} l^6 \sum_{i=0}^{N_{\epsilon,l}} \sum_{j=0}^{N_{\epsilon,l}} \int_{\substack{\boldsymbol{u} \in x\boldsymbol{e}_1 + [0,1]^3, \\ \boldsymbol{u}' \in x'\boldsymbol{e}_1 + [0,1]^3}}$$

$$\frac{\rho(x, \boldsymbol{u})\rho(x', \boldsymbol{u}')}{\left| x\boldsymbol{e}_1 + l\left(\boldsymbol{Q}^i\boldsymbol{u} + i\boldsymbol{e}_1\right) - x'\boldsymbol{e}_1 - l\left(\boldsymbol{Q}^j\boldsymbol{u}' + j\boldsymbol{e}_1\right) \right|} dV_{\boldsymbol{u}} dV_{\boldsymbol{u}'} \tag{2.3.15}$$

Using the mean value theorem for integral and substituting the scaling of ρ in Equation 2.3.13, in the limit, we get

$$E_{nonlocal} = \sum_{\substack{x,x' \in \Omega^s \cap (\epsilon\mathbb{Z}), \\ x \neq x'}} (\epsilon/l)^2 l^6 \int_{\substack{\boldsymbol{u} \in x\boldsymbol{e}_1 + [0,1]^3, \\ \boldsymbol{u}' \in x'\boldsymbol{e}_1 + [0,1]^3}} \frac{\rho(x, \boldsymbol{u})\rho(x', \boldsymbol{u}')}{|x\boldsymbol{e}_1 - x'\boldsymbol{e}_1|} dV_{\boldsymbol{u}} dV_{\boldsymbol{u}'}$$

$$= \int_{\substack{x,x' \in \Omega^s, \\ x \neq x'}} \left[\int_{\substack{\boldsymbol{u} \in x\boldsymbol{e}_1 + [0,1]^3, \\ \boldsymbol{u}' \in x'\boldsymbol{e}_1 + [0,1]^3}} \frac{\tilde{\rho}(x, \boldsymbol{u})\tilde{\rho}(x', \boldsymbol{u}')}{|x\boldsymbol{e}_1 - x'\boldsymbol{e}_1|} dV_{\boldsymbol{u}} dV_{\boldsymbol{u}'} \right] dl_x dl_{x'} \tag{2.3.16}$$

2.3.5 Continuum limit

We write the final expression of the limit here

$$E_{local}(x) = \lim_{N \to \infty} \int_{\substack{\boldsymbol{u} \in x\boldsymbol{e}_1 + \bigcup_{i=0}^{N}(g_1^i([0,1]^3)), \\ \boldsymbol{u}' \in x\boldsymbol{e}_1 + [0,1]^3}} \frac{\tilde{\rho}(x,\boldsymbol{u})\tilde{\rho}(x,\boldsymbol{u}')}{|\boldsymbol{u} - \boldsymbol{u}'|} dV_{\boldsymbol{u}} dV_{\boldsymbol{u}'} \qquad (2.3.17)$$

$$E_{nonlocal}(x, x') = \frac{q(x)q(x')}{|x\boldsymbol{e}_1 - x'\boldsymbol{e}_1|} \qquad (2.3.18)$$

and

$$E_{local} = \int_{x \in \Omega_s} E_{local}(x) dl_x \qquad (2.3.19)$$

$$E_{nonlocal} = \int_{\substack{x,x' \in \Omega_s, \\ x \neq x'}} E_{nonlocal}(x, x') dl_x dl_{x'} \qquad (2.3.20)$$

In the limit $N \to \infty$, the domain $\boldsymbol{u} \in x\boldsymbol{e}_1 + \bigcup_{i=0}^{N}(g_1^i([0,1]^3))$ will be the infinite length helical tube with scaling of 1.

Where, $q(x)$ is a total charge within a material point, defined as

$$q(x) := \int_{\boldsymbol{u} \in x\boldsymbol{e}_1 + [0,1]^3} \tilde{\rho}(x, \boldsymbol{u}) dV_{\boldsymbol{u}} \qquad (2.3.21)$$

Clearly, local energy is due to the charge-charge interaction within material point, while non-local energy is due to the charge-charge interaction between two material points.

2.4 Electrostatics calculations for the random media

In this section, we will analyze the electrostatics energy when the charge density field is a random field. The main reason for doing this calculation is that we want to develop a multiscale numerical method for ionic solids at finite temperature. As we know that the atoms randomly fluctuate when the material is at finite temperature, the charge density field will be a random field. We want to see how the interactions take place in the continuum limit.

Consider the Figure 2.4.1 where we show two ways the atoms can be arranged within a material point. In one case, we have a crystal structure, and in the other we have a

random arrangement of atoms, at some time t. The atomic length scale is same in both of this arrangement. In what follows, we will first talk about the material domain, the random charge density field, and some of the key properties we want our charge density field to satisfy. This work requires some knowledge of probability theory. Therefore, we first present a short overview of probability theory.
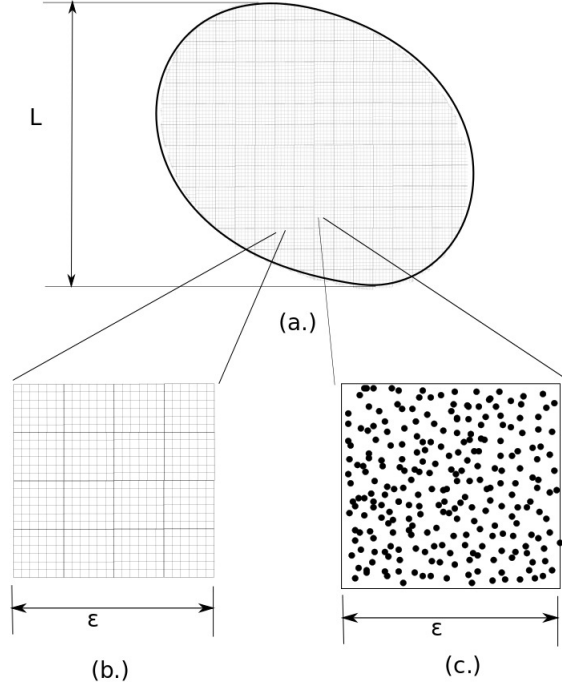
Figure 2.4.1: (a.) Typical material with material points (b.) Periodically arranged atoms (c.) Randomly arranged atoms.

2.4.1 Short overview of the probability theory

In this subsection, the basic concept of the probability theory is presented. We have used [Ostoja-Starzewski, 2008] (Chapter 1 and 2) and [Jikov et al., 1994] (Chapter 7) as a reference for this subsection.

Probability space

Let $(D, \mathcal{D}, \mu)$ be the probability space. Here D is a set of sample points, $\mathcal{D}$ is event space and is σ- algebra of D and μ is a probability measure of $\mathcal{D}$.

Random variable

A measurable function $\psi : D \to \mathbb{R}$ is called random variable. ψ satisfies following :
$\forall B \in \mathcal{B}(\mathbb{R})$,

$$B_\psi = \{\omega \in D : \psi(\omega) \in B\} \tag{2.4.1}$$

is in $\mathcal{D}$.

We define the expectation of ψ if it exists, as

$$\mathbb{E}[\psi(\cdot)] := \int_D \psi(\omega)\mu(\omega) \tag{2.4.2}$$

This is also called mean of the random variable.

We define variance of the random variable as

$$V[\psi] := \mathbb{E}[(\psi(\cdot) - \mathbb{E}[\psi])^2] \tag{2.4.3}$$

This measures the variation of random variable from its mean value. We can introduce new probability measure P_ψ on $(\mathbb{R}, \mathcal{B}(\mathbb{R}))$ using ψ as follows

$$P_\psi(B) := \mu(\{\omega \in D : \psi(\omega) \in B\}) = \mu(\psi \in B) \tag{2.4.4}$$

This is called the probability distribution of ψ in $(\mathbb{R}, \mathcal{B}(\mathbb{R}))$. We define distribution function $F_\psi : \mathbb{R} \to [0, 1]$ of ψ as

$$F_\psi(x) := \mu(\{\omega \in D : \psi(\omega) \leq x\}) \tag{2.4.5}$$

Random process

Random process is a collection of random variables parameterized by the element of some set K.

Continuum random process   Let $K \subset \mathbb{R}$ is some set, possibly equal to $\mathbb{R}$. Let $\psi_t : D \to \mathbb{R}$ be the random variable for all $t \in K$. We define a random process, parametrized by set K, as

$$\boldsymbol{X}(t,\omega) = \psi_t(\omega) \tag{2.4.6}$$

Measurable functions of type $\boldsymbol{X} : K \times D \to \mathbb{R}$ are random processes. We define its probability distribution $P_{\boldsymbol{X}}$ as

$$P_{\boldsymbol{X}}(B) = \mu(\{\omega : \boldsymbol{X}(t,\omega) \in B, \forall t \in K\}) \quad \forall B \in \boldsymbol{\mathcal{B}}(\mathbb{R}) \tag{2.4.7}$$

We can also define the finite probability distribution of $\boldsymbol{X}$. Let $(t_i)_{i=1}^n \subset K$. Then we define n-point finite probability distribution of $\boldsymbol{X}$ as follows

$$P_{t_1,\dots,t_n}(B) = \mu(\{\omega : \boldsymbol{X}(t_i,\omega) \in B, \forall i = 1\dots n\}) \quad \forall B \in \boldsymbol{\mathcal{B}}(\mathbb{R}) \tag{2.4.8}$$

We will have to work with random process that are parametrized by $\Omega \times \mathbb{R}^d$, $d = 3$. Thus we define random process $\boldsymbol{X}(\boldsymbol{x},\boldsymbol{y},\omega)$ as

$$\boldsymbol{X} : \Omega \times \mathbb{R}^d \times D \to \mathbb{R}. \tag{2.4.9}$$

We will impose certain properties on $\boldsymbol{X}$ in its second argument.

Dynamical system with d-dimensional time

We define the Dynamical system, [Jikov et al., 1994], with d-dimensional time (d-dimensional dynamical system) as a family of transformations $(T_{\boldsymbol{y}})_{\mathbb{R}^d}$, where for each $\boldsymbol{y} \in \mathbb{R}^d$, $T_{\boldsymbol{y}} : D \to D$ is a linear transformation on D, and it satisfies following properties

1. **Group property :** (a) $T_{\boldsymbol{0}}\omega = \omega$, $\forall \omega \in D$ is identity map.

   (b) $\forall \boldsymbol{x}, \boldsymbol{y} \in \mathbb{R}^d$ we have $T_{\boldsymbol{x}+\boldsymbol{y}} = T_{\boldsymbol{x}}T_{\boldsymbol{y}}$

2. **Measure preserving property :** For all $\boldsymbol{y} \in \mathbb{R}^d$ transformation $T_{\boldsymbol{y}}$ preserves measure μ. That is

$$\forall A \in \boldsymbol{\mathcal{D}}, (\forall \boldsymbol{y} \in \mathbb{R}^d) \Rightarrow \mu(T_{\boldsymbol{y}}A) = \mu(A) \tag{2.4.10}$$

3. **Measurability :** Let $\psi : D \to \mathbb{R}$ is random variable. Then random process $\boldsymbol{X} : \mathbb{R}^d \times D \to \mathbb{R}$ defined as $\boldsymbol{X}(\boldsymbol{y},\omega) = \psi(T_{\boldsymbol{y}}\omega)$ is measurable in $\mathbb{R}^d \times D$.

Invariant random variable and invariant set : Any random variable $\psi : D \to \mathbb{R}$ is said to be invariant if $\psi(T_{\boldsymbol{y}}\omega) = \psi(\omega), \forall \boldsymbol{y} \in \mathbb{R}^d$. Similarly, we say that a set $A \in \mathcal{D}$ is invariant if the random variable $\chi_A(\omega)$ (characteristic function of A) is invariant. In other words A is invariant if

$$\forall \boldsymbol{y} \in \mathbb{R}^d \Rightarrow T_{\boldsymbol{y}}A = A \tag{2.4.11}$$

Stationary random process

Let $\boldsymbol{X} : \mathbb{R}^d \times D \to \mathbb{R}$ is a random process. We say random process is stationary if there exist a random variable $\psi : D \to \mathbb{R}$ and also a dynamical system T, on D, indexed by space $\mathbb{R}^d$, such that

$$\boldsymbol{X}(\boldsymbol{y}, \omega) = \psi(T_{\boldsymbol{y}}\omega), \quad \forall \boldsymbol{y} \in \mathbb{R}^d, \text{ a.e.} \tag{2.4.12}$$

We can also define the stationary random process as follows: Random process is stationary if its finite probability distribution is invariant w.r.t. any translation $\boldsymbol{h} \in \mathbb{R}^d$. Here, we show that if we represent $\boldsymbol{X}$, which satisfies Equation 2.4.12, $\boldsymbol{X}$ is stationary.

Proposition 1. *For any $n \in \mathbb{N}$, and for any finite subset $(t_i)_{i=1}^n \subset \mathbb{R}^d$ and for any $\boldsymbol{h} \in \mathbb{R}^d$ we have*

$$P_{t_1,\dots,t_n}(B) = P_{t_1+\boldsymbol{h},\dots,t_n+\boldsymbol{h}}(B), \quad \forall B \in \mathcal{B}(\mathbb{R}) \tag{2.4.13}$$

Proof. We use the definition of P and proceed as below

$$P_{t_1+\boldsymbol{h},\dots,t_n+\boldsymbol{h}}(B) = \mu(\{\omega : \boldsymbol{X}(t_i + \boldsymbol{h}, \omega) \in B, \forall i = 1\dots n\})$$

$$= \mu(\{\omega : \psi(T_{t_i+\boldsymbol{h}}\omega) \in B, \forall i = 1\dots n\})$$

$$= \mu(\{\omega : \psi(T_{t_i}(T_{\boldsymbol{h}}\omega)) \in B, \forall i = 1\dots n\})$$

$$= \mu(\{T_{-\boldsymbol{h}}\omega : \psi(T_{t_i}(T_{\boldsymbol{h}}T_{-\boldsymbol{h}}\omega)) \in B, \forall i = 1\dots n\})$$

$$= \mu(\{T_{-\boldsymbol{h}}\omega : \psi(T_{t_i}(\omega)) \in B, \forall i = 1\dots n\})$$

$$= \mu(T_{-\boldsymbol{h}}\{\omega : \psi(T_{t_i}(\omega)) \in B, \forall i = 1\dots n\})$$

$$= \mu(\{\omega : \psi(T_{t_i}(\omega)) \in B, \forall i = 1\dots n\})$$

$$= P_{t_1,\dots,t_n}(B)$$

Where, in the fourth step, we just used the fact that

$$\{\omega : f(\omega) \in B\} = \{T_{\boldsymbol{x}}\omega : f(T_{\boldsymbol{x}}\omega) \in B\}, \forall \boldsymbol{x} \in \mathbb{R}^d$$

In the second last step, we used the fact that $\mu(T_{\boldsymbol{a}}M) = \mu(M)$, i.e. measure preserving property of dynamical system. $\qquad\square$

Also, for any $\boldsymbol{h}, \boldsymbol{y} \in \mathbb{R}^d$, we have

$$\int_D \boldsymbol{X}(\boldsymbol{y}, \omega) d\mu(\omega) = \int_D \boldsymbol{X}(\boldsymbol{y} + \boldsymbol{h}, \omega) d\mu(\omega) = \int_D \psi(\omega) d\mu(\omega) = \mathbb{E}[\psi] \qquad (2.4.14)$$

where ψ is related to $\boldsymbol{X}$ from Equation 2.4.12.

Stationary in second argument: Two parameters random process

Let $\boldsymbol{X} : \Omega \times \mathbb{R}^d \times D \to \mathbb{R}$ is a random process. We say that $\boldsymbol{X}$ is stationary in second argument if there exist another random process $\psi : \Omega \times D \to \mathbb{R}$, and dynamical system T, such that

$$\boldsymbol{X}(\boldsymbol{x}, \boldsymbol{y}, \omega) = \psi(\boldsymbol{x}, T_{\boldsymbol{y}}\omega), \quad \forall \boldsymbol{x} \in \Omega, \ \forall \boldsymbol{y} \in \mathbb{R}^d, \text{ a.e.} \qquad (2.4.15)$$

This implies $\forall \boldsymbol{x} \in \Omega$ and $\forall \boldsymbol{y}, \boldsymbol{h} \in \mathbb{R}^d$

$$\int_D \boldsymbol{X}(\boldsymbol{x}, \boldsymbol{y} + \boldsymbol{h}, \omega) d\mu(\omega) = \int_D \boldsymbol{X}(\boldsymbol{x}, \boldsymbol{y}, \omega) d\mu(\omega) = \mathbb{E}[\psi(\boldsymbol{x}, \cdot)] \qquad (2.4.16)$$

Ergodicity

Dynamical system $(T_{\boldsymbol{y}})_{\mathbb{R}^d}$ is ergodic if every invariant random variable is constant almost everywhere in D. That is, if T is Ergodic, then

$$\text{if } (\forall \boldsymbol{y} \in \mathbb{R}^d) \, \psi(T_{\boldsymbol{y}}\omega) = \psi(\omega) \Rightarrow \psi(\omega) = c \text{ a.e.} \tag{2.4.17}$$

In this case, we can also say that measure μ is ergodic w.r.t. T. One important implication of above definition is that: if set $A \in \mathcal{D}$ is invariant and if T is Ergodic then we have

$$\mu(A) = 0 \text{ or } 1 \tag{2.4.18}$$

Mean value of function Let f is a locally integrable function in $\mathbb{R}^d$, i.e. $f \in L^1_{loc}(\mathbb{R}^d)$. We define the mean value $M[f]$ of f as

$$\lim_{\epsilon \to 0} \int_K f(\boldsymbol{x}/\epsilon) d\boldsymbol{x} = |K| \, M[f] \tag{2.4.19}$$

for any Lebesgue measurable and bounded set $K \in \mathcal{B}(\mathbb{R}^d)$. Here $|K|$ is a Lebesgue measure of K. Another way to write the definition of mean value of a function is as follows

$$\lim_{N \to \infty} \frac{1}{N^d \, |K|} \int_{K_N} f(\boldsymbol{x}) d\boldsymbol{x} = M[f], \quad |K| \neq 0 \tag{2.4.20}$$

where $K_N = \{\boldsymbol{x} : \boldsymbol{x}/N \in K\}$.

Remark : For fixed $\omega \in D$, we call $f(T_{\boldsymbol{y}}\omega)$ a realization of w and it is a function of $\boldsymbol{y} \in \mathbb{R}^d$. For all $f \in L^p(D), p \geq 1$, almost all realization $f(T_{\boldsymbol{y}}\omega)$, as a function of $\boldsymbol{y} \in \mathbb{R}^d$, are in space $L^p_{loc}(\mathbb{R}^d)$. Similarly, the convergence of f in $L^p(D)$ implies the convergence of almost all realization $f(T_{\boldsymbol{y}}\omega)$ in $L^p_{loc}(\mathbb{R}^d)$ (upto subsequence).

We now state the main result for the random ergodic functions that we will be using in our work.

Theorem 2. *Birkhoff ergodic theorem* *Let $f \in L^p(D)$, $p \geq 1$. Then for almost all $w \in D$ the realization $f(T_{\boldsymbol{x}}\omega)$, as a function of $\boldsymbol{x} \in \mathbb{R}^d$, has mean value $M[f(T_{\boldsymbol{x}}\omega)]$.*

31

Further, this mean value $M[f(T(\boldsymbol{x})\omega)]$, as a function of ω, is invariant and also it satisfies following relation

$$\mathbb{E}[f(\omega)] = \int_D f(\omega)d\mu(\omega) = \int_D M[f(T_{\boldsymbol{x}}\omega)]d\mu(\omega) \qquad (2.4.21)$$

If T is ergodic, then we have

$$M[f(T_{\boldsymbol{x}}\omega)] = \mathbb{E}[f(\omega)] \quad \text{for almost all } \omega \in D \qquad (2.4.22)$$

For proof, we refer the reader to [Jikov et al., 1994].

Ergodicity theorem for the two parameters random process

In much of our work, we deal with random process of type $\boldsymbol{X} : \Omega \times \mathbb{R}^d \times D \to \mathbb{R}$.

Mean value of function: Let $f : \Omega \times \mathbb{R}^d \to \mathbb{R}$ is in $L^p[\Omega, L^1_{loc}(\mathbb{R}^d)]$. We define the mean value $M_2[f(\boldsymbol{x}, \cdot)]$ of f with respec to the second argument as follows

$$M_2[f(\boldsymbol{x}, \cdot)] := \lim_{N \to \infty} \frac{1}{N^d |K|} \int_{K_N} f(\boldsymbol{x}, \boldsymbol{y})d\boldsymbol{y}, \quad \text{a.e. } \boldsymbol{x} \qquad (2.4.23)$$

where $K \subset \mathbb{R}^d$, with $|K| \neq 0$, is bounded and Lebesgue measurable. Note that $M_2[f(\boldsymbol{x}, \cdot)]$ is a function of $\boldsymbol{x}$. We will assume that this is well defined and measurable function.

We assume $p, q, \alpha \geq 1$. Let a random process $\psi : \Omega \times D \to \mathbb{R}$ is L^p integrable in first argument and is L^α integrable in second argument. We denote the space of this random process as $L^p[\Omega, L^\alpha(D)]$. We now state the theorem

Theorem 3. *Let $\psi \in L^p[\Omega, L^\alpha(D)]$, $p, \alpha \geq 1$. Then for almost all $\omega \in D$, and for almost all $\boldsymbol{x} \in \Omega$, the realization $\psi(\boldsymbol{x}, T_{\boldsymbol{y}}\omega)$, as a function of $\boldsymbol{x} \in \Omega$ and $\boldsymbol{y} \in \mathbb{R}^d$, has a mean value $M_2[\psi(\boldsymbol{x}, T.\omega)]$ (see definition). Further, this mean value $M_2[\psi(\boldsymbol{x}, T.w)]$, as function of $\boldsymbol{x} \in \Omega$ and $w \in D$ (or as a random process in $\Omega \times D$), is invariant and satisfies following relation*

$$\mathbb{E}[\psi(\boldsymbol{x}, \cdot)] = \int_D \psi(\boldsymbol{x}, \omega)d\mu(\omega) = \int_D M_2[\psi(\boldsymbol{x}, T_{\boldsymbol{y}}\omega)]d\mu(\omega) \qquad \forall \boldsymbol{y} \qquad (2.4.24)$$

If T is ergodic, then we have

$$M_2[\psi(\boldsymbol{x}, T_{\boldsymbol{y}}\omega)] = \mathbb{E}[\psi(\boldsymbol{x}, \cdot)] \quad a.e. \ \boldsymbol{x} \ a.e. \ \omega \tag{2.4.25}$$

Remark: We write the following remark presented in [Jikov et al., 1994]

"As a result of simple operations with stationary random process, such as differentiation in $\boldsymbol{y}$, or convolution with a suitable Kernel, we again obtain stationary random field."

2.4.2 Final expression of energy

We first state our result.

Theorem 4. *Let $(D, \boldsymbol{\mathcal{D}}, \mu)$ be probability space with measure μ. Let $\rho : \Omega \times \mathbb{R}^3 \times D \to \mathbb{R}$ be the random charge density field. Let T be the ergodic dynamical system.*

We assume ρ to be ergodic and stationary. Therefore, assume that there exists $\bar{\rho} : \Omega \times D \to \mathbb{R}$ such that

$$\rho(\boldsymbol{x}, \boldsymbol{z}, \omega) = \bar{\rho}(\boldsymbol{x}, T_{\boldsymbol{z}}w) \qquad \forall \boldsymbol{x} \in \Omega, \boldsymbol{z} \in \mathbb{R}^3, \omega \in D$$

We define scaled charge density field ρ_l as

$$\rho_l(\boldsymbol{x}, \boldsymbol{y}, \omega) = \frac{\rho(\boldsymbol{x}, \boldsymbol{y}/l, \omega)}{l} = \frac{\bar{\rho}(\boldsymbol{x}, T_{\boldsymbol{y}/l}\omega)}{l}$$

We assume that the charge density field satisfies the condition of a charge neutrality. The charge neutrality condition is as follows

$$\mathbb{E}[\bar{\rho}(\boldsymbol{x}, \cdot)] = 0 \qquad \forall \boldsymbol{x} \in \Omega \tag{2.4.26}$$

Note that, using Birkhoff theorem, following holds for all $\boldsymbol{x} \in \Omega$, ω a.e.,

$$\lim_{r \to \infty} \frac{c}{|B_r(\boldsymbol{x})|} \int_{\boldsymbol{z} \in B_r(\boldsymbol{x})} \rho(\boldsymbol{x}, \boldsymbol{z}, \omega) dV_{\boldsymbol{z}} = \mathbb{E}[\bar{\rho}(\boldsymbol{x}, \cdot)] \tag{2.4.27}$$

where $c = 1/|B_1(\boldsymbol{0})|$, inverse of the volume of sphere of radius 1.

Then, electrostatics energy, in the limit is given by

$$E = E_{local} + E_{nonlocal} \tag{2.4.28}$$

$$E_{local} = \mathbb{E}\left[\int_{\boldsymbol{x}\in\Omega}\left(\int_{\mathbb{R}^3}\frac{\rho(\boldsymbol{x},\boldsymbol{0},\cdot)\rho(\boldsymbol{x},\boldsymbol{z}',\cdot)}{|\boldsymbol{0}-\boldsymbol{z}'|}dV_{\boldsymbol{z}'}\right)dV_{\boldsymbol{x}}\right] \tag{2.4.29}$$

$$E_{nonlocal} = \int_{\substack{\boldsymbol{x},\boldsymbol{x}'\in\Omega,\\\boldsymbol{x}\neq\boldsymbol{x}'}}\mathbb{K}(\boldsymbol{x}-\boldsymbol{x}):\hat{\boldsymbol{p}}(\boldsymbol{x})\otimes\hat{\boldsymbol{p}}(\boldsymbol{x}')dV_{\boldsymbol{x}}d_{\boldsymbol{x}'} \tag{2.4.30}$$

where $\hat{\boldsymbol{p}}(\boldsymbol{x})$ is the dipole moment at $\boldsymbol{x}$ and is independent of ω.

$$\hat{\boldsymbol{p}}(\boldsymbol{x}) = \boldsymbol{p}(\boldsymbol{x},w) = \lim_{r\to\infty}\frac{1}{|B_r(\boldsymbol{x})|}\int_{\boldsymbol{z}\in B_r(\boldsymbol{x})}\rho(\boldsymbol{x},\boldsymbol{z},\omega)\boldsymbol{z}dV_{\boldsymbol{z}}$$

Proof of this theorem is in next two sections. We will first construct the random charge density field, and then analyze the total energy in two parts, namely local and nonlocal part.

2.4.3 Charge density field

Let $B_\epsilon(\boldsymbol{x}) \subset \mathbb{R}^3$ be the sphere of radius ϵ, at material point $\boldsymbol{x} \in \Omega$.

Let $\rho : \Omega \times \mathbb{R}^3 \times D \to \mathbb{R}$ be a random process. We assume ρ to be stationary and ergodic. Therefore, we assume that there exists a ergodic dynamical system $T_{\boldsymbol{y}}$ for $\boldsymbol{y} \in \mathbb{R}^3$ and also another random process $\bar{\rho} : \Omega \times D \to \mathbb{R}$, such that ρ has following representation

$$\rho(\boldsymbol{x},\boldsymbol{z},\omega) = \bar{\rho}(\boldsymbol{x},T_{\boldsymbol{z}}\omega) \quad \forall\boldsymbol{x}\in\Omega, \forall\boldsymbol{z}\in\mathbb{R}^3, \forall\omega\in D$$

For materials with length scale $L >> \epsilon >> l$, we define scaled charge density field ρ_l, as we did in the case of nanostructures, as follows

$$\rho_l(\boldsymbol{x},\boldsymbol{y},\omega) = \rho(\boldsymbol{x},\frac{\boldsymbol{y}}{l},\omega) = \bar{\rho}(\boldsymbol{x},T_{\boldsymbol{y}/l}\omega) \tag{2.4.31}$$

2.4.4 Electrostatic energy

We now write the expression of electrostatic energy, as a realization of event $\omega \in D$, as follows

$$E(\omega) = \sum_{\substack{\boldsymbol{x} \in \Omega_\epsilon \\ \boldsymbol{x}' \in \Omega_\epsilon}} \int_{\substack{\boldsymbol{z} \in B_\epsilon(\boldsymbol{x}), \\ \boldsymbol{z}' \in B_\epsilon(\boldsymbol{x}')}} \frac{\rho_l(\boldsymbol{x}, \boldsymbol{z}, \omega) \rho_l(\boldsymbol{x}', \boldsymbol{z}', \omega)}{|\boldsymbol{x} + \boldsymbol{z} - \boldsymbol{x}' - \boldsymbol{z}'|} dV_{\boldsymbol{z}} dV_{\boldsymbol{z}'} \tag{2.4.32}$$

where $\Omega_\epsilon = \Omega \cap (\epsilon \mathbb{Z})^3$.

Local energy

Fix $\omega \in D$. In this section, we will compute the limit of Local energy. Local energy is given by

$$E_{local} = \sum_{\boldsymbol{x} \in \Omega_\epsilon} \int_{\boldsymbol{z}, \boldsymbol{z}' \in B_\epsilon(\boldsymbol{x})} \frac{\rho_l(\boldsymbol{x}, \boldsymbol{z}, \omega) \rho_l(\boldsymbol{x}, \boldsymbol{z}', \omega)}{|\boldsymbol{z} - \boldsymbol{z}'|} dV_{\boldsymbol{z}} dV_{\boldsymbol{z}'} \tag{2.4.33}$$

After rescaling the integral we get

$$\begin{aligned}
E_{local} &= \sum_{\boldsymbol{x} \in \Omega_\epsilon} \int_{\boldsymbol{z}, \boldsymbol{z}' \in B_{\epsilon/l}(\boldsymbol{x})} l^6 \frac{\rho(\boldsymbol{x}, \boldsymbol{z}, \omega) \rho(\boldsymbol{x}, \boldsymbol{z}', \omega)}{l \, |\boldsymbol{z} - \boldsymbol{z}'|} dV_{\boldsymbol{z}} dV_{\boldsymbol{z}'} \\
&= \sum_{\boldsymbol{x} \in \Omega_\epsilon} \int_{\boldsymbol{z}, \boldsymbol{z}' \in B_{\epsilon/l}(\boldsymbol{x})} l^5 \frac{\rho(\boldsymbol{x}, \boldsymbol{z}, \omega) \rho(\boldsymbol{x}, \boldsymbol{z}', \omega)}{|\boldsymbol{z} - \boldsymbol{z}'|} dV_{\boldsymbol{z}} dV_{\boldsymbol{z}'}
\end{aligned}$$

If ρ is ergodic and stationary than following function is also ergodic and stationary, see [Jikov et al., 1994],

$$h(\boldsymbol{x}, \boldsymbol{z}, \omega) := \int_{\mathbb{R}^3} \frac{\rho(\boldsymbol{x}, \boldsymbol{z}', \omega)}{|\boldsymbol{z} - \boldsymbol{z}'|} dV_{\boldsymbol{z}'} \tag{2.4.34}$$

Thus, there exist $\bar{h} : \Omega \times D \to \mathbb{R}$ such that

$$h(\boldsymbol{x}, \boldsymbol{z}, \omega) = \bar{h}(\boldsymbol{x}, T_{\boldsymbol{z}} \omega) \quad \forall \boldsymbol{x} \in \Omega, \ \forall \boldsymbol{z} \in \mathbb{R}^3, \ \forall \omega \in D \tag{2.4.35}$$

Also, note that by the Ergodicity theorem we have

$$\lim_{\epsilon/l \to \infty} \frac{1}{|B_{\epsilon/l}(\boldsymbol{x})|} \int_{\boldsymbol{z} \in B_{\epsilon/l}(\boldsymbol{x})} \mathcal{P}(\boldsymbol{x}, \boldsymbol{z}, \omega) \rho(\boldsymbol{x}, \boldsymbol{z}, \omega) dV_{\boldsymbol{z}}$$

$$= \frac{1}{|B_1(\boldsymbol{x})|} \mathbb{E}\left[\bar{\mathcal{P}}(\boldsymbol{x}, \cdot) \bar{\rho}(\boldsymbol{x}, \cdot)\right] \tag{2.4.36}$$

$$= \frac{1}{|B_1(\boldsymbol{x})|} \int_{\omega \in D} \bar{\mathcal{P}}(\boldsymbol{x}, \omega) \bar{\rho}(\boldsymbol{x}, \omega) d\mu(\omega) \tag{2.4.37}$$

Now, consider local energy

$$E_{local} = \sum_{\boldsymbol{x} \in \Omega_\epsilon} \frac{|B_{\epsilon/l}(\boldsymbol{x})|}{|B_{\epsilon/l}(\boldsymbol{x})|} l^5 \int_{\boldsymbol{z} \in B_{\epsilon/l}(\boldsymbol{x})} \rho(\boldsymbol{x}, \boldsymbol{z}, \omega) \left(\int_{\boldsymbol{z}' \in B_{\epsilon/l}(\boldsymbol{x})} \frac{\rho(\boldsymbol{x}, \boldsymbol{z}', \omega)}{|\boldsymbol{z} - \boldsymbol{z}'|} dV_{\boldsymbol{z}'} \right) dV_{\boldsymbol{z}}$$

$$= \frac{4\pi}{3} \sum_{\boldsymbol{x} \in \Omega_\epsilon} \epsilon^3 l^2 \left(\frac{1}{|B_{\epsilon/l}(\boldsymbol{x})|} \int_{\boldsymbol{z} \in B_{\epsilon/l}(\boldsymbol{x})} \rho(\boldsymbol{x}, \boldsymbol{z}, \omega) h(\boldsymbol{x}, \boldsymbol{z}, \omega) dV_{\boldsymbol{z}} \right) \quad (2.4.38)$$

$$- \sum_{\boldsymbol{x} \in \Omega_\epsilon} l^5 \int_{\boldsymbol{z} \in B_{\epsilon/l}(\boldsymbol{x})} \rho(\boldsymbol{x}, \boldsymbol{z}, \omega) \left(\int_{\boldsymbol{z}' \in \mathbb{R}^3 - B_{\epsilon/l}(\boldsymbol{x})} \frac{\rho(\boldsymbol{x}, \boldsymbol{z}, \omega)}{|\boldsymbol{z} - \boldsymbol{z}'|} dV_{\boldsymbol{z}'} \right) dV_{\boldsymbol{z}} \quad (2.4.39)$$

The second term will go to zero in the limit. We will use Equation 2.4.36 for term inside the bracket.

Scaling on the charge density field As we argued the in the previous section of nanostructures, we make a similar argument here. We do not want local energy to go to zero or infinity trivially in the limit. In Equation 2.4.39, we find that the energy has l^4, and, hence, energy will go to zero in the limit. Therefore, we revisit the Equation 2.4.31, where we had defined the scaled charge density field ρ_l. Correct scaled charge density field is as follows

$$\rho_l(\boldsymbol{x}, \boldsymbol{y}, \omega) = \frac{\rho(\boldsymbol{x}, \frac{\boldsymbol{y}}{l}, \omega)}{l} = \frac{\bar{\rho}(\boldsymbol{x}, T_{\boldsymbol{y}/l}\omega)}{l} \quad (2.4.40)$$

We substitute above scaling on ρ, and also use Equation 2.4.36, to finally get

$$E_{local} = \int_{\boldsymbol{x} \in \Omega} \left(\mathbb{E}[\bar{\rho}(\boldsymbol{x}, \cdot) \bar{h}(\boldsymbol{x}, \cdot)] \right) dV_{\boldsymbol{x}} \quad (2.4.41)$$

We can further write the expression of E_{local} as follows:

Assuming $T_{\boldsymbol{0}}$ is the identity element of group, i.e. $T_{\boldsymbol{0}}\omega = \omega, \forall \omega \in D$. Then

$$\bar{\rho}(\boldsymbol{x}, \omega) \bar{h}(\boldsymbol{x}, \omega) = \bar{\rho}(\boldsymbol{x}, T_{\boldsymbol{0}}\omega) \bar{h}(\boldsymbol{x}, T_{\boldsymbol{0}}\omega)$$
$$= \rho(\boldsymbol{x}, \boldsymbol{0}, \omega) \int_{\mathbb{R}^3} \frac{\rho(\boldsymbol{x}, \boldsymbol{z}', \omega)}{|\boldsymbol{z}'|} dV_{\boldsymbol{z}'}$$

substituting this in local energy expression

36

$$E_{local} = \int_{\boldsymbol{x} \in \Omega} \left[\int_D \left\{ \rho(\boldsymbol{x}, \boldsymbol{0}, \omega) \int_{\mathbb{R}^3} \frac{\rho(\boldsymbol{x}, \boldsymbol{z}', \omega)}{|\boldsymbol{z}'|} dV_{\boldsymbol{z}'} \right\} d\mu(\omega) \right] dV_{\boldsymbol{x}}$$

$$= \int_D \left\{ \int_{\boldsymbol{x} \in \Omega} \left[\int_{\mathbb{R}^3} \frac{\mathcal{P}(\boldsymbol{x}, \boldsymbol{0}, \omega) \mathcal{P}(\boldsymbol{x}, \boldsymbol{z}', \omega)}{|\boldsymbol{0} - \boldsymbol{z}'|} dV_{\boldsymbol{z}'} \right] dV_{\boldsymbol{x}} \right\} d\mu(\omega)$$

Finally, we can write local energy, in limit, as follows

$$E_{local} = \mathbb{E} \left[\int_{\boldsymbol{x} \in \Omega} \left(\int_{\mathbb{R}^3} \frac{\rho(\boldsymbol{x}, \boldsymbol{0}, \cdot) \rho(\boldsymbol{x}, \boldsymbol{z}', \cdot)}{|\boldsymbol{0} - \boldsymbol{z}'|} dV_{\boldsymbol{z}'} \right) dV_{\boldsymbol{x}} \right] \tag{2.4.42}$$

$$= c \mathbb{E} \left[\text{realization of local energy corresponding to event } \omega \right] := c \mathbb{E}[e_{local}(\omega)] \tag{2.4.43}$$

Remark: We make following two remarks on calculations so far:

1 Energy $e_{local}(w)$, term inside square bracket in Equation 2.4.42, and E_{local}, for the periodic ρ, are similar. In the periodic case, local energy was due to the interactions of the charge density field within one unit cell, and the charge density field within the material point. In the case of random stationary charge density field, the local energy is due to the interactions of the charge density field, at some point $\boldsymbol{y}$ (we choose $\boldsymbol{y} = \boldsymbol{0}$), and the charge density field within the material point.

2 The choice of $\boldsymbol{0}$ in $\int_{\mathbb{R}^3} \frac{\mathcal{P}(\boldsymbol{x}, \boldsymbol{0}, w) \mathcal{P}(\boldsymbol{x}, \boldsymbol{z}', w)}{|\boldsymbol{0} - \boldsymbol{z}'|} dV_{\boldsymbol{z}'}$ was arbitrary. We can choose any other point $\boldsymbol{y} \in \mathbb{R}^3$ and evaluate E_{local}. That is if

$$e^{\boldsymbol{y}}_{local}(w) = \int_{\boldsymbol{x} \in \Omega} \left(\int_{\mathbb{R}^3} \frac{\mathcal{P}(\boldsymbol{x}, \boldsymbol{y}, w) \mathcal{P}(\boldsymbol{x}, \boldsymbol{z}', w)}{|\boldsymbol{y} - \boldsymbol{z}'|} dV_{\boldsymbol{z}'} \right) dV_{\boldsymbol{x}} \tag{2.4.44}$$

is calculated by choosing any $\boldsymbol{y} \in \mathbb{R}^3$ then

$$E_{local} = \mathbb{E}[e^{\boldsymbol{y}}_{local}(w)] = \mathbb{E}[e^{\boldsymbol{0}}_{local}(w)] = \mathbb{E}[e_{local}(w)] \tag{2.4.45}$$

This is again consistent with the periodic case. In periodic case the choice of unit cell U_0 was arbitrary, in the sense it is a unit cube, but the center can be any point of $\mathbb{Z}^3$.

Non-local energy

After rescaling the variable in the expression of non-local energy and using the modified definition of scaled charge density field, we get

$$E_{nonlocal} = \sum_{\substack{\boldsymbol{x},\boldsymbol{x}'\in\Omega_\epsilon,\\ \boldsymbol{x}\neq\boldsymbol{x}'}} l^4 \int_{\substack{\boldsymbol{z}\in B_{\epsilon/l}(\boldsymbol{x}),\\ \boldsymbol{z}'\in B_{\epsilon/l}(\boldsymbol{x}')}} \frac{\rho(\boldsymbol{x},\boldsymbol{z},\omega)\rho(\boldsymbol{x}',\boldsymbol{z}',\omega)}{|\boldsymbol{x}+l\boldsymbol{z}-\boldsymbol{x}'-l\boldsymbol{z}'|}dV_{\boldsymbol{z}}dV_{\boldsymbol{z}'} \tag{2.4.46}$$

After multiplying and dividing by $\left|B_{\epsilon/l}(\boldsymbol{x})\right|\left|B_{\epsilon/l}(\boldsymbol{x}')\right|$, we get

$$E_{nonlocal} = \left(\frac{4\pi}{3}\right)^2 \sum_{\substack{\boldsymbol{x},\boldsymbol{x}'\in\Omega_\epsilon,\\ \boldsymbol{x}\neq\boldsymbol{x}'}} \epsilon^6 \left(\frac{1}{l^2}\frac{1}{\left|B_{\epsilon/l}(\boldsymbol{x})\right|}\frac{1}{\left|B_{\epsilon/l}(\boldsymbol{x}')\right|}\right.$$

$$\left.\int_{\substack{\boldsymbol{z}\in B_{\epsilon/l}(\boldsymbol{x}),\\ \boldsymbol{z}'\in B_{\epsilon/l}(\boldsymbol{x}')}} \frac{\rho(\boldsymbol{x},\boldsymbol{z},\omega)\rho(\boldsymbol{x}',\boldsymbol{z}',\omega)}{|\boldsymbol{x}+l\boldsymbol{z}-\boldsymbol{x}'-l\boldsymbol{z}'|}dV_{\boldsymbol{z}}dV_{\boldsymbol{z}'}\right) \tag{2.4.47}$$

We focus on the term inside the bracket. It has $\frac{1}{l^2}$. Since we do not want energy to go to zero or infinity trivially, we do Taylor series expansion as follows, and look for the condition.

$$\frac{1}{|\boldsymbol{x}+l\boldsymbol{z}-\boldsymbol{x}'-l\boldsymbol{z}'|} = \frac{1}{|\boldsymbol{x}-\boldsymbol{x}'|} + \left[\frac{\partial}{\partial\boldsymbol{y}}\frac{1}{|\boldsymbol{y}|}\right]_{\boldsymbol{y}=\boldsymbol{x}-\boldsymbol{x}'} l\cdot(\boldsymbol{z}-\boldsymbol{z}')$$

$$+ \left[\frac{\partial^2}{\partial\boldsymbol{y}^2}\frac{1}{|\boldsymbol{y}|}\right]_{\boldsymbol{y}=\boldsymbol{x}-\boldsymbol{x}'} l^2 : (\boldsymbol{z}-\boldsymbol{z}')\otimes(\boldsymbol{z}-\boldsymbol{z}') + O(l^3) \tag{2.4.48}$$

Where, we identify the second order term $\frac{\partial^2}{\partial\boldsymbol{x}^2}\frac{1}{|\boldsymbol{x}|}$ as <u>dipole field kernel</u> $\boldsymbol{K}(\boldsymbol{x})$. It is defined as below:

$$\boldsymbol{K}(\boldsymbol{x}) := -\frac{1}{4\pi\left|\boldsymbol{x}\right|^3}\left\{\boldsymbol{I}-3\frac{\boldsymbol{x}}{|\boldsymbol{x}|}\otimes\frac{\boldsymbol{x}}{|\boldsymbol{x}|}\right\}, \quad \boldsymbol{x}\in\mathbb{R}^3 \tag{2.4.49}$$

We substitute Equation 2.4.48 into the expression of non-local energy. Analyzing the first term, after substitution,

$$\sum_{\substack{\boldsymbol{x},\boldsymbol{x}'\in\Omega_\epsilon, \\ \boldsymbol{x}\neq\boldsymbol{x}'}} \epsilon^6 \left(\frac{1}{l^2} \frac{1}{|\boldsymbol{x}-\boldsymbol{x}'|} \left\{ \frac{1}{|B_{\epsilon/l}(\boldsymbol{x})|} \int_{\boldsymbol{z}\in B_{\epsilon/l}(\boldsymbol{x})} \rho(\boldsymbol{x},\boldsymbol{z},\omega)dV_{\boldsymbol{z}} \right\} \right.$$

$$\left. \left\{ \frac{1}{|B_{\epsilon/l}(\boldsymbol{x}')|} \int_{\boldsymbol{z}'\in B_{\epsilon/l}(\boldsymbol{x}')} \rho(\boldsymbol{x}',\boldsymbol{z}',\omega)dV_{\boldsymbol{z}'} \right\} \right)$$

This term will go to infinity in a continuum limit. However, if we have following condition

$$\lim_{\epsilon/l\to\infty} \frac{1}{|B_{\epsilon/l}(\boldsymbol{x})|} \int_{\boldsymbol{z}\in B_{\epsilon/l}(\boldsymbol{x})} \rho(\boldsymbol{x},\boldsymbol{z},\omega)dV_{\boldsymbol{z}} = 0 \quad \forall \boldsymbol{x}\in\Omega \tag{2.4.50}$$

then, the term containing l^{-2} (among other terms too) will go to zero. We now state this condition precisely using the Ergodic Theorem.

Charge neutrality condition for random and ergodic charge density field

$$\mathbb{E}[\bar{\rho}(\boldsymbol{x},\cdot)] = \int_D \bar{\rho}(\boldsymbol{x},\omega)d\mu(\omega) = 0 \quad \forall \boldsymbol{x}\in\Omega \tag{2.4.51}$$

Using the Ergodic Theorem, we have

$$\lim_{r\to\infty} \frac{1}{|B_r(\boldsymbol{x})|} \int_{\boldsymbol{z}\in B_r(\boldsymbol{x})} \rho(\boldsymbol{x},\boldsymbol{z},\omega)dV_{\boldsymbol{z}} = |B_1(\boldsymbol{0})|\,\mathbb{E}[\bar{\rho}(\boldsymbol{x},\cdot)] \tag{2.4.52}$$

Given that ρ satisfies the charge neutrality condition Equation 2.4.50, we find that contribution from the zeroth order term, and the first order term, in Taylor expansion Equation 2.4.48, is zero. And, contribution from the second order term, with $\boldsymbol{z}\otimes\boldsymbol{z}$ and $\boldsymbol{z}'\otimes\boldsymbol{z}'$ will be zero. Contribution from the third order term will also be zero. Therefore, the non-local energy, in the continuum limit, is given by

$$E_{nonlocal} = \sum_{\substack{\boldsymbol{x},\boldsymbol{x}'\in\Omega_\epsilon, \\ \boldsymbol{x}\neq\boldsymbol{x}'}} \epsilon^6 \mathbb{K}(\boldsymbol{x}-\boldsymbol{x}') : \left\{ \frac{1}{|B_{\epsilon/l}(\boldsymbol{x})|} \int_{\boldsymbol{z}\in B_{\epsilon/l}(\boldsymbol{x})} \rho(\boldsymbol{x},\boldsymbol{z},\omega)\boldsymbol{z}dV_{\boldsymbol{z}} \right\}$$

$$\otimes \left\{ \frac{1}{|B_{\epsilon/l}(\boldsymbol{x}')|} \int_{\boldsymbol{z}'\in B_{\epsilon/l}(\boldsymbol{x}')} \rho(\boldsymbol{x}',\boldsymbol{z}',\omega)\boldsymbol{z}'dV_{\boldsymbol{z}'} \right\}$$

$$= \int_{\substack{\boldsymbol{x},\boldsymbol{x}'\in\Omega, \\ \boldsymbol{x}\neq\boldsymbol{x}'}} \mathbb{K}(\boldsymbol{x}-\boldsymbol{x}') : \boldsymbol{p}(\boldsymbol{x},\omega)\otimes\boldsymbol{p}(\boldsymbol{x}',\omega)dV_{\boldsymbol{x}}d_{\boldsymbol{x}'}$$

Where, $\boldsymbol{p}(\boldsymbol{x}, \omega)$ is a polarization within the material point. It is defined as

$$\boldsymbol{p}(\boldsymbol{x}, \omega) = \lim_{r \to \infty} \frac{c}{|B_r(\boldsymbol{x})|} \int_{\boldsymbol{z} \in B_r(\boldsymbol{x})} \rho(\boldsymbol{x}, \boldsymbol{z}, \omega) \boldsymbol{z} dV_{\boldsymbol{z}} \tag{2.4.53}$$

Where, $c = 1/|B_1(\boldsymbol{0})|$ is inverse of volume of sphere of radius 1.

The analysis of non-local energy is not complete, as we see that integrand in non-local energy is the function of $\omega \in D$. Therefore, the continuum limit of non-local energy appears to be the function of ω in probability space. This is in contrast to local energy, where the final expression of the limit of energy, was mean of energy.

Proposition 5. *Dipole moment $\boldsymbol{p}(\boldsymbol{x}, \omega)$, as defined in Equation 2.4.53, is invariant, i.e. for all $\boldsymbol{a} \in \mathbb{R}^3$, we have*

$$\boldsymbol{p}(\boldsymbol{x}, T_{\boldsymbol{a}}\omega) = \boldsymbol{p}(\boldsymbol{x}, \omega)$$

Further, since T is the ergodic dynamical system, $\boldsymbol{p}$ is independent of ω. Therefore, the integrand of non-local energy is independent of ω and hence non-local energy is independent of ω.

Proof. We use the definition of $\boldsymbol{p}$ to show invariance, using change of variable $\boldsymbol{y} = \boldsymbol{z} - \boldsymbol{a}$, as follows

$$\begin{aligned}
\boldsymbol{p}(\boldsymbol{x}, \omega) &= \lim_{r \to \infty} \frac{c}{|B_r(\boldsymbol{x})|} \int_{\boldsymbol{z} \in B_r(\boldsymbol{x})} \rho(\boldsymbol{x}, \boldsymbol{z}, \omega) \boldsymbol{z} dV_{\boldsymbol{z}} \\
&= \lim_{r \to \infty} \frac{c}{|B_r(\boldsymbol{x})|} \int_{\boldsymbol{y} \in B_r(\boldsymbol{x}) - \boldsymbol{a}} \rho(\boldsymbol{x}, \boldsymbol{y} + \boldsymbol{a}, \omega)(\boldsymbol{y} + \boldsymbol{a}) dV_{\boldsymbol{y}} \\
&= \lim_{r \to \infty} \frac{c}{|B_r(\boldsymbol{x})|} \int_{\boldsymbol{y} \in B_r(\boldsymbol{x}) - \boldsymbol{a}} \bar{\rho}(\boldsymbol{x}, T_{\boldsymbol{y}+\boldsymbol{a}}\omega) \boldsymbol{y} dV_{\boldsymbol{y}} \\
&\quad + \left[\lim_{r \to \infty} \frac{c}{|B_r(\boldsymbol{x})|} \int_{\boldsymbol{y} \in B_r(\boldsymbol{x}) - \boldsymbol{a}} \bar{\rho}(\boldsymbol{x}, T_{\boldsymbol{y}+\boldsymbol{a}}\omega) dV_{\boldsymbol{y}} \right] \boldsymbol{a} \\
&= \lim_{r \to \infty} \frac{c}{|B_r(\boldsymbol{x})|} \int_{\boldsymbol{y} \in B_r(\boldsymbol{x}) - \boldsymbol{a}} \rho(\boldsymbol{x}, \boldsymbol{y}, T_{\boldsymbol{a}}\omega) \boldsymbol{y} dV_{\boldsymbol{y}} \\
&\quad + \left[\mathbb{E}[\bar{\rho}(\boldsymbol{x}, \cdot)] \right] \boldsymbol{a} \\
&= \boldsymbol{p}(\boldsymbol{x}, T_{\boldsymbol{a}}\omega) \tag{2.4.54}
\end{aligned}$$

Where, we have used the Ergodic theorem and the charge neutrality condition. We have also used following property of the Mean value of a function $\boldsymbol{f}$,

$$
\begin{aligned}
M[\boldsymbol{f}] &= \lim_{r\to\infty} \frac{c}{|B_r(\boldsymbol{x})|} \int_{\boldsymbol{y}\in B_r(\boldsymbol{x})} \boldsymbol{f}(\boldsymbol{y},\omega)dV_{\boldsymbol{y}} \\
&= \lim_{r\to\infty} \frac{c}{|B_r(\boldsymbol{x}+\boldsymbol{a})|} \int_{\boldsymbol{z}\in B_r(\boldsymbol{x})+\boldsymbol{a}} \boldsymbol{f}(\boldsymbol{x},\boldsymbol{z},\omega)\boldsymbol{z}dV_{\boldsymbol{z}} \quad\quad (2.4.55)
\end{aligned}
$$

So we have shown that $\boldsymbol{p}(\boldsymbol{x},\omega) = \boldsymbol{p}(\boldsymbol{x}, T_{\boldsymbol{a}}\omega)$ for all $\boldsymbol{a} \in \mathbb{R}^3$.

Since we assumed T to be the ergodic dynamical system, we have

$$
\boldsymbol{p}(\boldsymbol{x},\omega) = \hat{\boldsymbol{p}}(\boldsymbol{x}) \quad\quad \forall \omega \in D \quad\quad (2.4.56)
$$

Now, we substitute this in $E_{nonlocal}$, and use the Riemann definition of integral, to get

$$
E_{nonlocal} = \int_{\substack{\boldsymbol{x},\boldsymbol{x}'\in\Omega, \\ \boldsymbol{x}\neq\boldsymbol{x}'}} \mathbb{K}(\boldsymbol{x}-\boldsymbol{x}') : \hat{\boldsymbol{p}}(\boldsymbol{x})\otimes\hat{\boldsymbol{p}}(\boldsymbol{x}')dV_{\boldsymbol{x}}d_{\boldsymbol{x}'} \quad\quad (2.4.57)
$$

$\square$

2.4.5   Discussion

The final expression of energy is similar to the case of periodic charge density field. In fact, in the next subsection, we will show that the periodic and the quasi-periodic charge density field are special case of our random charge density field.

We see that in the continuum limit, the local energy is an expectation of the local energy as a random function. This suggests that in designing the numerical method for material with random charge density field, we need to compute the phase average of local energy. As expected, non-local energy is independent of ω. The reason for this is, as we tend to continuum limit, the size of the material point ϵ is much greater than size of atomic spacing. Since non-local energy is due to one material point interacting with another material point, the distance between interacting charges, in non-local interactions, are of the order of ϵ. Compare this to the case of local energy, where the energy is due to the interaction of charges from a material point. There, the distance between charges is of

the order of atomic spacing. Therefore, the atomic fluctuations, or rather randomness of charge density field, can be seen in local energy. Whereas, in the case of non-local energy, due to the huge separation between interacting charges, all it matters was the average behavior of charge density field.

Periodic and quasi-periodic media In this paragraph, we show that periodic and quasi-periodic charge density field are special case of random charge density field.

Periodic case

Define probability space, D, as $D = [0,1]^3$, and define $T_{\boldsymbol{x}}$ as follows

$$T_{\boldsymbol{u}}(\boldsymbol{y}) = \boldsymbol{u} + \boldsymbol{y} \qquad \boldsymbol{y} \in D, \boldsymbol{y} \in \mathbb{R}^3$$

Then,

$$\mathcal{P}(\boldsymbol{x}, \boldsymbol{u}, \boldsymbol{y}) = \bar{\mathcal{P}}(\boldsymbol{x}, T_{\boldsymbol{u}}\boldsymbol{y}) = \bar{\mathcal{P}}(\boldsymbol{x}, \boldsymbol{u} + \boldsymbol{y})$$

If we substitute this definition of D, and $T_{\boldsymbol{x}}$, we recover the continuum limit for periodic charge density field.

Quasi-periodic case

We can also find the continuum limit of Electrostatic energy, when ρ is quasi-periodic. Define $D = [0,1]^3$. Let $\boldsymbol{M}$ is 3×3 matrix. Then, define $T_{\boldsymbol{u}}$ as follows

$$T_{\boldsymbol{u}}(\boldsymbol{y}) = \boldsymbol{M}\boldsymbol{u} + \boldsymbol{y} \qquad \boldsymbol{y} \in D, \boldsymbol{u} \in \mathbb{R}^3$$

2.5 Continuum limit of the energy due to the system of dipole moments

In this section, we present our continuum limit calculation of energy, for the system of dipole moments. The main idea is to attach dipole moments at equal spacing, on the straight line, and helix, and then compute the limit of energy as the spacing between the

dipoles go to zero. This is an extension of work in [James and Müller, 1994] to nanostructures.

As shown in the thesis of [Xiao, 2004], computing continuum limit of electrostatics energy using the charge density field is equivalent to computing the continuum limit using the system of dipole moments. Therefore, the continuum limit calculation we did in section 2.3 is similar to the calculation presented in this section. The proof of the theorem, for the case of the 1-D system of dipole moments, is interesting and hence, we want to present it in the thesis.

We describe Helix using second order rotational tensor. If we set the tensor to identity, we will have the straight line. This is related to how we described the objective nanorod in section 2.3.

2.5.1 Dipole system along the helix

Let $s \in \mathbb{R}$ be a parameter to define point $\boldsymbol{x} \in \mathbb{R}^3$ on helix. $\boldsymbol{x}$ on helix is given by

$$\boldsymbol{x}(s) := \boldsymbol{Q}^s \boldsymbol{x}_0 + s\boldsymbol{c}$$

Here, $\boldsymbol{Q}$ is orthogonal rotation tensor, $\boldsymbol{x}_0$ is a vector in plane perpendicular to vector $\boldsymbol{c}$. $\boldsymbol{c}$ is the axis of helix. To simplify the calculation, we take $\boldsymbol{x}_0 = \boldsymbol{e}_1$, $\boldsymbol{c} = \boldsymbol{e}_3$, and hence

$$\boldsymbol{x}(s) = \boldsymbol{Q}^s \boldsymbol{e}_1 + s\boldsymbol{e}_3$$

Cross-section of the helix is a circle and for our case the radius of this circle is unity. Further, the axis is along $\boldsymbol{e}_3$ direction. See Figure 2.5.1 below for schematic view.

Straight line: If we set $\boldsymbol{Q} = \boldsymbol{I}$, we will have straight line. Therefore, the calculation we present for the helix also holds for the straight line.

Before we proceed with our calculation, we define some relevant quantities as follows

- $\mathcal{L}_\lambda := \lambda\mathbb{Z}$. $\mathcal{L}_\lambda$ This is discretization in parametric space.

- We define map $\hat{s}_\lambda : \mathbb{R} \to \mathcal{L}_\lambda$ as

$$\hat{s}_\lambda(y) = s, \quad \text{if } y \in [s, s + \lambda) \tag{2.5.1}$$

43

$$x(s) = Q^s e_1 + s e_3$$
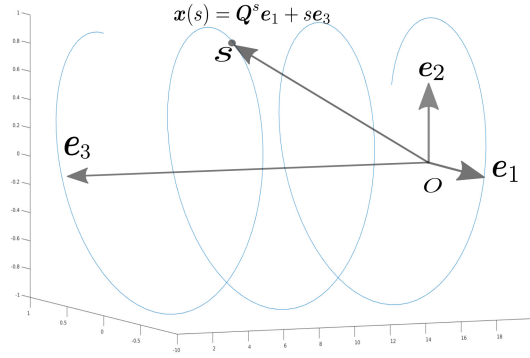
(a)
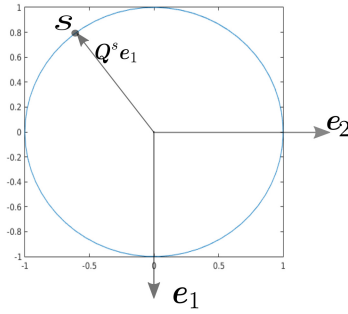
(b)

Figure 2.5.1: (a) Helix with axis in e_3 direction (b) cross-section of the helix

- $U_\lambda(s) = [s, s + \lambda)$.

- $d_\lambda : \mathcal{L}_\lambda \to \mathbb{R}^3$ is the system of dipole moments located at points given by parametric domain $\mathcal{L}_\lambda$.

- e_λ is magnetostatic energy.

- $f_\lambda : \mathbb{R} \to \mathbb{R}^3$ is background dipole field, function of parameter s.

2.5.2 Dipole moment and the background dipole field

Let $f_\lambda \in L^2\left(\mathbb{R}, \mathbb{R}^3\right)$, for $\lambda \in (0, 1]$, such that

$$f_\lambda \xrightarrow[\lambda \to 0]{} f_0 \quad \in L^2\left(\mathbb{R}, \mathbb{R}^3\right). \tag{2.5.2}$$

We define the system of dipole moments d_λ, using the background dipole filed f_λ, as follows

$$d_\lambda(x) := \int_{U_\lambda(x)} f_\lambda(s) ds \quad \forall x \in \mathcal{L}_\lambda \tag{2.5.3}$$

44

We define the dipole density $\tilde{\boldsymbol{d}}_\lambda : \mathbb{R} \to \mathbb{R}^3$, using piecewise constant extension, as follows

$$\tilde{\boldsymbol{d}}_\lambda(y) = \frac{\boldsymbol{d}_\lambda(x)}{\lambda} \qquad \forall y \in [x, x+\lambda), \forall x \in \mathcal{L}_\lambda$$

Convergence of the dipole field We have the following result on the convergence of the dipole field.

Let $\boldsymbol{f}_\lambda \in L^2(\mathbb{R}, \mathbb{R}^3)$, be sequence of vector field. If

$$\boldsymbol{f}_\lambda \xrightarrow[\lambda \to 0]{} \boldsymbol{f} \qquad \in L^2(\mathbb{R}, \mathbb{R}^3)$$

then, we have

$$\tilde{\boldsymbol{d}}_\lambda \xrightarrow[\lambda \to 0]{} \boldsymbol{f} \qquad \in L^2(\mathbb{R}, \mathbb{R}^3)$$

2.5.3 Energy

We define the energy of system of dipole moments $\boldsymbol{d}_\lambda$ as follows

$$e_\lambda := -\frac{1}{2}\lambda^2 \sum_{\substack{s,s' \in \mathcal{L}_\lambda, \\ s \neq s'}} \boldsymbol{d}_\lambda(s) \cdot \boldsymbol{K}(\boldsymbol{x}(s) - \boldsymbol{x}(s'))\boldsymbol{d}_\lambda(\boldsymbol{x}(s')) \tag{2.5.4}$$

$$= -\frac{1}{2}\lambda^2 \int_\mathbb{R} \int_\mathbb{R} \boldsymbol{f}_\lambda(s) \cdot \boldsymbol{K}_\lambda(s, s')\boldsymbol{f}_\lambda(s')ds ds'$$

$$= -\frac{1}{2} \int_\mathbb{R} \boldsymbol{f}_\lambda(s) \cdot (T_\lambda \boldsymbol{f}_\lambda)$$

$$= -\frac{1}{2}\langle \boldsymbol{f}_\lambda, T_\lambda \boldsymbol{f}_\lambda \rangle_{L^2(\mathbb{R}, \mathbb{R}^3)} \tag{2.5.5}$$

Where,

$$\boldsymbol{K}_\lambda(s, s') := \sum_{\substack{u,v \in \mathcal{L}_\lambda, \\ u \neq v}} \chi_{U_\lambda(u)}(s)\boldsymbol{K}(\boldsymbol{x}(u) - \boldsymbol{x}(v))\chi_{U_\lambda(v)}(s') \tag{2.5.6}$$

We define the map $T_\lambda : L^2(\mathbb{R}, \mathbb{R}^3) \to L^2(\mathbb{R}, \mathbb{R}^3)$ as

$$(T_\lambda \boldsymbol{f})(s) := \lambda^2 \int_\mathbb{R} \boldsymbol{K}_\lambda(s, s')\boldsymbol{f}(s')ds' \tag{2.5.7}$$

Scaling of K_λ

We will use this scaling to prove the next result on boundedness of map T_λ. For any given $a, b \in \mathcal{L}_\lambda$, we have

$$
\begin{aligned}
\boldsymbol{x}(\lambda a) - \boldsymbol{x}(\lambda b) &= \boldsymbol{Q}^{\lambda a}\boldsymbol{e}_1 + \lambda a \boldsymbol{e}_3 - \boldsymbol{Q}^{\lambda b}\boldsymbol{e}_1 + \lambda b \boldsymbol{e}_3 \\
&= \left(\lambda \boldsymbol{Q}^a \boldsymbol{e}_1 + \lambda a \boldsymbol{e}_3 + \boldsymbol{Q}^{\lambda a}\boldsymbol{e}_1 - \lambda \boldsymbol{Q}^a \boldsymbol{e}_1 \right) \\
&\quad - \left(\lambda \boldsymbol{Q}^b \boldsymbol{e}_1 + \lambda b \boldsymbol{e}_3 + \boldsymbol{Q}^{\lambda b}\boldsymbol{e}_1 - \lambda \boldsymbol{Q}^b \boldsymbol{e}_1 \right) \\
&= \lambda(\boldsymbol{x}(a) - \boldsymbol{x}(b)) + \lambda \boldsymbol{A}_\lambda(a, b)\boldsymbol{e}_1 \quad\quad\quad (2.5.8)
\end{aligned}
$$

Where, we have defined the second order tensor $\boldsymbol{A}_\lambda$, as a function of two parameters on $\mathbb{R}$, as follows

$$
\boldsymbol{A}_\lambda(a, b) := \frac{\boldsymbol{Q}^{\lambda a} - \boldsymbol{Q}^{\lambda b} - \lambda \boldsymbol{Q}^a + \lambda \boldsymbol{Q}^b}{\lambda} \quad\quad\quad (2.5.9)
$$

Note that, if $\boldsymbol{Q} = \boldsymbol{I}$ then $\boldsymbol{A}_\lambda(a, b) = \boldsymbol{0}$, for all $a, b \in \mathbb{R}$.

Now,

$$
\begin{aligned}
\boldsymbol{K}_\lambda(s, s') &= \sum_{\substack{u,v \in \mathcal{L}_\lambda, \\ u \neq v}} \chi_{U_\lambda(u)}(s) \boldsymbol{K}(\boldsymbol{x}(u) - \boldsymbol{x}(v)) \chi_{U_\lambda(v)}(s') \\
&= \sum_{\substack{u,v \in \mathcal{L}_1, \\ u \neq v}} \chi_{U_\lambda(\lambda u)}(s) \boldsymbol{K}(\boldsymbol{x}(\lambda u) - \boldsymbol{x}(\lambda v)) \chi_{U_\lambda(\lambda v)}(s') \\
&= \sum_{\substack{u,v \in \mathcal{L}_1, \\ u \neq v}} \chi_{U_1(u)}(s/\lambda) \boldsymbol{K}(\lambda\left(\boldsymbol{x}(u) - \boldsymbol{x}(v) + \boldsymbol{A}_\lambda(u, v)\boldsymbol{e}_1\right)) \chi_{U_1(v)}(s'/\lambda) \\
&= \frac{1}{\lambda^3} \sum_{\substack{u,v \in \mathcal{L}_1, \\ u \neq v}} \chi_{U_1(u)}(s/\lambda) \boldsymbol{K}(\boldsymbol{x}(u) - \boldsymbol{x}(v) + \boldsymbol{A}_\lambda(u, v)\boldsymbol{e}_1) \chi_{U_1(v)}(s'/\lambda) \quad (2.5.10)
\end{aligned}
$$

$$(2.5.11)$$

Where, we have used the fact that $\chi_{U_\lambda(\lambda u)}(s) = \chi_{U_1(u)}(s/\lambda)$. We define new term $\boldsymbol{K}_{1,\lambda}(s, s')$ as follows

$$
\boldsymbol{K}_{1,\lambda}(s, s') := \sum_{\substack{u,v \in \mathcal{L}_1, \\ u \neq v}} \chi_{U_1(u)}(s) \boldsymbol{K}(\boldsymbol{x}(u) - \boldsymbol{x}(v) + \boldsymbol{A}_\lambda(u, v)\boldsymbol{e}_1) \chi_{U_1(v)}(s') \quad\quad (2.5.12)
$$

Note that, if $\mathbf{Q} = \mathbf{I}$, the case of straight line, we have $\mathbf{K}_{1,\lambda}(s, s') = \mathbf{K}_1(s, s')$ as $\mathbf{A}_\lambda(u, v) = \mathbf{0}$.

Thus, we have following scaling relation for $\mathbf{K}_\lambda$

$$\mathbf{K}_\lambda(s, s') = \frac{1}{\lambda^3}\mathbf{K}_{1,\lambda}(s/\lambda, s'/\lambda) \tag{2.5.13}$$

We also define new map $T_{1,\lambda}$ similar to T_1 as follows

$$(T_{1,\lambda}\mathbf{f})(s) := \int_{\mathbb{R}} \mathbf{K}_{1,\lambda}(s, s')\mathbf{f}(s')ds' \tag{2.5.14}$$

Note that, if $\mathbf{Q} = \mathbf{I}$ then $T_{1,\lambda} = T_1$. Here, by $T_1, \mathbf{K}_1$ we mean $T_\lambda, \mathbf{K}_\lambda$ at $\lambda = 1$.

2.5.4 Boundedness of map T

We first show that norm of $T_{1,\lambda}$ and T_λ are equal. Then we show that $T_{1,\lambda}$ is bounded for all the functions in $C_0^\infty(\mathbb{R}, \mathbb{R})$ and hence the norm is bounded for each λ.

Proposition 6. *The map $T_{1,\lambda}$ and T_λ are bounded for all $\lambda > 0$. This also satisfies following property*

$$\|T_\lambda\|_{\mathcal{L}(L^2, L^2)} = \|T_{1,\lambda}\|_{\mathcal{L}(L^2, L^2)} \tag{2.5.15}$$

Above holds for all rotational second order tensor including $\mathbf{Q} = \mathbf{I}$.

Proof. We first prove the property of map. Let $S_\lambda : L^2(\mathbb{R}, \mathbb{R}^3) \to L^2(\mathbb{R}, \mathbb{R}^3)$ is a isometry. It will be sufficient to show, $\forall \mathbf{f} \in L^2(\mathbb{R}, \mathbb{R}^3)$

$$\|T_\lambda\mathbf{f}\|_{L^2(\mathbb{R}, \mathbb{R}^3)} = \|T_{1,\lambda}\mathbf{f}\|_{L^2(\mathbb{R}, \mathbb{R}^3)} \tag{2.5.16}$$

Note

$$\begin{aligned}
(T_\lambda\mathbf{f})(s) &= \lambda^2 \int_{\mathbb{R}} \mathbf{K}_\lambda(s, s')\mathbf{f}(s')ds' \\
&= \lambda^2 \int_{\mathbb{R}} \frac{1}{\lambda^3}\mathbf{K}_{1,\lambda}(s/\lambda, s'/\lambda)\left(\lambda^{-1/2}(S_\lambda\mathbf{f})(s'/\lambda)\right)ds' \\
&= \lambda^{-3/2} \int_{\mathbb{R}} \mathbf{K}_{1,\lambda}(s/\lambda, s')(S_\lambda\mathbf{f})(s')\lambda ds' \\
&= \lambda^{-1/2}(T_{1,\lambda}(S_\lambda\mathbf{f}))(s/\lambda) \\
&= (S_\lambda^{-1}T_{1,\lambda}S_\lambda\mathbf{f})(s) \tag{2.5.17}
\end{aligned}$$

Where, we have used the fact that $(S_\lambda^{-1}\boldsymbol{f})(s) = \lambda^{(-1/2)}\boldsymbol{f}(s/\lambda)$. Now, to prove the claim 1 we only need to use the definition of norm of map on $L^2(\mathbb{R},\mathbb{R}^3)$ as follows

$$
\begin{aligned}
\|T_\lambda\|_{\mathcal{L}(L^2,L^2)} &= \sup_{\|\boldsymbol{f}\|\neq 0} \frac{\|T_\lambda\boldsymbol{f}\|_{L^2(\mathbb{R},\mathbb{R}^3)}}{\|\boldsymbol{f}\|_{L^2(\mathbb{R},\mathbb{R}^3)}} \\
&= \sup_{\|\boldsymbol{f}\|\neq 0} \frac{\left\|S_\lambda^{-1}(T_{1,\lambda}S_\lambda\boldsymbol{f})\right\|_{L^2(\mathbb{R},\mathbb{R}^3)}}{\|\boldsymbol{f}\|_{L^2(\mathbb{R},\mathbb{R}^3)}} \\
&= \sup_{\|\boldsymbol{f}\|\neq 0} \frac{\|T_{1,\lambda}(S_\lambda\boldsymbol{f})\|_{L^2(\mathbb{R},\mathbb{R}^3)}}{\|\boldsymbol{f}\|_{L^2(\mathbb{R},\mathbb{R}^3)}} \\
&= \sup_{\|S_\lambda\boldsymbol{f}\|\neq 0} \frac{\|T_{1,\lambda}(S_\lambda\boldsymbol{f})\|_{L^2(\mathbb{R},\mathbb{R}^3)}}{\|S_\lambda\boldsymbol{f}\|_{L^2(\mathbb{R},\mathbb{R}^3)}} \\
&= \|T_{1,\lambda}\|_{\mathcal{L}(L^2,L^2)} \tag{2.5.18}
\end{aligned}
$$

We will only show the bound on $\boldsymbol{K}_{1,\lambda}$ as the bound on norm of $T_{1,\lambda}$, see definition Equation 2.5.14, will follow from the Young's inequality.

From the definition of $\boldsymbol{A}_\lambda$,

$$
\begin{aligned}
|\boldsymbol{A}_\lambda(a,b)\boldsymbol{e}_1| &= \left|\frac{\boldsymbol{Q}^{\lambda a} - \boldsymbol{Q}^{\lambda b} - \lambda\boldsymbol{Q}^a + \lambda\boldsymbol{Q}^b}{\lambda}\right| \\
&= \left|\frac{1}{\lambda}(\boldsymbol{Q}^{\lambda a}\boldsymbol{e}_1 - \boldsymbol{Q}^{\lambda b}\boldsymbol{e}_1) - (\boldsymbol{Q}^a\boldsymbol{e}_1 - \boldsymbol{Q}^b\boldsymbol{e}_1)\right| \\
&\leq \left|(\boldsymbol{Q}^{\lambda a}\frac{1}{\lambda}\boldsymbol{e}_1 - \boldsymbol{Q}^{\lambda b}\frac{1}{\lambda}\boldsymbol{e}_1)\right| + |\boldsymbol{Q}^a\boldsymbol{e}_1 - \boldsymbol{Q}^b\boldsymbol{e}_1| \\
&\leq |a-b| + 2 \tag{2.5.19}
\end{aligned}
$$

Where, we have used the fact that any two points on a circle of unit radius can have maximum distance of 2. To see $\left|(\boldsymbol{Q}^{\lambda a}\frac{1}{\lambda}\boldsymbol{e}_1 - \boldsymbol{Q}^{\lambda b}\frac{1}{\lambda}\boldsymbol{e}_1)\right| \leq |a-b|$, consider the circle of a radius $\frac{1}{\lambda}$.

Let $\boldsymbol{x}_0 := \frac{1}{\lambda}\boldsymbol{e}_1$, $\boldsymbol{x}_1 := \boldsymbol{Q}^{\lambda a}\frac{1}{\lambda}\boldsymbol{e}_1$, and $\boldsymbol{x}_2 := \boldsymbol{Q}^{\lambda b}\frac{1}{\lambda}\boldsymbol{e}_1$. We use the the fact that the arc length of angle is an upper bound for the distance between point $\boldsymbol{x}_0$ and rotation of point $\boldsymbol{x}_0$ by an angle λa. We have

$$
|\boldsymbol{x}_1 - \boldsymbol{x}_0| \leq \frac{1}{\lambda}|\lambda a| = |a| \tag{2.5.20}
$$

$$
|\boldsymbol{x}_2 - \boldsymbol{x}_0| \leq \frac{1}{\lambda}|\lambda b| = |b| \tag{2.5.21}
$$

48

Where, we have used the formula that arc length of angle θ is $r\theta$. For our case $r = \dfrac{1}{\lambda}$. From above bounds, we also have

$$|\boldsymbol{x}_1 - \boldsymbol{x}_2| \leq |a - b| \tag{2.5.22}$$

Thus, for a and b such that $|a - b| > 1$, we have

$$|\boldsymbol{A}_\lambda(a, b)\boldsymbol{e}_1| \leq c_1 |a - b| \tag{2.5.23}$$

For $s, s' \in \mathbb{R}$, and $|s - s'| < 1$, we have $\boldsymbol{K}_{1,\lambda}(s, s') = \boldsymbol{0}$. So we only need to show the bound on $\boldsymbol{K}_{1,\lambda}$ for $|s - s'| > 1$. Using the fact that $\boldsymbol{A}_\lambda(a, b)\boldsymbol{e}_1$ is bounded by $|a - b|$, we have, for $|s - s'| > 1$,

$$|\boldsymbol{K}_{1,\lambda}(s, s')| \leq c_2 \frac{1}{|\boldsymbol{x}(\hat{s}_1(s)) - \boldsymbol{x}(\hat{s}_1(s')) + \boldsymbol{A}_\lambda(a, b)\boldsymbol{e}_1|^3} \qquad \leq \frac{c_3}{|s - s'|^3} \tag{2.5.24}$$

Recall that $\hat{s}_1(x) = a$, where, a is such that $a \in \mathcal{L}_1$ and $x \in [a, a+1)$. Basically, $\hat{s}_1(x)$ returns the point in set $\mathcal{L}_1$ such that x is in unit cell of that point.

We have also used the fact that $|\boldsymbol{I} - 3\boldsymbol{n} \otimes \boldsymbol{n}| \leq 4$ for any unit vector $\boldsymbol{n} \in \mathbb{R}^3$. Also, note that for any $s, s' \in \mathbb{R}$, $|s - s'| \leq |\hat{s}_1(s) - \hat{s}_1(s')| + 2$.

To complete the bound on $\boldsymbol{K}_{1,\lambda}(s, s')$, we note that $\boldsymbol{K}_{1,\lambda}$ is bounded, by 0, for $|s - s'| < 1$. Thus, we add another constant at the denominator of 2.5.24. So, for all $s, s' \in \mathbb{R}$, we have

$$|\boldsymbol{K}_{1,\lambda}(s, s')| \leq \frac{c_4}{c_5 + |s - s'|^3} \tag{2.5.25}$$

where c_4, c_5 are positive constants and independent of s, s' and λ.

Since $\boldsymbol{K}_{1,\lambda}$ is bounded by function $g(s) = \dfrac{c_4}{c_5 + |s|^3}$ which is in $L^1(\mathbb{R}, \mathbb{R})$, we have the bound on map $T_{1,\lambda}$ for all λ.

$\square$

2.5.5 Limit of map T

We want to know the limit of $T_\lambda \boldsymbol{f}$ as $\lambda \to 0$ in $L^2\left(\mathbb{R}, \mathbb{R}^3\right)$. We can simplify this calculation by utilizing the fact that T_λ is a bounded map. Let $\boldsymbol{f} \in L^2\left(\mathbb{R}, \mathbb{R}^3\right)$ and let there is a sequence of functions $\boldsymbol{f}^k \in C_0^\infty\left(\mathbb{R}, \mathbb{R}\right)$, $k \in \mathbb{N}$ such that

$$\boldsymbol{f}^k \xrightarrow[k \to \infty]{} \boldsymbol{f} \quad \text{in } L^2\left(\mathbb{R}, \mathbb{R}^3\right) \tag{2.5.26}$$

Then,

$$T_\lambda(\boldsymbol{f}) = T_\lambda(\boldsymbol{f}^k) + T_\lambda(\boldsymbol{f} - \boldsymbol{f}^k) \tag{2.5.27}$$

Since the second term is bounded by $\left\|\boldsymbol{f} - \boldsymbol{f}^k\right\|$ and it will go to zero as $k \to \infty$, we only need to analyze the $T_\lambda(\boldsymbol{f}^k)$, for any $\boldsymbol{f}^k \in C_0^\infty\left(\mathbb{R}, \mathbb{R}\right)$, in the limit $\lambda \to 0$.

Before we analyze the map T_λ in the limit, we will show results which will be used in the limit calculation of map T_λ. We define new function $\boldsymbol{H}_\lambda$ as follows

$$\boldsymbol{H}_\lambda(s) := \int_{\mathbb{R}} \boldsymbol{K}_{1,\lambda}(s, s')ds' \tag{2.5.28}$$

Proposition 7. *For any $\lambda > 0$, and $s, s' \in \mathbb{R}$, we have*

$$\boldsymbol{K}_{1,\lambda}(s, s' + \hat{s}_1(s)) = \boldsymbol{Q}^{\lambda\hat{s}_1(s)} \boldsymbol{K}_{1,\lambda}(0, s')\boldsymbol{Q}^{-\lambda\hat{s}_1(s)} \tag{2.5.29}$$

Further, for any $s \in \mathbb{R}$ and $\lambda > 0$ we have

$$\boldsymbol{H}_\lambda(s) = \boldsymbol{Q}^{\lambda\hat{s}_1(s)} \boldsymbol{H}_\lambda(0)\boldsymbol{Q}^{-\lambda\hat{s}_1(s)} \tag{2.5.30}$$

Note that for $s = 0$, $\hat{s}_1(s) = 0$, hence 2.5.30 is not ill-defined at $s = 0$. Also, this holds for all rotational second order tensor including $\boldsymbol{Q} = \boldsymbol{I}$.

Proof. For the first part of claim, we use the following identity

50

$$K(Qx) = QK(x)Q^T \qquad \forall a, b \in \mathbb{R}^3, Q \in \text{Orth}^+(\mathbb{R}^3) \tag{2.5.31}$$

Where we have used the fact that $|Qa| = |a|, \forall a$, and

$$Q(a \otimes b)Q^T = (Qa) \otimes (Qb) \qquad \forall a, b \in \mathbb{R}^3$$

Further,

$$
\begin{aligned}
K(Qx) &= \frac{-1}{4\pi |Qx|^3} \left[I - \frac{3}{|Qx|^2} Qx \otimes Qx \right] \\
&= \frac{-1}{4\pi |x|^3} \left[QIQ^T - \frac{3}{|x|^2} Q(x \otimes x)Q^T \right] \\
&= Q \left(\frac{-1}{4\pi |x|^3} \left[I - \frac{3}{|x|^2} x \otimes x \right] \right) Q^T \\
&= QK(x)Q^T \tag{2.5.32}
\end{aligned}
$$

Let $s \in [a, a+1), a \in \mathcal{L}_1$. Then $\hat{s}_1(s) = a$. We have

$$
\begin{aligned}
&K_{1,\lambda}\big(s, \hat{s}_1(s) + s'\big) \\
&= \sum_{\substack{v \in \mathcal{L}_1, \\ v \neq \hat{s}_1(s)}} \chi_{U_1(v)}(\hat{s}_1(s) + s') K\left(x(\hat{s}_1(s)) - x(v) + A_\lambda(\hat{s}_1(s), v)e_1\right) \\
&= \sum_{\substack{v \in \mathcal{L}_1, \\ v \neq a}} \chi_{U_1(v)}(a + s') K\left(x(a) - x(v) + A_\lambda(a, v)e_1\right) \\
&= \sum_{\substack{v' \in a + \mathcal{L}_1, \\ v' \neq 0}} \chi_{U_1(v')}(s') K\left(x(a) - x(v' + a) + A_\lambda(a, v' + a)e_1\right) \tag{2.5.33}
\end{aligned}
$$

In the second step, we have just substituted $\hat{s}_1(s) = a$. In the third step, we translated the set $\mathcal{L}_1$ by an amount a in the sum. Note that $\mathcal{L}_1 + a = \mathcal{L}_1$ and $\chi_{U_1(v'+a)}(a + s') = \chi_{U_1(v')}(s')$.

To prove our claim, we only need to analyze the argument of K in above equation, i.e. $x(a) - x(v' + a) + A_\lambda(a, v' + a)e_1$. We have

$$\boldsymbol{x}(a) - \boldsymbol{x}(v' + a) + \boldsymbol{A}_\lambda(a, v' + a)\boldsymbol{e}_1$$

$$= \boldsymbol{Q}^a \boldsymbol{e}_1 + a\boldsymbol{e}_3 - \boldsymbol{Q}^{v'+a}\boldsymbol{e}_1 - (v' + a)\boldsymbol{e}_3$$

$$+ \frac{1}{\lambda}\left(\boldsymbol{Q}^{\lambda a} - \boldsymbol{Q}^{v'\lambda+a\lambda}\right)\boldsymbol{e}_1 - \left(\boldsymbol{Q}^a - \boldsymbol{Q}^{v'+a}\right)\boldsymbol{e}_1$$

$$= -v'\boldsymbol{e}_3 + \frac{1}{\lambda}\left(\boldsymbol{Q}^{\lambda a} - \boldsymbol{Q}^{v'\lambda+a\lambda}\right)\boldsymbol{e}_1$$

$$= \boldsymbol{Q}^{\lambda a}\left[\frac{1}{\lambda}\left(\boldsymbol{I} - \boldsymbol{Q}^{\lambda v'}\right)\boldsymbol{e}_1 - v'\boldsymbol{e}_3\right]$$

$$= \boldsymbol{Q}^{\lambda a}\left[-v'\boldsymbol{e}_3 - \boldsymbol{Q}^{v'}\boldsymbol{e}_1 + \boldsymbol{Q}^{v'}\boldsymbol{e}_1 + \boldsymbol{Q}^0\boldsymbol{e}_1 - \boldsymbol{Q}^0\boldsymbol{e}_1 - 0\boldsymbol{e}_3 + \frac{1}{\lambda}\left(\boldsymbol{Q}^0 - \boldsymbol{Q}^{\lambda v'}\right)\boldsymbol{e}_1\right]$$

$$= \boldsymbol{Q}^{\lambda a}\left[\boldsymbol{x}(0) - \boldsymbol{x}(v') + \boldsymbol{A}_\lambda(0, v')\boldsymbol{e}_1\right] \tag{2.5.34}$$

From 2.5.31, we have

$$\boldsymbol{K}_{1,\lambda}(s, \hat{s}_1(s) + s')$$

$$= \sum_{\substack{v' \in a + \mathcal{L}_1, \\ v' \neq 0}} \chi_{U_1(v')}(s')\boldsymbol{K}\left(\boldsymbol{Q}^{\lambda a}\left[\boldsymbol{x}(0) - \boldsymbol{x}(v') + \boldsymbol{A}_\lambda(0, v')\boldsymbol{e}_1\right]\right)$$

$$= \sum_{\substack{v' \in \mathcal{L}_1, \\ v' \neq 0}} \chi_{U_1(v')}(s')\boldsymbol{Q}^{\lambda a}\boldsymbol{K}\left(\boldsymbol{x}(0) - \boldsymbol{x}(v') + \boldsymbol{A}_\lambda(0, v')\boldsymbol{e}_1\right)\boldsymbol{Q}^{-\lambda a}$$

$$= \boldsymbol{Q}^{\lambda a}\left[\sum_{\substack{v' \in \mathcal{L}_1, \\ v' \neq 0}} \chi_{U_1(v')}(s')\boldsymbol{K}\left(\boldsymbol{x}(0) - \boldsymbol{x}(v') + \boldsymbol{A}_\lambda(0, v')\boldsymbol{e}_1\right)\right]\boldsymbol{Q}^{-\lambda a}$$

$$= \boldsymbol{Q}^{\lambda a}\boldsymbol{K}_{1,\lambda}(0, s')\boldsymbol{Q}^{-\lambda a} \tag{2.5.35}$$

For second part, we use 2.5.31, and change of variable, to get

$$\boldsymbol{H}_\lambda(s) = \int_{\mathbb{R}} \boldsymbol{K}_{1,\lambda}(s, s')ds'$$

$$= \int_{\mathbb{R}} \boldsymbol{K}_{1,\lambda}(s, u + \hat{s}_1(s))du$$

$$= \int_{\mathbb{R}} \boldsymbol{Q}^{\lambda \hat{s}_1(s)}\boldsymbol{K}_{1,\lambda}(0, u)\boldsymbol{Q}^{-\lambda \hat{s}_1(s)}du$$

$$= \boldsymbol{Q}^{\lambda \hat{s}_1(s)}\boldsymbol{H}_\lambda(0)\boldsymbol{Q}^{-\lambda \hat{s}_1(s)} \tag{2.5.36}$$

This completes the proof. $\qquad\square$

We now analyze the map T_λ in the limit.

Proposition 8. *Let $\boldsymbol{f} \in C_0^\infty (\mathbb{R}, \mathbb{R})$. Then, we have*

$$(T_\lambda \boldsymbol{f})(s) \xrightarrow[\lambda \to 0]{} \mathcal{K}(s)\boldsymbol{f}(s) \tag{2.5.37}$$

Where,

$$\mathcal{K}(s) := \boldsymbol{Q}^{\hat{s}_1(s)} \left[\lim_{\rho \to \infty} \sum_{\substack{v \in \mathcal{L}_1 \cap (-\rho, \rho), \\ v \neq 0}} \boldsymbol{K}(v\boldsymbol{Q}'\boldsymbol{e}_1 + v\boldsymbol{e}_3) \right] \boldsymbol{Q}^{-\hat{s}_1(s)} \tag{2.5.38}$$

$\boldsymbol{Q}'$ is given by

$$\boldsymbol{Q}' = \lim_{h \to 0} \frac{\boldsymbol{Q}^h - \boldsymbol{Q}^0}{h} \tag{2.5.39}$$

i.e., $\boldsymbol{Q}'$ is derivative of tensor $T(s) = \boldsymbol{Q}^s$ with respect to s at $s = 0$. Note that, if $\boldsymbol{Q} = \boldsymbol{I}$, for the case of straight line, $\boldsymbol{Q}' = \boldsymbol{0}$.

We can further simplify $\mathcal{K}$ as follows

$$\mathcal{K}(s) = c\boldsymbol{Q}^{\hat{s}_1(s)} \boldsymbol{K}(\boldsymbol{Q}'\boldsymbol{e}_2 + \boldsymbol{e}_3)\boldsymbol{Q}^{-\hat{s}_1(s)} \tag{2.5.40}$$

Where, constant c is given by

$$c = \sum_{v \in \mathcal{L}_1 - 0} \frac{1}{|v|^3} \tag{2.5.41}$$

Proof. Using Equation 2.5.13, i.e. scaling of $\boldsymbol{K}_\lambda$, we have

$$\begin{aligned}
T_\lambda(\boldsymbol{f})(s) &= \lambda^2 \int_\mathbb{R} \frac{1}{\lambda^3} \boldsymbol{K}1, \lambda(s/\lambda, s'/\lambda)\boldsymbol{f}(s')ds' \\
&= \left(\frac{1}{\lambda} \int_\mathbb{R} \boldsymbol{K}_{1,\lambda}(s/\lambda, s'\lambda)ds' \right) \boldsymbol{f}(s) \\
&\quad + \left(\frac{1}{\lambda} \int_\mathbb{R} \boldsymbol{K}_{1,\lambda}(s/\lambda, s'\lambda)(\boldsymbol{f}(s') - \boldsymbol{f}(s))ds' \right)
\end{aligned} \tag{2.5.42}$$

53

We analyze the term multiplying $\boldsymbol{f}(s)$ in first equation above. Using bound on $\boldsymbol{K}_{1,\lambda}$, see Equation 2.5.25, wwe have, for $R > 0$,

$$\frac{1}{\lambda} \int_{|s-s'| \geq R\lambda} \boldsymbol{K}_{1,\lambda}(s/\lambda, s'\lambda) ds'$$

$$\leq \frac{1}{\lambda} \int_{|s-s'| \geq R\lambda} \frac{c_4}{c_5 + |s/\lambda - s'/\lambda|^3} ds'$$

$$= \lambda^2 \int_{|s-s'| \geq R\lambda} \frac{c_4}{c_5 \lambda^3 + |s - s'|^3} ds'$$

$$= \lambda^2 \int_{|t| \geq R} \frac{c_4}{c_5 \lambda^3 + |\lambda t|^3} \lambda dt$$

$$= \int_{|t| \geq R} \frac{c_4}{c_5 + |t|^3} dt \tag{2.5.43}$$

In second last step, we did change in variable. From above, we find that the upper bound on $\frac{1}{\lambda} \int_{|s-s'| \geq R\lambda} \boldsymbol{K}_{1,\lambda}(s/\lambda, s'\lambda) ds'$ is independent of λ and it goes to zero as $R \to \infty$. Considering the second term in Equation 2.5.42

$$\frac{1}{\lambda} \int_{\mathbb{R}} \boldsymbol{K}_{1,\lambda}(s/\lambda, s'\lambda)(\boldsymbol{f}(s') - \boldsymbol{f}(s)) ds'$$

$$= \frac{1}{\lambda} \int_{|s-s'| \geq R\lambda} \boldsymbol{K}_{1,\lambda}(s/\lambda, s'\lambda) \boldsymbol{f}(s') ds' - \frac{1}{\lambda} \int_{|s-s'| \geq R\lambda} \boldsymbol{K}_{1,\lambda}(s/\lambda, s'\lambda) ds' \boldsymbol{f}(s)$$

$$+ \frac{1}{\lambda} \int_{|s-s'| \leq R\lambda} \boldsymbol{K}_{1,\lambda}(s/\lambda, s'\lambda)(\boldsymbol{f}(s') - \boldsymbol{f}(s)) ds' \tag{2.5.44}$$

We will first let $\lambda \to 0$ and then $R \to \infty$. In the limit $\lambda \to 0$, third term will go to zero, as $\boldsymbol{f} \in C_0^\infty (\mathbb{R}, \mathbb{R})$. First and the second term have an upper bound, independent of λ, as shown in Equation 2.5.43, and as $R \to \infty$, the upper bound goes to zero. Therefore, we have

$$\lim_{\lambda \to 0} T_\lambda(\boldsymbol{f})(s) = \lim_{\lambda \to 0} \left(\frac{1}{\lambda} \int_{\mathbb{R}} \boldsymbol{K}_{1,\lambda}(s/\lambda, s'\lambda) ds' \right) \boldsymbol{f}(s)$$

$$= \left[\lim_{\lambda \to 0} \int_{\mathbb{R}} \boldsymbol{K}_{1,\lambda}(s/\lambda, s'') ds'' \right] \boldsymbol{f}(s)$$

$$= \left[\lim_{\lambda \to 0} \boldsymbol{H}_\lambda(s/\lambda) \right] \boldsymbol{f}(s) \tag{2.5.45}$$

Where, we did change in variable in s' in second step, and used definition of $\boldsymbol{H}_\lambda$ in third step. Combining Equation 2.5.45 and Equation 2.5.30, we get

$$\lim_{\lambda \to 0} T_\lambda(\boldsymbol{f})(s) = \lim_{\lambda \to 0} \boldsymbol{Q}^{\lambda \hat{s}_1(s/\lambda)} \boldsymbol{H}_\lambda(0) \boldsymbol{Q}^{-\lambda \hat{s}_1(s/\lambda)} \boldsymbol{f}(s)$$

$$= \lim_{\lambda \to 0} \boldsymbol{Q}^{\hat{s}_1(s)} \boldsymbol{H}_\lambda(0) \boldsymbol{Q}^{-\hat{s}_1(s)} \boldsymbol{f}(s)$$

$$= \boldsymbol{Q}^{\hat{s}_1(s)} \left[\lim_{\lambda \to 0} \boldsymbol{H}_\lambda(0) \right] \boldsymbol{Q}^{-\hat{s}_1(s)} \boldsymbol{f}(s) \qquad (2.5.46)$$

Where, we have used the fact that $\lambda \hat{s}_1(s) = \hat{s}_1(s)$. So, we need to analyze $\boldsymbol{H}_\lambda(0)$ in the limit. We have

$$\lim_{\lambda \to 0} \boldsymbol{H}_\lambda(0) = \lim_{\lambda \to 0} \sum_{v \in \mathcal{L}_1 - 0} \boldsymbol{K}(\boldsymbol{x}(0) - \boldsymbol{x}(v) + \boldsymbol{A}_\lambda(0, v)\boldsymbol{e}_1)$$

$$= \lim_{\lambda \to 0} \sum_{v \in \mathcal{L}_1 - 0} \boldsymbol{K}(-\frac{1}{\lambda}(\boldsymbol{Q}^{\lambda v} - \boldsymbol{I})\boldsymbol{e}_1 - v\boldsymbol{e}_3) \qquad (2.5.47)$$

We show that the term $\frac{1}{\lambda}(\boldsymbol{Q}^{\lambda v} - \boldsymbol{I})\boldsymbol{e}_1$ is derivative of second order tensor as a function of $t \in \mathbb{R}$. We have

$$\lim_{\lambda \to 0} \frac{(\boldsymbol{Q}^{\lambda v} - \boldsymbol{I})\boldsymbol{e}_1}{\lambda} = \lim_{\lambda \to 0} \frac{(\boldsymbol{Q}^{0+\lambda v} - \boldsymbol{Q}^0)\boldsymbol{e}_1}{\lambda}$$

$$= v \left[\lim_{\lambda v \to 0} \frac{(\boldsymbol{Q}^{0+\lambda v} - \boldsymbol{Q}^0)}{\lambda v} \right] \boldsymbol{e}_1$$

$$= v \left[\lim_{h \to 0} \frac{\boldsymbol{Q}^{0+h} - \boldsymbol{Q}^0}{h} \right] \boldsymbol{e}_1$$

$$= v\boldsymbol{Q}' \qquad (2.5.48)$$

Where, $\boldsymbol{Q}'$ is defined as

$$\boldsymbol{Q}' := \frac{d\boldsymbol{Q}^x}{dx} \Big|_{x=0} \qquad (2.5.49)$$

Thus,

$$\lim_{\lambda \to 0} \boldsymbol{H}_\lambda(0) = \sum_{v \in \mathcal{L}_1 - 0} \boldsymbol{K}(-v\boldsymbol{Q}'\boldsymbol{e}_1 - v\boldsymbol{e}_3)$$

$$= \sum_{v \in \mathcal{L}_1 - 0} \boldsymbol{K}(v\boldsymbol{Q}'\boldsymbol{e}_1 + v\boldsymbol{e}_3)$$

$$= \left[\sum_{v \in \mathcal{L}_1 - 0} \frac{1}{|v|^3} \right] \boldsymbol{K}(\boldsymbol{Q}'\boldsymbol{e}_1 + \boldsymbol{e}_3) \tag{2.5.50}$$

Second and the third step follows from the definition of dipole field kernel $\boldsymbol{K}(\boldsymbol{x})$. Therefore, we have

$$\lim_{\lambda \to 0} T_\lambda(\boldsymbol{f})(s) = \boldsymbol{Q}^{\hat{s}_1(s)} \left[\sum_{v \in \mathcal{L}_1 - 0} \boldsymbol{K}(v\boldsymbol{Q}'\boldsymbol{e}_1 + v\boldsymbol{e}_3) \right] \boldsymbol{Q}^{-\hat{s}_1(s)} \boldsymbol{f}(s) \tag{2.5.51}$$

$$= \mathcal{K}(s)\boldsymbol{f}(s) \tag{2.5.52}$$

Where, we $\mathcal{K}(s) = \boldsymbol{Q}^{\hat{s}_1(s)} \left[\sum_{v \in \mathcal{L}_1 - 0} \boldsymbol{K}(v\boldsymbol{Q}'\boldsymbol{e}_1 + v\boldsymbol{e}_3) \right] \boldsymbol{Q}^{-\hat{s}_1(s)}$. This completes the proof. $\square$

2.5.6 Main results

We present the main result here.

Theorem 9. *Let $\boldsymbol{f}_\lambda \in L^2(\mathbb{R}, \mathbb{R}^3)$ with $\boldsymbol{f} \in L^2(\mathbb{R}, \mathbb{R}^3)$ such that*

$$\boldsymbol{f}_\lambda \xrightarrow[\lambda \to 0]{} \boldsymbol{f} \quad in \ L^2(\mathbb{R}, \mathbb{R}^3). \tag{2.5.53}$$

Let the system of dipole moments, located at 1-D lattice points $\mathcal{L}_\lambda$ along the helix, is given by

$$\boldsymbol{d}_\lambda(s) = \int_{U_\lambda(s)} \boldsymbol{f}_\lambda(s')ds' \quad \forall s \in \mathcal{L}_\lambda. \tag{2.5.54}$$

Let the helix is described by paramtetric mapping : $\boldsymbol{x} : \mathbb{R} \to \mathbb{R}^3$

$$\boldsymbol{x}(s) = \boldsymbol{Q}^s \boldsymbol{e}_1 + s\boldsymbol{e}_3 \tag{2.5.55}$$

Where, $\boldsymbol{Q}$ is the second order rotational tensor. $\boldsymbol{e}_3$ is the axis of helix, and, hence $\boldsymbol{Q}\boldsymbol{e}_3 = \boldsymbol{e}_3$.

Let e_λ and T_λ are defined by 2.5.4 and 2.5.7.

Then

$$(T_\lambda \boldsymbol{f}_\lambda) \xrightarrow[\lambda \to 0]{} \mathcal{K}\boldsymbol{f} \quad \text{in } L^2\left(\mathbb{R}, \mathbb{R}^3\right) \tag{2.5.56}$$

and

$$e_\lambda = -\frac{1}{2}\langle \boldsymbol{f}, T_\lambda \boldsymbol{f}\rangle_{L^2(\mathbb{R},\mathbb{R}^3)} \xrightarrow[\lambda \to 0]{} -\frac{1}{2}\langle \boldsymbol{f}, \mathcal{K}\boldsymbol{f}\rangle_{L^2(\mathbb{R},\mathbb{R}^3)} \tag{2.5.57}$$

Where, $\mathcal{K}$ is defined in Equation 2.5.38.

This holds for all rotational tensor $\boldsymbol{Q}$. If we set $\boldsymbol{Q} = \boldsymbol{I}$, we will have the system of dipole moments along the straight line.

Proof. As the map T_λ is bounded, we have,

$$\lim_{\lambda \to 0}(T_\lambda \boldsymbol{f}_\lambda) = \lim_{\lambda \to 0}(T_\lambda \boldsymbol{f}) + \lim_{\lambda \to 0}(T_\lambda(\boldsymbol{f}_\lambda - \boldsymbol{f})) \tag{2.5.58}$$

$$= \lim_{\lambda \to 0}(T_\lambda \boldsymbol{f}) \tag{2.5.59}$$

Now, let $\boldsymbol{f}^k \in C_0^\infty(\mathbb{R}, \mathbb{R})$ are sequence of function such that $\boldsymbol{f}^k \to \boldsymbol{f}$. Then

$$\lim_{\lambda \to 0}(T_\lambda \boldsymbol{f}) = \lim_{k \to \infty} \lim_{\lambda \to 0}(T_\lambda \boldsymbol{f}^k) + \lim_{k \to \infty} \lim_{\lambda \to 0}(T_\lambda(\boldsymbol{f} - \boldsymbol{f}^k))$$

$$= \lim_{k \to \infty} \lim_{\lambda \to 0}(T_\lambda \boldsymbol{f}^k)$$

$$= \lim_{k \to \infty}\left(\mathcal{K}\boldsymbol{f}^k\right)$$

$$= \mathcal{K}\boldsymbol{f} \tag{2.5.60}$$

Note that

$$-\frac{1}{2}\langle \boldsymbol{f}_\lambda, T_\lambda \boldsymbol{f}_\lambda\rangle_{L^2(\mathbb{R},\mathbb{R}^3)}$$

$$= -\frac{1}{2}\left[\langle \boldsymbol{f}_\lambda - \boldsymbol{f}, T_\lambda \boldsymbol{f}_\lambda\rangle_{L^2(\mathbb{R},\mathbb{R}^3)} + \langle \boldsymbol{f}, T_\lambda \boldsymbol{f}_\lambda\rangle_{L^2(\mathbb{R},\mathbb{R}^3)}\right]$$

$$= -\frac{1}{2}\left[\langle \boldsymbol{f}_\lambda - \boldsymbol{f}, T_\lambda \boldsymbol{f}_\lambda\rangle_{L^2(\mathbb{R},\mathbb{R}^3)} + \langle \boldsymbol{f}, T_\lambda \boldsymbol{f}\rangle_{L^2(\mathbb{R},\mathbb{R}^3)} + \langle \boldsymbol{f}, T_\lambda(\boldsymbol{f}_\lambda - \boldsymbol{f})\rangle_{L^2(\mathbb{R},\mathbb{R}^3)}\right] \tag{2.5.61}$$

$$\tag{2.5.62}$$

The first and second term goes to zero. Finally, we have

$$\lim_{\lambda \to 0} -\frac{1}{2}\langle \boldsymbol{f}_\lambda, T_\lambda \boldsymbol{f}_\lambda \rangle_{L^2(\mathbb{R},\mathbb{R}^3)} = -\frac{1}{2}\langle \boldsymbol{f}, \mathcal{K}\boldsymbol{f} \rangle_{L^2(\mathbb{R},\mathbb{R}^3)} \tag{2.5.63}$$

This completes the proof.

$\square$

2.6 Electric and magnetic interactions are different in nanostructures

In general, we would expect the electric and magnetic interactions to be long range even in materials like nanostructures and thin film. However, it is not the case. Our calculations, in section 2.5, and section 2.3, show that the electric and magnetic interactions are short range, in the continuum limit, for nanostructures and thin film. In support of our calculation, we also note the work of Gioia and James, see [Gioia and James, 1997], where they compute the magnetostatics energy in the limit thickness of film goes to zero. They find that the limit of energy does not have a long-range term.

Since nonlocal energy, in the limit, means two charged material domain, very far away from each other, interact with each other. As, they are far away, at the limit, their interactions will involve dipole field kernel $\boldsymbol{K}$. Therefore, the reason that nanostructures do not have a nonlocal interaction is related to the dipole field kernel.

Dipole field kernel has $1/r^3$ scaling. Consider 1-D, 2-D and 3-D lattice with a net unit dipole moment in each unit cell. We can estimate the energy as follows

1. **1-D dipole system** $E = \sum_{r=1}^{\infty} \frac{1}{r^3} * 1 = \sum_{r=1}^{\infty} \frac{1}{r^3}$. This sum is well behaved and bounded. At r^{th} unit cell there will be unit dipole moment.

2. **2-D dipole system** $E = \sum_{r=1}^{\infty} \frac{1}{r^3} * r$. This sum is also well behaved and bounded. At the circumference of circle of radius r, there will be roughly r amount of dipole moment.

3. **3-D dipole system** $E = \sum_{r=1}^{\infty} \frac{1}{r^3} * r * r$. This sum is divergent. Although, this estimate is unbounded, the actual energy density considering the vector nature of

dipole moment and tensor nature of $\boldsymbol{K}$, we find the sum to be the conditionally convergent.

Here, we can see that the energy density for 1-D dipole and 2-D dipole system are bounded, as opposed to the case of 3-D dipole system. Therefore, the case of 1-D and 2-D system does not have a long-range interaction. In other words, the dipole field is decaying very fast, for 1-D and 2-D system, and hence, energy at one atom can be computed by looking at atoms within some cutoff region. For 3-D, the decay of kernel is not fast enough.

Chapter 3

Quasicontinuum formulation: Finite temperature with electrostatics

In this chapter, we will talk about the multiscale method for electrostatics interactions at finite temperature. We will follow the multiscale method developed in [Kulkarni et al., 2008]. Although the method in [Kulkarni et al., 2008] was designed for a single lattice, we extend it to multi-lattice. The extension is straight forward. For the sake of completeness of the thesis, we will go through the derivation of QC formulation.

In chapter 2, we computed the continuum limit of electrostatics energy for the random media. The aim of that calculation was to develop the multiscale method which can do electrostatics calculations at the finite temperature. We, instead of developing the multiscale framework, decided to make use of existing methods. We did a survey of available methods and broadly discovered that there are two choices available for the finite temperature multiscale calculations. One choice was to use the multiscale method developed by Tadmor group, see [Dupuy et al., 2005], [Tadmor et al., 2013], [Kim et al., 2014]. Another choice was to use the method developed by Knap and Ortiz group, see [Kulkarni et al., 2008]. Further, our colleague Jason Marshall [Marshall and Dayal, 2013] had already used the code from Knap and Ortiz group, and modified it extensively, to implement the electrostatics. His work was for the system of atoms with no thermal fluctuations. The multiscale method presented in [Kulkarni et al., 2008] was easier to implement into the existing code.

As proposed in [Kulkarni et al., 2008], we refer to their method as *max-ent* method.

Apart from extending the *max-ent* method to multi-lattice, we did not require to modify or extend it further. As for numerical implementation, we modified the QC code developed by Marshall, see [Marshall and Dayal, 2013], and implemented the method presented in this chapter. We add the electrostatics calculation to the *max-ent* method. However, the main work for the electrostatics was to compute the continuum limit for the random media. In rest of this chapter, we will talk about QC method, and how we integrated the electrostatics.

We also observed that in the quasi-harmonic approximation, the contribution from the electrostatics energy is zero. We can easily generalize this observation to all the potentials which have $1/r$ scaling. The trace of second order derivative of such potentials are zero, and, hence, their contribution is zero in quasi-harmonic approximation.

The *max-ent* method simplifies the calculation in two broad ways: it simplifies the probability distribution function, and by approximating the statistics problem (calculation of phase average over configuration space) to the minimization problem. Though, the second simplification is a consequence of a first. One of the main assumptions of the method is that the system has some well defined mean state, and the atomic fluctuations are not significant from its mean state. We use the mean value approximation to construct the probability distribution function, which has mean state variables as its parameters. Now, to determine these parameters, we use the variational mean field theory, which says the best probability distribution function is the one which minimizes the free energy. Therefore, we finally have a minimization problem on the mean state variables.

3.1 Notations

We will use following notations in this chapter.

- (n, a) : a^{th} atom of nth lattice

- $\mathcal{L}^n = \{(n, a) : a = 1, 2, ..., N\}$: set of indices of all the atoms of nth lattice

- $\mathcal{L} = \{(n, a) : n = 1, 2, .., Q, \ a = 1, 2, ..., N\} = \bigcup_{i=1}^{Q} \mathcal{L}^i$: set of indices of all the atoms

- m_a^n : atomic mass of atom (n, a)

- $\boldsymbol{p}_a^n$: momenta of atom (n, a)

- $\boldsymbol{q}_a^n$: position of atom (n, a)

- $\mathbf{q}$: vector of positions of all the atoms

- $\mathbf{p}$: vector of momentas of all the atoms

- Q : total number of lattices

- N : number of atoms in each lattice

- $\Gamma = \mathbb{R}^{3N} \times \mathbb{R}^{3N}$: phase space of one lattice

- $\bar{\Gamma} = \Gamma^Q$: phase space of whole system

- $p : \bar{\Gamma} \to [0, 1]$: probability density function of whole system

- Z : partition function of whole system

- p_a^n : probability density function of atom (n, a)

- Z_a^n : partition function of atom (n, a)

- $\boldsymbol{q}^n$: vector of positions of all the atoms of n$^{\text{th}}$ lattice

- $\boldsymbol{p}^n$: vector of momenta of all the atoms of n$^{\text{th}}$ lattice

- $\boldsymbol{q}_a^n$: position of (n, a) atom

- $\boldsymbol{p}_a^n$: momenta of (n, a) atom

- $\bar{\boldsymbol{q}}_a^n$: mean position of (n, a) atom

- $\bar{\boldsymbol{p}}_a^n$: mean momenta of (n, a) atom

- τ_a^n : standard deviation of position from mean position of (n, a) atom

- σ_a^n : standard deviation of momenta from mean momenta of (n, a) atom

- w_a^n : mean frequency of (n, a) atom

- τ^n : vector of τ_a^n of all the atoms of nth lattice

- σ^n : vector of σ_a^n of all the atoms of nth lattice

- w^n : vector of w_a^n of all the atoms of nth lattice

- τ : vector of τ_a^n of all the atoms

- σ : vector of σ_a^n of all the atoms

- w : vector of w_a^n of all the atoms

- $< f >:= \dfrac{1}{(QN)!h^{3QN}} \int_{\bar{\Gamma}} p(\{\boldsymbol{q}\},\{\boldsymbol{p}\}) f(\{\boldsymbol{q}\},\{\boldsymbol{p}\}) \prod_{n=1}^{Q} d\boldsymbol{q}^n d\boldsymbol{p}^n$: phase average of phase function f.

3.2 Maximum entropy principle and the variational mean field theory

For multi-lattice with the Q number of species and the N number of atoms in each species, state of a system at any time can be described by the momenta vector and the position vector of all the atoms. Let $(\mathbf{q}, \mathbf{p}) \in \bar{\Gamma}$ be the state of system, also called <u>microstate</u> of the system. Then Hamiltonian of system will be

$$H(\mathbf{q}, \mathbf{p}) := \sum_{(n,a)} \frac{1}{2} |\boldsymbol{p}_a^n|^2 + V(\mathbf{q}) + \Phi(\mathbf{q}) \tag{3.2.1}$$

Where the first term is kinetic energy, the second term is potential energy, and the third term is an electrostatic energy.

There exists a probability density function $p : \bar{\Gamma} \to [0, 1]$, which gives the probability of a system being at given microstate $(\mathbf{q}, \mathbf{p})$. Exact probability function p_{exact} is given by

$$p_{exact}(\mathbf{q}, \mathbf{p}) = \frac{\exp[-\beta H(\mathbf{q}, \mathbf{p})]}{Z_{exact}} \tag{3.2.2}$$

where Z_{exact} is a partition function, defined as

$$Z_{exact} = \frac{1}{(QN)! h^{3QN}} \int_{\bar{\Gamma}} e^{[-\beta H(\mathbf{q},\mathbf{p})]} d\mathbf{q} d\mathbf{p} \qquad (3.2.3)$$

p_{exact} is a function of the state of atoms through Hamilton, and it is numerically expensive to compute phase average of a function using p_{exact}, for a large system of atoms/particles. We want to approximate p_{exact} and find simple functional form of p. For that, we will use variational mean field theory together with maximum entropy principle.

3.2.1 Entropy of a system

We define a global entropy of system as follows

$$S[p] := -\frac{k_B}{(QN)! h^{3QN}} \int_{\bar{\Gamma}} p \log p \prod_{n=1}^{Q} d\boldsymbol{q}^n d\boldsymbol{p}^n \qquad (3.2.4)$$

The best probability function will be the one which maximizes the entropy, subjected to all known constraints. See [Jaynes, 1957a] for the detailed reasoning behind this postulate. Here, we will mention it very briefly.

The function that is positive, which increases with increasing uncertainty, and is additive for independent sources of uncertainty, is similar to $S[p]$. Entropy, as defined above, is also a measure of the amount of uncertainty, when probability density function represents the uncertainty associated with state of the system. Jaynes, [Jaynes, 1957a], writes

"It is now evident how to solve our problem; in making inferences on the basis of partial information we must use that probability distribution function which has maximum entropy subject to whatever is known. This is the only unbiased assignment we can make; to use any other would amount to an arbitrary assumption of information which by hypothesis we do not have."

3.2.2 Introducing the mean field parameters into the system

Let $\bar{\boldsymbol{q}}_a^n$ and $\bar{\boldsymbol{p}}_a^n$ are the mean position and momenta of atom (n, a). Let $\sqrt{3}\tau_a^n$ and $\sqrt{3}\sigma_a^n$ are standard deviation from mean position and mean momenta. We have

$$< \boldsymbol{q}_a^n > := \bar{\boldsymbol{q}}_a^n \quad \forall n = 1, 2, .., Q \,\, \forall a = 1, 2, ..., N \tag{3.2.5}$$

$$< \boldsymbol{p}_a^n > := \bar{\boldsymbol{p}}_a^n \quad \forall n = 1, 2, .., Q \,\, \forall a = 1, 2, ..., N \tag{3.2.6}$$

$$< |\boldsymbol{q}_a^n - \bar{\boldsymbol{q}}_a^n|^2 > := 3(\tau_a^n)^2 \quad \forall n = 1, 2, .., Q \,\, \forall a = 1, 2, ..., N \tag{3.2.7}$$

$$< |\boldsymbol{p}_a^n - \bar{\boldsymbol{p}}_a^n|^2 > := 3(\sigma_a^n)^2 \quad \forall n = 1, 2, .., Q \,\, \forall a = 1, 2, ..., N \tag{3.2.8}$$

Combining last two constraints into one as follows

$$< |\boldsymbol{p}_a^n - \bar{\boldsymbol{p}}_a^n|^2 > + (w_a^n)^2 < |\boldsymbol{q}_a^n - \bar{\boldsymbol{q}}_a^n|^2 > = 6(\sigma_a^n)^2 \tag{3.2.9}$$

Where, we call w_a^n the mean frequency of atom (n, a) and define it as follows

$$w_a^n := \frac{\sigma_a^n}{\tau_a^n}$$

3.2.3   Maximum entropy principle

First, the probability density function must satisfy following normalization condition

$$\frac{1}{(QN)! h^{3QN}} \int_{\bar{\Gamma}} p \prod_{n=1}^{Q} d\boldsymbol{q}^n d\boldsymbol{p}^n = 1 \tag{3.2.10}$$

Following is the statement of maximum entropy principle subjected to constraint Equation 3.2.9 and Equation 3.2.10

$$\sup_{p:\bar{\Gamma} \to [0,1]} - \frac{k_B}{(QN)! h^{3QN}} \int_{\bar{\Gamma}} [p \log p + \lambda p +$$

$$p \sum_{a=1}^{N} \sum_{n=1}^{Q} \beta_a^n \left[|\boldsymbol{p}_a^n - \bar{\boldsymbol{p}}_a^n|^2 (w_a^n)^2 |\boldsymbol{q}_a^n - \bar{\boldsymbol{q}}_a^n|^2 \right] \Bigg] \prod_{m=1}^{Q} d\boldsymbol{q}^m d\boldsymbol{p}^m \tag{3.2.11}$$

where λ is a Lagrange multiplier corresponding to normalization constraint, and $\left\{ (\beta_a^n)_1^N \right\}_{n=1}^{Q}$ are QN number of Lagrange multiplier corresponding to the standard deviation constraint as written in Equation 3.2.9.

Taking the variation of functional, and enforcing its value to be zero, we get the desired probability density function. Further, by using constraint equations we determine the values of Lagrange multipliers. The results are as follows

$$p\left(\mathbf{q}, \mathbf{p} | \bar{\mathbf{q}}, \bar{\mathbf{p}}, w, \sigma\right) = \frac{1}{Z} \prod_{n=1}^{Q} \prod_{a=1}^{N} \exp \left[-\frac{|\boldsymbol{p}_a^n - \bar{\boldsymbol{p}}_a^n|^2 + (w_a^n)^2 |\boldsymbol{q}_a^n - \bar{\boldsymbol{q}}_a^n|^2}{2(\sigma_a^n)^2} \right] \tag{3.2.12}$$

and the partition function is

$$Z = \frac{1}{(QN)! h^{3QN}} \prod_{n=1}^{Q} \prod_{a=1}^{N} \left(\pi 2(\sigma_a^n)^2\right)^{3/2} \left(\pi 2 \frac{(\sigma_a^n)^2}{(w_a^n)^2}\right)^{3/2} \tag{3.2.13}$$

We observe that we can also write the probability density function and partition function as the product of the atomic probability density function and atomic partition function. Let us denote p_a^n as a probability density function of atom (n, a) and Z_a^n as a partition function of atom (n, a). We note that the probability of individual atom only depend on its mean position, mean momenta, and standard deviation parameters.

We write the probability density function and Z in atomic form as follows

$$p\left(\mathbf{q}, \mathbf{p} | \bar{\mathbf{q}}, \bar{\mathbf{p}}, w, \sigma\right) := \prod_{n=1}^{Q} \prod_{a=1}^{N} p_a^n(\boldsymbol{q}_a^n, \boldsymbol{p}_a^n | \bar{\boldsymbol{q}}_a^n, \bar{\boldsymbol{p}}_a^n, w_a^n, \sigma_a^n) \tag{3.2.14}$$

$$Z := \prod_{n=1}^{Q} \prod_{a=1}^{N} Z_a^n \tag{3.2.15}$$

where

$$p_a^n(\boldsymbol{q}_a^n, \boldsymbol{p}_a^n | \bar{\boldsymbol{q}}_a^n, \bar{\boldsymbol{p}}_a^n, w_a^n, \sigma_a^n) := \frac{1}{Z_a^n} \exp \left[-\frac{|\boldsymbol{p}_a^n - \bar{\boldsymbol{p}}_a^n|^2 + (w_a^n)^2 |\boldsymbol{q}_a^n - \bar{\boldsymbol{q}}_a^n|^2}{2(\sigma_a^n)^2} \right] \tag{3.2.16}$$

and

$$Z_a^n := \frac{1}{[(QN)!]^{1/QN} h^3} \left(\pi 2(\sigma_a^n)^2\right)^{3/2} \left(\pi 2 \frac{(\sigma_a^n)^2}{(w_a^n)^2}\right)^{3/2} \tag{3.2.17}$$

3.2.4 Variational mean field theory

Once we have the simplified functional form of p, we now need to determine the mean field parameters in the p. We use the variational mean field theory to determine the mean field parameters. We explain the theory in next few paragraphs.

Let F be the exact free energy and let F_p be the free energy associated to p. They are defined as follows

$$\exp[-\beta F] = Z_{exact} = \frac{1}{(QN)!h^{3QN}} \int_{\bar{\Gamma}} e^{[-\beta H(\mathbf{q}, \mathbf{p})]} d\mathbf{q} d\mathbf{p} \qquad (3.2.18)$$

and

$$F_p = <H>_p -TS[p] \qquad (3.2.19)$$

where T is the temperature and is defined as

$$T = \left(\frac{\partial E}{\partial S}\right)_{\mathbf{q}} \qquad (3.2.20)$$

According to the variational mean field theory, the best probability density function is the one which minimizes F_p. Following inequality, see [Chaikin and Lubensky, 1995], then is used to find the mean field parameters in p such that F_p is minimum and closest to the exact free energy F

$$F \leq F_p \qquad (3.2.21)$$

3.3 Internal energy, free energy and statement of problem

In this section, we will talk about the derivation of free energy as a function of mean position, mean momenta, mean frequency, and temperature. The minimization problem for the system is also presented in this section.

3.3.1 Entropy

We use expression Equation 3.2.4 to compute entropy

$$
\begin{aligned}
S &= \frac{-k_B}{(QN)!h^{3QN}} \int_{\bar{\Gamma}} p \log p \prod_{m=1}^{Q} d\boldsymbol{q}^m d\boldsymbol{p}^m \\
&= \frac{-k_B}{(QN)!h^{3QN}} \int_{\bar{\Gamma}} p \log \left[\prod_{n=1}^{Q} \prod_{a=1}^{N} p_a^n \right] \prod_{m=1}^{Q} d\boldsymbol{q}^m d\boldsymbol{p}^m \\
&= k_B \left\{ -\log \left[(QN)! \right] + 3QN + 3\log \left[\prod_{n=1}^{Q} \prod_{a=1}^{N} \frac{(\sigma_a^n)^2}{\hbar w_a^n} \right] \right\}
\end{aligned}
\tag{3.3.1}
$$

approximating $\log \left[(QN)! \right]$ by assuming QN to be very large number

$$
\log \left[(QN)! \right] \approx QN \log(QN) - QN
\tag{3.3.2}
$$

Finally, we get

$$
S = k_B \left\{ -QN \log(QN) + 4QN + 3\log \left[\prod_{n=1}^{Q} \prod_{a=1}^{N} \frac{(\sigma_a^n)^2}{\hbar w_a^n} \right] \right\}
\tag{3.3.3}
$$

We can also express the entropy as the sum of atomic entropies $S = \sum_{n=1}^{Q} \sum_{a=1}^{N} S_a^n$, where,

$$
S_a^n := 3k_B \log \left[\frac{(\sigma_a^n)^2}{\hbar w_a^n} \right] + 4k_B - k_B \log(QN)
\tag{3.3.4}
$$

After inverting the Equation 3.3.4, we get

$$
\sigma_a^n = \sqrt{\hbar w_a^n} \exp \left[\frac{S_a^n}{3k_B} - \frac{4}{3} + \frac{1}{3}\log(QN) \right]
\tag{3.3.5}
$$

3.3.2 Internal energy

Internal energy is defined as the phase average of Hamilton. We assume that the Hamilton of a system can be written as atomic sum. That is,

$$H(\mathbf{q}, \mathbf{p}) = \sum_{n=1}^{Q} \sum_{a=1}^{N} H_a^n(\mathbf{q}, \mathbf{p}) \tag{3.3.6}$$

Where, we define H_a^n as

$$H_a^n(\mathbf{q}, \mathbf{p}) = \frac{1}{2} |\boldsymbol{p}_a^n|^2 + V_a^n(\mathbf{q}) + \Phi_a^n(\mathbf{q}) \tag{3.3.7}$$

V_a^n is the interatomic potential and Φ_a^n is the electrostatic energy.

Internal energy is given by

$$E(\bar{\mathbf{q}}, \bar{\mathbf{p}}, w_a^n, \sigma_a^n) = < H >_p = \frac{1}{(QN)! h^{3QN}} \int_{\bar{\Gamma}} H(\mathbf{q}, \mathbf{p}) d\mathbf{q} d\mathbf{p} \tag{3.3.8}$$

In Appendix B, we talk about the calculation of phase average of kinetic energy, potential energy, and electrostatic energy. We also discuss the calculation of forces, which are derivatives of free energy on mean field parameters.

3.3.3 Temperature and entropy

Our goal is to derive the energy as a function of mean parameters and temperature. To incorporate the temperature in a system, we use the fundamental result of statistical mechanics: equipartition of energy.

Equipartition of energy: For a canonical system in thermal equilibrium, each quadratic term in the Hamiltonian contributes $k_B T/2$ to the mean Hamiltonian (or Internal Energy) of the system. See [Weiner, 2002].

We enforce the equipartition of energy through local kinetic energy, i.e.

$$< \frac{1}{2} |\boldsymbol{p}_a^n|^2 > = \frac{3}{2} k_B T_a^n \tag{3.3.9}$$

Assumption: We are interested in modeling the quasi-static process. Thus, we can assume $\bar{\boldsymbol{p}}_a^n = 0$, i.e. mean momenta is zero for all the atoms.

With the assumption of quasi-static and the equipartition of energy, we have

$$(\sigma_a^n)^2 = k_B T_a^n \tag{3.3.10}$$

Substituting above equation in entropy-sigma equation Equation 3.3.4, we get the equilibrium relation between the local entropy and the local temperature

$$S_a^n := 3k_B \log\left[\frac{k_B T_a^n}{\hbar w_a^n}\right] + 4k_B - k_B \log(QN) \tag{3.3.11}$$

3.3.4 Helmholtz free energy

Helmholtz free energy is defined as a Legendre transformation of the internal energy with respect to the entropy. For quasi-static process, we have

$$F\left(\mathbf{q}, \{T_a^n\}, \{w_a^n\}\right) = \inf_{\{S_a^n\}}\left\{E\left(\mathbf{q}, \{S_a^n\}, \{w_a^n\}\right) - \sum_{m=1}^{Q}\sum_{b=1}^{N} T_b^m S_b^m\right\} \tag{3.3.12}$$

Condition for infimum in Equation 3.3.12 is

$$\frac{\partial}{\partial S_b^m} E\left(\mathbf{q}, \{S_a^n\}, \{w_a^n\}\right) = T_b^m \tag{3.3.13}$$

In Equation 3.3.13, one has to compute the derivative of phase average of potential energy and electrostatic energy with respect to the entropy S_b^m. Relation in Equation 3.3.13 is the exact entropy-temperature relation. However, it is a difficult task. So, instead of using the relation between T and S as per Equation 3.3.13, we will use the relation given in Equation 3.3.11.

Then, the free energy is

$$F\left(\mathbf{q}, \{T_a^n\}, \{w_a^n\}\right) = \sum_{(n,a)\in\mathcal{L}} \frac{3}{2} k_B T_a^n + \sum_{(n,a)\in\mathcal{L}} <V_a^n>_p$$
$$+ \sum_{(n,a)\in\mathcal{L}} <\Phi_a^n>_p - \sum_{(n,a)\in\mathcal{L}} T_a^n\left(3k_B \log\left[\frac{k_B T_a^n}{\hbar w_a^n}\right] + 4k_B - k_B \log(QN)\right)$$
$$\tag{3.3.14}$$

3.3.5 Minimization problem

Mean field parameters, which are still unknown, will be determined by solving the following minimization problem for the quasi-static constant temperature problem

$$\min_{\bar{\mathbf{q}},\{w_a^n\}} \left[F\left(\mathbf{q}, T, \{w_a^n\}\right) + F_{ext}\left(\mathbf{q}, T, \{w_a^n\}\right) \right] \tag{3.3.15}$$

where T of the system is fixed and given, and F_{ext} is energy due to external field or force.

3.4 Quasicontinuum framework

In this section, we will talk about QC approximation of minimization problem stated in Equation 3.3.15. There are two main steps: selection of representative nodes, and using interpolation to write the field at other nodes in term of representative nodes. Let us also denote $\mathbf{q}$ as the mean displacement, without the bar on top, for simplicity. We will be only dealing with constant temperature (or equilibrium) and the quasi-static process. Thus, the temperature will be fixed and given, and the mean momenta will be zero.

3.4.1 Meshing of the lattice and interpolation

Recall that $\mathcal{L}$ represents the set of atom indices for whole system and $\mathcal{L}^n$ represents the atom indices of nth lattice. We mesh each lattice independently, and out of N number of atoms in each lattice, we chose c^n number of atoms, as a representative atoms. Let $\hat{\mathcal{L}}^n$ be list of representative atoms for n^{th} lattice. Let $\hat{\mathcal{K}}^n$ be triangulation of $\hat{\mathcal{L}}^n$. We will denote $\hat{\Psi}^n(\cdot; (n, a))$ the value of interpolation function, corresponding to rep. atom $(n, a) \in \hat{\mathcal{L}}^n$ of nth lattice, and, which takes value 1 at (n, a) and zero at all other rep. atoms.

$\hat{\Psi}^n$ satisfies

$$\hat{\Psi}^n((n, b); (n, a)) = \delta_{(n,b),(n,a)} \quad \forall (n, a), (n, b) \in \hat{\mathcal{L}}^n$$

Now, denote $\hat{\mathbf{q}}_a^n$ and $\hat{w}_a^n$ as displacement and mean frequency of rep. atoms of nth lattice. Then, displacement and frequency at remaining atoms will be given by

$$q_b^n = \sum_{(n,a) \in \hat{\mathcal{L}}^n} \hat{q}_a^n \hat{\Psi}^n(X_b^n; (n,a)) \quad \forall (n,b) \in \mathcal{L}^n \tag{3.4.1}$$

$$w_b^n = \sum_{(n,a) \in \hat{\mathcal{L}}^n} \hat{w}_a^n \hat{\Psi}^n(X_b^n; (n,a)) \quad \forall (n,b) \in \mathcal{L}^n \tag{3.4.2}$$

Thus, the field at atoms other than rep. atoms, depends on the field at rep. atoms through the interpolation function.

3.4.2 Minimization problem for unknowns at rep. atoms

We substitute Equation 3.4.1, Equation 3.4.2 in the expression of free energy Equation 3.3.14. Let F_{QC} denote the free energy as function of mean displacement and mean frequency of rep. atoms.

$$F_{QC}\left(\{\{\hat{q}_i^n\}_{i=1}^{c^n}\}_{n=1}^{Q}, \{\{\hat{w}_i^n\}_{i=1}^{c^n}\}_{n=1}^{Q}, T\right) = F\left(\mathbf{q}(\hat{q}), w(\hat{w}), T\right) \tag{3.4.3}$$

where $\mathbf{q}(\hat{q})$ means q_a^n is function of displacement at rep. atoms.

Minimization problem, for the unknowns at rep. atoms, is as follows

$$\min_{\hat{\mathbf{q}}, \hat{w}} \left[F_{QC}\left(\hat{\mathbf{q}}, \hat{w}, T\right) + F_{QC,ext}\left(\hat{\mathbf{q}}, \hat{w}, T\right)\right] \tag{3.4.4}$$

Where $\hat{\mathbf{q}}$ and $\hat{w}$ are the vector of displacement vector and frequency of all the rep. atoms. $\sum_{i=1}^{Q} c^i$ is the number of displacement vector unknowns and frequency unknowns in the system. This is compared to total QN number of displacement vector and frequency unknowns in minimization problem Equation 3.3.15.

3.4.3 Equations to solve

A derivative of the total energy, $F_{QC} + F_{QC,ext}$, with respect to the position and frequency of the rep. atom has to be zero to minimize the total energy. Thus, we need to solve the following non-linear equation

$$\frac{\partial}{\partial \hat{\boldsymbol{q}}_a^n} F_{QC}\left(\hat{\mathbf{q}}, \{\hat{w}_a^n\}, T\right) = \mathbf{0} \tag{3.4.5}$$

$$\frac{\partial}{\partial \hat{w}_a^n} F_{QC}\left(\hat{\mathbf{q}}, \{\hat{w}_a^n\}, T\right) = 0 \tag{3.4.6}$$

We have

$$\hat{\boldsymbol{f}}_a^n(\hat{\mathbf{q}}, \hat{w}) := \frac{\partial}{\partial \hat{\boldsymbol{q}}_a^n} F_{QC}\left(\hat{\mathbf{q}}, \{\hat{w}_a^n\}, T\right)$$

$$= \sum_{(n,b)\in\mathcal{L}^n} \left[\frac{\partial}{\partial \boldsymbol{q}_b^n} F\left(\mathbf{q}(\hat{\mathbf{q}}), w(\hat{w}), T\right)\right] \Psi((n,b);(n,a)) \tag{3.4.7}$$

Where F is the free energy given in Equation 3.3.14, and $\mathbf{q}(\hat{\mathbf{q}})$ shows that the displacement of an atom is the function of the displacement of rep. atom. So, to compute the force at each rep. atom, one has to calculate the term in the square bracket in Equation 3.4.7, for each atom in a material.

Consider the sum S

$$S = \sum_{(n,a)\in\mathcal{L}^n} g((n,a)) \tag{3.4.8}$$

Where g is some function of atoms of the lattice. The expression of force $\hat{\boldsymbol{f}}_a^n$ is similar to summation in S.

We can see in Equation 3.4.7, or in S, that forces on rep. atom is the sum of forces on a large number of atoms. Therefore, we need to approximate and simplify the force calculation at rep. atoms.

Simplified force calculation

Node based summation

One way we can approximate S is by computing the g at rep. atoms and summing these with some weight $\hat{n}$. Then

$$S \approx \hat{S} = \sum_{(n,a)\in\hat{\mathcal{L}}^n} \hat{n}(n,a)g(n,a) \tag{3.4.9}$$

where choice of weight $\hat{n}$ is such that summation of interpolation function $\Psi(\cdot; (n, a))$ is exact. That is

$$S = \sum_{(n,b)\in\mathcal{L}^n} \Psi(n, b; n, a) = \sum_{(n,c)\in\hat{\mathcal{L}}^n} \hat{n}(n, c)\Psi(n, c; n, a) = \hat{n}(n, a) \qquad (3.4.10)$$

$$\Rightarrow \hat{n}(n, a) = \sum_{(n,b)\in\mathcal{L}^n} \Psi(n, b; n, a) \qquad (3.4.11)$$

In [Knapp and Ortiz, 2001], we can see that above choice of lattice sum is not appropriate. So, we improve this approximation.

Cluster based summation

We improve the node based summation by considering set of atoms, around each rep. atoms, and summing over these atoms and multiplying by weights for each rep. atoms. Define set of cluster sites, $\hat{\mathcal{C}}(n, a)$ for rep. atom (n, a) as follows

$$\hat{\mathcal{C}}(n, a) := \{(n, b) \in \mathcal{L}^n : |\boldsymbol{X}_a^n - \boldsymbol{X}_b^n| \leq \hat{r}(n, a)\} \qquad (3.4.12)$$

where $\hat{r}(n, a)$ is some cluster radius corresponding to (n, a).

We approximate sum as

$$S \approx \hat{S} = \sum_{(n,a)\in\hat{\mathcal{L}}^n} \hat{n}(n, a) \left[\sum_{(n,b)\in\hat{\mathcal{C}}(n,a)} g(n, b) \right] \qquad (3.4.13)$$

As cluster radius increases the number of atoms in summation increases. Moreover, for smaller cluster radius we will have stability issues, pointed out in [Knapp and Ortiz, 2001]. Thus, choice of cluster radius is such that it balances the stability concern and computational expense.

Equations to solve : Cluster based summation

We chose cluster based summation approximation. Following are the set of equations we will have to solve

$$\hat{\boldsymbol{f}}_a^n(\hat{\mathbf{q}}, \hat{w})$$

$$= \sum_{(n,b)\in\hat{\mathcal{L}}^n} \hat{n}(n,b) \left\{ \sum_{(n,c)\in\hat{\mathcal{C}}(n,b)} \frac{\partial}{\partial \boldsymbol{q}_c^n} \left[F(\mathbf{q}(\hat{\mathbf{q}}), w(\hat{w}), T) + F_{ext}(\mathbf{q}(\hat{\mathbf{q}}), w(\hat{w}), T) \right] \right\} \Psi((n,b);(n,a))$$

$$= \mathbf{0} \tag{3.4.14}$$

$$\hat{f}_{wa}^{\,n}(\hat{\mathbf{q}}, \hat{w})$$

$$= \sum_{(n,b)\in\hat{\mathcal{L}}^n} \hat{n}(n,b) \left\{ \sum_{(n,c)\in\hat{\mathcal{C}}(n,b)} \frac{\partial}{\partial w_c^n} \left[F(\mathbf{q}(\hat{\mathbf{q}}), w(\hat{w}), T) + F_{ext}(\mathbf{q}(\hat{\mathbf{q}}), w(\hat{w}), T) \right] \right\} \Psi((n,b);(n,a))$$

$$= \mathbf{0} \tag{3.4.15}$$

3.4.4   Adaptive meshing

The code has adaptive meshing, meaning at each iteration it checks the energy and deformation of each element, and if needed further divides the element into smaller parts. We briefly mention the criteria for meshing. Let $\Pi_E(e)$ be the second invariant of deviatoric part of the Lagrangian strain tensor for element e. We define adaption indicator, $\epsilon(e)$ of element e as

$$\epsilon(e) = \sqrt{|\Pi_E(e)|} h(e) \tag{3.4.16}$$

where $h(e)$ is the size of element e. Then, element e is accepted if it satisfies following criteria

$$\frac{\epsilon(e)}{b} < TOL \tag{3.4.17}$$

where TOL is tolerance, and b is the magnitude of the smallest burgers vector of the crystal.

3.5   Numerical strategy for the electrostatic energy

Since nonlocal energy is a constant random function, we need to find the dipole field for the mean state configuration and then compute the nonlocal energy. Further, as for local

energy, the interatomic potentials include local electrostatics interaction. Hence, the phase average of interatomic potential also includes the phase average of local electrostatics energy.

3.5.1 Electrostatics energy density

Consider Figure 3.5.1. Suppose we want to compute the electric field at atom shown in red color. We consider the box with the red point at the center. We use continuum limit approximation, i.e. energy due to dipole field at elements outside the box. For all the atoms inside the box, we do exact Coulombic interaction. Since energy due to dipole field is sensitive to the boundary conditions, see [Marshall and Dayal, 2013], we also take into account the surface charge density at the surface of intersection between the box and mesh element. We compute phase average of the interaction of the charges within a box with the charge at red atoms. For contribution outside the box, we use continuum limit expression of non-local energy. Moreover, non-local energy, as we observed in Chapter 2, does not depend on atomic fluctuations.

Energy due to dipole field We consider the linear interpolation in each element. Therefore, the deformation gradient is constant in each element. As a result, dipole moment would be constant in each element as it is a linear function of deformation gradient. The nonlocal energy, see Equation 2.4.29 of subsection 2.4.2, can also be written as follows

$$
\begin{aligned}
\int_{\substack{\boldsymbol{x},\boldsymbol{x}'\in\Omega,\\ \boldsymbol{x}\neq\boldsymbol{x}'}} \hat{\boldsymbol{p}}(\boldsymbol{x}')\cdot\boldsymbol{K}(\boldsymbol{x}-\boldsymbol{x}')\hat{\boldsymbol{p}}(\boldsymbol{x})dV_{\boldsymbol{x}}dV_{\boldsymbol{x}'} &= \int_{\substack{\boldsymbol{x},\boldsymbol{x}'\in\Omega,\\ \boldsymbol{x}\neq\boldsymbol{x}'}} \boldsymbol{\nabla}\cdot\hat{\boldsymbol{p}}(\boldsymbol{x}')G(\boldsymbol{x}-\boldsymbol{x}')\hat{\boldsymbol{p}}(\boldsymbol{x})dV_{\boldsymbol{x}}dV_{\boldsymbol{x}'} \\
&+ \int_{\substack{\boldsymbol{x},\boldsymbol{x}'\in\partial\Omega,\\ \boldsymbol{x}\neq\boldsymbol{x}'}} \boldsymbol{n}(\boldsymbol{x}')\cdot\hat{\boldsymbol{p}}(\boldsymbol{x}')G(\boldsymbol{x}-\boldsymbol{x}')\boldsymbol{n}(\boldsymbol{x})\cdot\hat{\boldsymbol{p}}(\boldsymbol{x})dS_{\boldsymbol{x}}dS_{\boldsymbol{x}'} \\
&- 2\int_{\substack{\boldsymbol{x}\in\Omega,\boldsymbol{x}'\in\partial\Omega,\\ \boldsymbol{x}\neq\boldsymbol{x}'}} \boldsymbol{n}(\boldsymbol{x}')\cdot\hat{\boldsymbol{p}}(\boldsymbol{x}')G(\boldsymbol{x}-\boldsymbol{x}')\boldsymbol{\nabla}\cdot\hat{\boldsymbol{p}}(\boldsymbol{x})dV_{\boldsymbol{x}}dS_{\boldsymbol{x}'}
\end{aligned}
\tag{3.5.1}
$$

where G is the Green's function and satisfies $\boldsymbol{K}(\boldsymbol{x}) = \boldsymbol{\nabla}\cdot\boldsymbol{\nabla}G(\boldsymbol{x})$.

Since $\hat{\boldsymbol{p}}$ is constant in each element, we do not need to compute the energy due to $\boldsymbol{\nabla}\cdot\hat{\boldsymbol{p}}$ inside the element. All we need to compute is the energy due to jump in $\boldsymbol{n}\cdot\hat{\boldsymbol{p}}$ at all

surface. Note that all this is possible because $\hat{\boldsymbol{p}}$ is a constant random function, as shown in section 2.4.
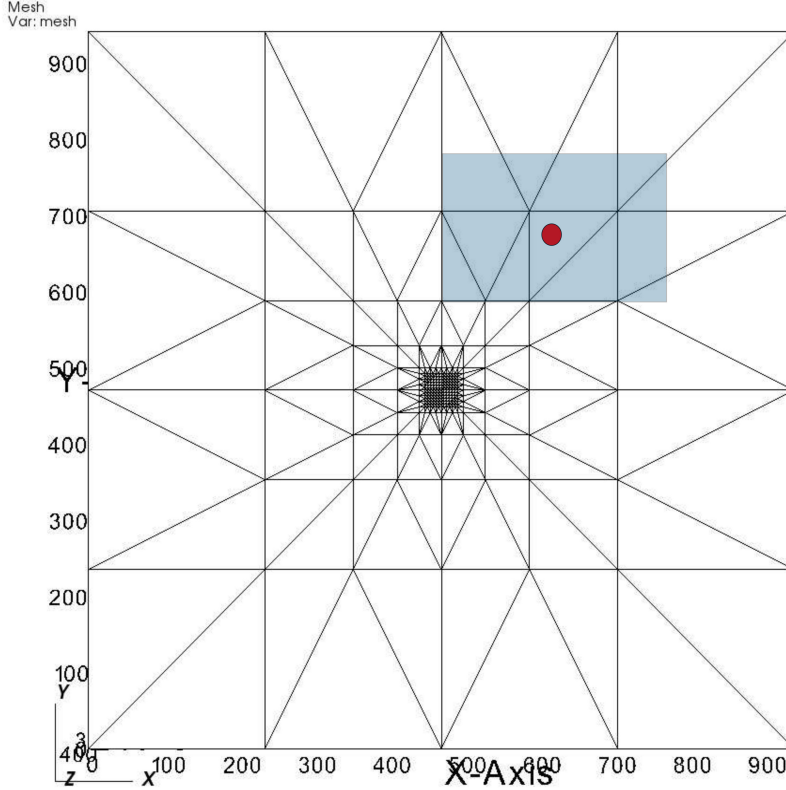
Figure 3.5.1: Typical mesh in Quasicontinuum method

3.5.2 Dependence of the phase average of charge-charge interaction on fluctuations

Let (n, a) is index corresponding to atom in Figure 3.5.1. We will now show that dependence of Coulombic energy on mean frequency decays very fast as the distance between atom (n, a) and (m, b) increases. This suggests that we should only compute phase average of Coulomb interaction for atom pair, very close to each other, say 2 to 3 atomic distance, and for the pair of the atom with more than 3 atomic distance away, we should approximate the energy using mean position of atoms.

By Taylor series expansion and integration:

77

$$\frac{1}{\left| \sqrt{2}\frac{\sigma_a^n}{w_a^n}\boldsymbol{x}_1 + \bar{\boldsymbol{q}}_a^n - \sqrt{2}\frac{\sigma_b^m}{w_b^m}\boldsymbol{x}_2 - \bar{\boldsymbol{q}}_b^m \right|}$$

$$= \frac{1}{|\bar{\boldsymbol{q}}_a^n - \bar{\boldsymbol{q}}_b^m|} + \left[\frac{\partial}{\partial \boldsymbol{q}}\frac{1}{|\boldsymbol{q}|} \right]_{\boldsymbol{q}=\bar{\boldsymbol{q}}_a^n - \bar{\boldsymbol{q}}_b^m} \cdot \left(\sqrt{2}\frac{\sigma_a^n}{w_a^n}\boldsymbol{x}_1 - \sqrt{2}\frac{\sigma_b^m}{w_b^m}\boldsymbol{x}_2 \right)$$

$$+ \frac{1}{2}\left[\frac{\partial^2}{\partial \boldsymbol{q}\partial \boldsymbol{q}}\frac{1}{|\boldsymbol{q}|} \right]_{\boldsymbol{q}=\bar{\boldsymbol{q}}_a^n - \bar{\boldsymbol{q}}_b^m} : \left(\sqrt{2}\frac{\sigma_a^n}{w_a^n}\boldsymbol{x}_1 - \sqrt{2}\frac{\sigma_b^m}{w_b^m}\boldsymbol{x}_2 \right) \otimes \left(\sqrt{2}\frac{\sigma_a^n}{w_a^n}\boldsymbol{x}_1 - \sqrt{2}\frac{\sigma_b^m}{w_b^m}\boldsymbol{x}_2 \right)$$

$$+ F_{third\ order} + F_{fourth\ order} \tag{3.5.2}$$

Then

$$\left\langle \frac{Q(n)Q(m)}{|\bar{\boldsymbol{q}}_a^n - \bar{\boldsymbol{q}}_b^m|} \right\rangle_p$$

$$= \left(\frac{1}{\sqrt{\pi}} \right)^6 \frac{Q(n)Q(m)}{|\bar{\boldsymbol{q}}_a^n - \bar{\boldsymbol{q}}_b^m|} \int_{\mathbb{R}^3 \times \mathbb{R}^3} \exp\left[-|\boldsymbol{x}_1|^2 - |\boldsymbol{x}_2|^2 \right] d\boldsymbol{x}_1 d\boldsymbol{x}_2$$

$$+ \left(\frac{1}{\sqrt{\pi}} \right)^6 \left[\frac{\partial}{\partial \boldsymbol{q}}\frac{1}{|\boldsymbol{q}|} \right]_{\boldsymbol{q}=\bar{\boldsymbol{q}}_a^n - \bar{\boldsymbol{q}}_b^m} \cdot \int_{\mathbb{R}^3 \times \mathbb{R}^3} \left(\sqrt{2}\frac{\sigma_a^n}{w_a^n}\boldsymbol{x}_1 - \sqrt{2}\frac{\sigma_b^m}{w_b^m}\boldsymbol{x}_2 \right) \exp[-|\boldsymbol{x}_1|^2 - |\boldsymbol{x}_2|^2]d\boldsymbol{x}_1 d\boldsymbol{x}_2$$

$$+ \frac{1}{2}\left(\frac{1}{\sqrt{\pi}} \right)^6 \left[\frac{\partial^2}{\partial \boldsymbol{q}\partial \boldsymbol{q}}\frac{1}{|\boldsymbol{q}|} \right]_{\boldsymbol{q}=\bar{\boldsymbol{q}}_a^n - \bar{\boldsymbol{q}}_b^m} : \int_{\mathbb{R}^3 \times \mathbb{R}^3} \left(\sqrt{2}\frac{\sigma_a^n}{w_a^n}\boldsymbol{x}_1 - \sqrt{2}\frac{\sigma_b^m}{w_b^m}\boldsymbol{x}_2 \right) \otimes \left(\sqrt{2}\frac{\sigma_a^n}{w_a^n}\boldsymbol{x}_1 - \sqrt{2}\frac{\sigma_b^m}{w_b^m}\boldsymbol{x}_2 \right)$$

$$\exp\left[-|\boldsymbol{x}_1|^2 - |\boldsymbol{x}_2|^2 \right] d\boldsymbol{x}_1 d\boldsymbol{x}_2$$

$$+ \int_{\mathbb{R}^3 \times \mathbb{R}^3} F_{third\ order} + F_{fourth\ order} \exp[-|\boldsymbol{x}_1|^2 - |\boldsymbol{x}_2|^2]d\boldsymbol{x}_1 d\boldsymbol{x}_2 \tag{3.5.3}$$

Where $Q(n)$ is charge of atom of nth lattice. Note that $\int_{\mathbb{R}} x \exp[-x^2]dx = 0$. Because of this property, first order and third order term will be zero, and some of the terms in second order will be zero.

Also, note that

$$\frac{1}{2}\left(\frac{1}{\sqrt{\pi}} \right)^6 \int_{\mathbb{R}^6} \left(\sqrt{2}\frac{\sigma_a^n}{w_a^n}\boldsymbol{x}_1 - \sqrt{2}\frac{\sigma_b^m}{w_b^m}\boldsymbol{x}_2 \right) \otimes \left(\sqrt{2}\frac{\sigma_a^n}{w_a^n}\boldsymbol{x}_1 - \sqrt{2}\frac{\sigma_b^m}{w_b^m}\boldsymbol{x}_2 \right) e^{(-|\boldsymbol{x}_1|^2 - |\boldsymbol{x}_2|^2)}d\boldsymbol{x}_1 d\boldsymbol{x}_2$$

$$= \left[\left(\frac{\sqrt{2}\sigma_a^n}{w_a^n} \right)^2 + \left(\frac{\sqrt{2}\sigma_b^m}{w_b^m} \right)^2 \right] \boldsymbol{I} \tag{3.5.4}$$

And

$$\left[\frac{\partial^2}{\partial \boldsymbol{q} \partial \boldsymbol{q}} \frac{1}{|\boldsymbol{q}|}\right]_{\boldsymbol{q}=\bar{\boldsymbol{q}}_a^n - \bar{\boldsymbol{q}}_b^m} : \boldsymbol{I} = \left(3\frac{(\bar{\boldsymbol{q}}_a^n - \bar{\boldsymbol{q}}_b^m)\otimes(\bar{\boldsymbol{q}}_a^n - \bar{\boldsymbol{q}}_b^m)}{|\bar{\boldsymbol{q}}_a^n - \bar{\boldsymbol{q}}_b^m|^5} - \frac{\boldsymbol{I}}{|\bar{\boldsymbol{q}}_a^n - \bar{\boldsymbol{q}}_b^m|^3}\right) : \boldsymbol{I} = 0 \qquad (3.5.5)$$

Thus, $\Psi_{(n,a)(m,b)}$ can be written as

$$\langle \frac{Q(n)Q(m)}{|\bar{\boldsymbol{q}}_a^n - \bar{\boldsymbol{q}}_b^m|}\rangle_p = \frac{Q(n)Q(m)}{|\bar{\boldsymbol{q}}_a^n - \bar{\boldsymbol{q}}_b^m|} + O(\frac{1}{R_{(n,a)}^5}) \qquad (3.5.6)$$

Thus, we have $1/r^5$ decay in dependence of Ψ on fluctuations. Meaning, for atoms far apart, we can use $\langle \frac{Q(n)Q(m)}{|\bar{\boldsymbol{q}}_a^n - \bar{\boldsymbol{q}}_b^m|}\rangle_p \approx \frac{Q(n)Q(m)}{|\bar{\boldsymbol{q}}_a^n - \bar{\boldsymbol{q}}_b^m|}$.

3.6 Mean frequency from quasi-harmonic approximation

We will analytically compute the mean frequency for the quasi-harmonic approximation of energy. Further, we will show that any potential which is of type $1/|\boldsymbol{x}|$ contributes nothing to mean frequency. Note that Coulombic interactions have $1/|\boldsymbol{x}|$. This is why we found in the previous section that dependence of energy on mean frequency decays like $1/r^5$. If it was not the case, the decay would have been of the type $1/r^3$.

Interatomic potential We do Taylor series expansion, up to second order, of potential energy as follows

$$V(\mathbf{q}) = V(\bar{\mathbf{q}}) + \frac{\partial V(\mathbf{q})}{\partial \mathbf{q}} |_{\mathbf{q}=\bar{\mathbf{q}}} \cdot (\mathbf{q} - \bar{\mathbf{q}}) + \frac{1}{2}\frac{\partial^2 V(\mathbf{q})}{\partial \mathbf{q}^2} |_{\mathbf{q}=\bar{\mathbf{q}}} : (\mathbf{q} - \bar{\mathbf{q}})\otimes(\mathbf{q} - \bar{\mathbf{q}}) \qquad (3.6.1)$$

Defining second order derivative of total potential energy as

$$\boldsymbol{H}(\bar{\mathbf{q}}) = \frac{\partial^2 V(\mathbf{q})}{\partial \mathbf{q}^2} |_{\mathbf{q}=\bar{\mathbf{q}}} \qquad (3.6.2)$$

$$\boldsymbol{H}_{(n,a),(m,b))}(\bar{\mathbf{q}}) = \frac{\partial^2 V(\mathbf{q})}{\partial \boldsymbol{q}_a^n \partial \boldsymbol{q}_b^m} |_{\substack{\boldsymbol{q}_a^n = \bar{\mathbf{q}}_a^n, \\ \boldsymbol{q}_b^m = \bar{\mathbf{q}}_b^m}} \qquad (3.6.3)$$

Thus

$$\frac{1}{2}\frac{\partial^2 V(\mathbf{q})}{\partial \mathbf{q}^2}\big|_{\mathbf{q}=\bar{\mathbf{q}}} : (\mathbf{q} - \bar{\mathbf{q}}) \otimes (\mathbf{q} - \bar{\mathbf{q}})$$

$$= \frac{1}{2}\sum_{(n,a),(m,b)} \boldsymbol{H}_{(n,a),(m,b))}(\bar{\mathbf{q}}) : (\boldsymbol{a}_a^n - \bar{\boldsymbol{q}}_a^n) \otimes (\boldsymbol{q}_b^m - \bar{\boldsymbol{q}}_b^m) \tag{3.6.4}$$

Taking phase average of Equation 3.6.1, and noting that phase average of $\bar{\boldsymbol{q}}_a^n - \boldsymbol{q}_a^n$ is zero, as $\bar{\boldsymbol{q}}_a^n$ is mean of position of atom (n, a), we have

$$< V > = V(\bar{\mathbf{q}}) + \frac{1}{2}\sum_{(n,a)} \left(\frac{\sigma_a^n}{w_a^n}\right)^2 \boldsymbol{I} : \boldsymbol{H}_{(n,a),(n,a)} \tag{3.6.5}$$

Electrostatics energy   For $\Phi(\mathbf{q}) = \sum_{(n,a),(m,b)} Q^n Q^m / |\boldsymbol{q}_a^n - \boldsymbol{q}_b^m|$, the trace of second derivative is zero. That is

$$\boldsymbol{I} : \frac{\partial^2}{\partial \boldsymbol{q}_a^n \partial \boldsymbol{q}_a^n} \frac{1}{|\boldsymbol{q}_a^n - \boldsymbol{q}_b^m|} = 0 \qquad \forall (n, a)(m, b) \tag{3.6.6}$$

We substitute the quasi-harmonic approximation to the free energy in Equation 3.3.14, we get

$$F(\bar{\mathbf{q}}, T_a^n, w_a^n) = \sum_{(n,a)} \frac{3}{2} k_B T_a^n + V(\bar{\mathbf{q}}) + \frac{1}{2}\sum_{(n,a)} \left(\frac{\sigma_a^n}{w_a^n}\right)^2 \boldsymbol{I} : \boldsymbol{H}_{(n,a),(n,a)}(\bar{\mathbf{q}})$$

$$- \sum_{(n,a)} T_a^n \left(3 k_B \log\left[\frac{k_B T_a^n}{\hbar w_a^n}\right] + 4 k_B - k_B \log(QN)\right) \tag{3.6.7}$$

Minimizing above free energy with respect to w_a^n and noting that $(\sigma_a^n)^2 = k_B T_a^n$, we get

$$(w_a^n)^2 = \frac{1}{3} Tr \boldsymbol{H}_{(n,a),(n,a)} \tag{3.6.8}$$

As we can see, the electrostatics energy contributes nothing to the mean frequency in quasi-harmonic approximation.

3.7 Analyzing interatomic potentials with zero trace of the second derivative

We would like to know which classes of Kernels have the trace of its second order derivative zero.

Proposition 10. *Let $\phi : \mathbb{R}^+ \to \mathbb{R}$ is pairwise potential. Let energy of system of N atoms is given by*

$$E(\{x\}) = \frac{1}{2} \sum_{\substack{i,j=1,\dots,N, \\ i \neq j}} \phi(|x_i - x_j|) \tag{3.7.1}$$

The energy given by above equation will have zero trace of the second derivative only if ϕ satisfies the following ordinary differential equation

$$r\phi''(r) + 2\phi'(r) = 0 \qquad \forall r > 0 \tag{3.7.2}$$

Further, it can be shown that only $\phi(r) = c_1 + c_2/r$, $r > 0$, satisfy the condition.

Proof. We compute the second derivative of Energy as follows

$$
\begin{aligned}
\boldsymbol{H}_{ii}(\{x\}) &= \frac{\partial^2 E}{\partial x_i \partial x_i} \\
&= \sum_{j \neq i} \frac{\partial^2 \phi(|x_i - x_j|)}{\partial x_i \partial x_i} \\
&= \sum_{j \neq i} \left[\phi'(|x_i - x_j|) \frac{\boldsymbol{I}}{|x_i - x_j|} - \phi'(|x_i - x_j|) \frac{(x_i - x_j) \otimes (x_i - x_j)}{|x_i - x_j|^3} \right. \\
&\quad \left. + \phi''(|x_i - x_j|) \frac{(x_i - x_j) \otimes (x_i - x_j)}{|x_i - x_j|^2} \right]
\end{aligned}
\tag{3.7.3}
$$

Trace of $\boldsymbol{H}_{ii}$ is

$$Tr\boldsymbol{H}_{ii}(\{x\}) = \sum_{j \neq i} \left[\frac{2\phi'(|x_1 - x_j|)}{|x_i - x_j|} + \phi''(|x_i - x_j|) \right] \tag{3.7.4}$$

Since, we want $\boldsymbol{H}_{ii}$ to be zero, for all i, and for all possible $\{bx_i\} \subset \mathbb{R}^{3N}$, ϕ mush satisfy following equation

$$\frac{2\phi'(r)}{r} + \phi''(r) = 0 \qquad \forall r > 0$$
$$\Rightarrow r\phi''(r) + 2\phi'(r) = 0 \qquad \forall r > 0 \tag{3.7.5}$$

So, ϕ needs to be the solution of above ordinary differential equation.

We can solve this ode analytically as follows :

$$\int r\phi''(r)dr + 2\phi'(r)dr = c_1 \tag{3.7.6}$$

let $u = r\phi'$ then $du = \phi'dr + r\phi''dr$, we have

$$\int \left[r\phi'' + \phi' \right] dr + \int \phi'dr = c_1$$
$$\Rightarrow u + \phi = c_1$$
$$\Rightarrow r\phi' + \phi = c_1 \tag{3.7.7}$$

integrating above equation further, and using change in variable $v = r\phi$, then $dv = \phi dr + r\phi'dr$, we get

$$\int dv = c_1 r + c_2$$
$$\Rightarrow v = c_1 r + c_2$$
$$\Rightarrow \phi(r) = c_1 + \frac{c_2}{r} \tag{3.7.8}$$

We have the desired result.

$\square$

We also note that any kernel with $1/r$ property will have energy which contributes zero in quasi-harmonic approximation.

Chapter 4

Results

In this chapter, we will present some results which will demonstrate the functioning of our QC code. Before we present the results, we would like to talk about the structure of the code.
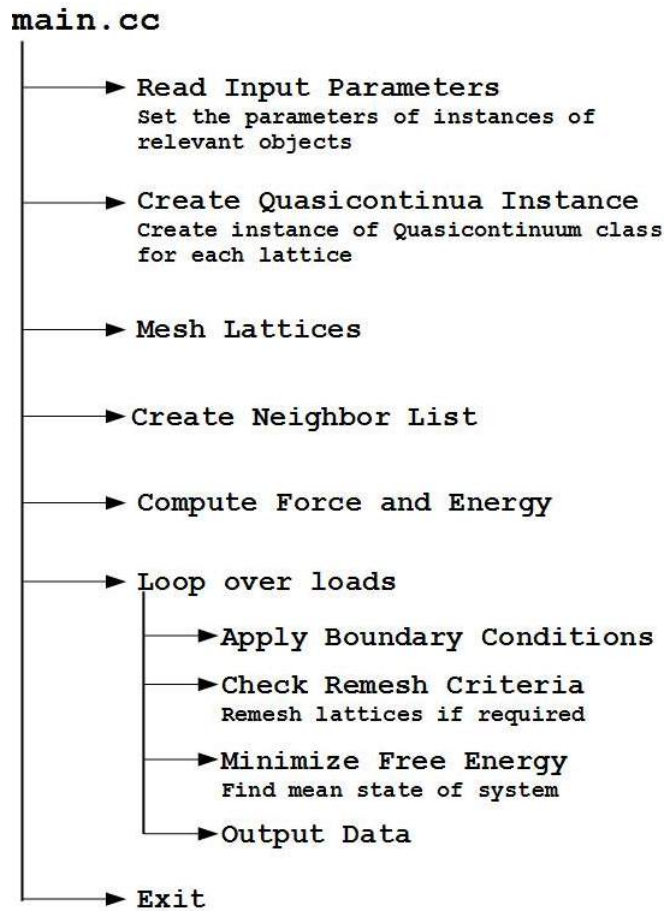
Figure 4.0.1: QC code flow

4.1 Structure of QC Code

The code is completely object oriented. We have main function main.cc which calls function of various classes. Some of the key classes and their functioning are

- *Quasicontinua* This is class object which contains *Quasicontinuum* class objects. For multilattice, think of this as class corresponding to a multilattice, and think of *Quasicontinuum* class as each individual lattices.

- *Quasicontinuum* This is a class object which contains information related to individual lattices. Since we mesh each lattice separately, each lattice will have its set of representative nodes. This is class contains getter and setter functions for data related to the lattice.

- *Input* This class deals with input related operation. main.cc calls *mainInput()* of this class, which reads parameter from input files, and sets the relevant parameters of each class. *Quasicontinuum* class's constructor calls *quasiInput()* of this class, which sets the parameters of each lattice.

- *CreateMesh* This class meshes lattices. It operates on data of *Quasicontinuum*.

- *PairPotentials* This class contains information about interatomic potential.

- *CrossNeighborList* This class creates a neighbor list, and stores them in its data bucket. This data will be used when we will compute forces on atoms.

- *ForceEnergyCalculations* This class computes forces on nodes of each lattice, from different interactions.

- *Electrostatics* This class computes forces and electric field for electrostatics interaction.

Apart from these, we also have few other class, like *Indent, Void, Node.*

4.2 Verification of force and energy calculation

We compare the results of new code with the zero temperature code. For same initial configuration, the results of old QC code, [Marshall and Dayal, 2013], and new QC code with τ (standard deviation of position) very small should be very close. This gives us the way by which we can test the accuracy of our QC code.

We remind the readers that forces at representative nodes of the mesh are computed using cluster based summation. Thus if forces and energy, at cluster sites, in new and old QC are close then it implies that forces and energy at representative nodes will also be close. Similarly, if the forces and energy, at representative nodes, are very close then the forces and energy, at cluster sites, has to be very close. To avoid the use of excess space, we will show the force and energy at representative nodes, except once at the beginning where we will show the force and energy at both rep. nodes and cluster sites.

4.2.1 NiAl system

To verify that the calculation of the code is correct, we can set the standard deviation of the position of atoms very small, and then compare the force and energy from the zero temperature QC code. We set the $\tau = 0.001$, $\tau = 0.01$, and $\tau = 0.1$. Table 4.1 gives the detail about NiAl system.

Table 4.1: NiAl system for force and energy verification of QC code

temperature	300K
system size	32x32x32
k_B, h, and ϵ_0	actual values
atomic mass Ni	58.693400
atomic mass Al	26.981540
potential	Mishin NiAl

Lennard-Jonnes Pairwise interaction

We present the results which show that new QC code calculates pairwise interactions correctly. We switch off the EAM part in *Mishin NiAl* interatomic potential. Thus, the

atoms interact only through pairwise potential.

Energy and Force at representative atoms Figure 4.2.1 and Figure 4.2.2 show the energy at representative nodes in old QC and new QC respectively. As we can see in the figure, the energies at nodes, of new QC, are very close to energies at nodes, of old QC. Similarly, Figure 4.2.3 and Figure 4.2.4 show the forces at reps. nodes.
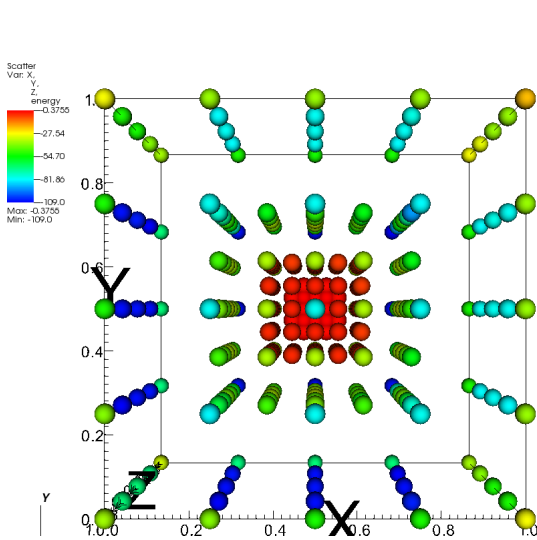
Figure 4.2.1: Zero temperature QC - Lennard Jonnes energy at initial configuration. NiAl system.
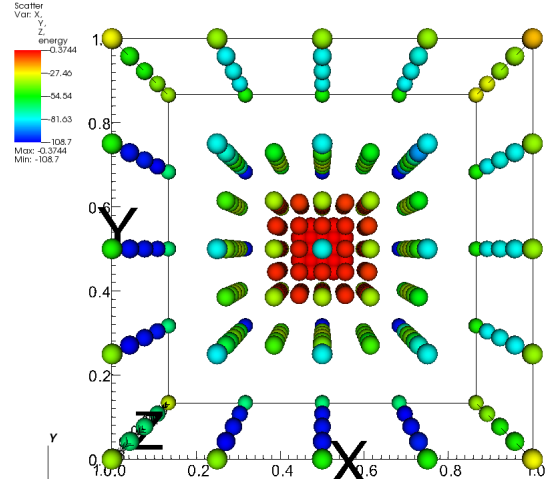
Figure 4.2.2: Finite temperature QC - Lennard Jonnes energy at mean state(initial configuration) with $\tau = 0.01$. NiAl system.

Energy and Force at the cluster sites Figure 4.2.5 and Figure 4.2.6 show that energy at cluster sites in both old and new QC code are very close. Figure 4.2.7 and Figure 4.2.8 show the force at cluster sites.

EAM without pairwise interaction

We now show that the implementation of EAM potential is correct in new QC code. We switch off the pairwise potential in *Mishin NiAl* for the calculations in this subsection. Figure 4.2.9 and Figure 4.2.10 show the energy at cluster sites for old and new QC code. Figure 4.2.11 and Figure 4.2.12 show the forces at cluster sites.
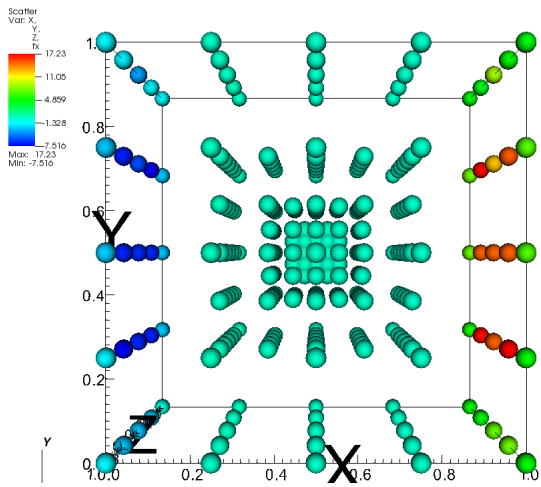
Figure 4.2.3: Zero temperature QC - Lennard Jonnes force $\boldsymbol{f_x}$ at initial configuration. NiAl system.
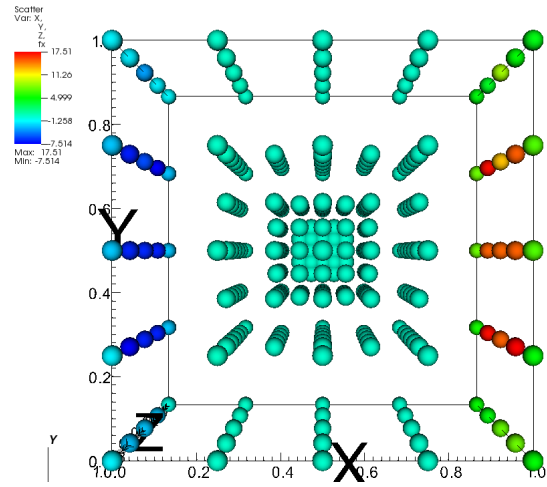
Figure 4.2.4: Finite temperature QC - Lennard Jonnes force $\boldsymbol{f_x}$ at mean state(initial configuration) with $\tau = 0.01$. NiAl system.
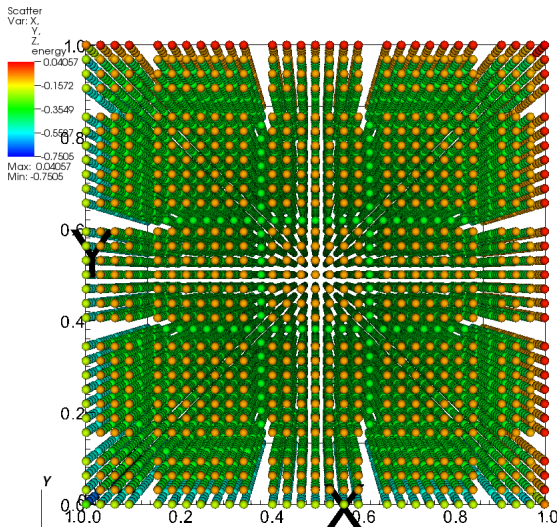
Figure 4.2.5: Zero temperature QC - Lennard Jonnes energy at cluster site at initial configuration. NiAl system.
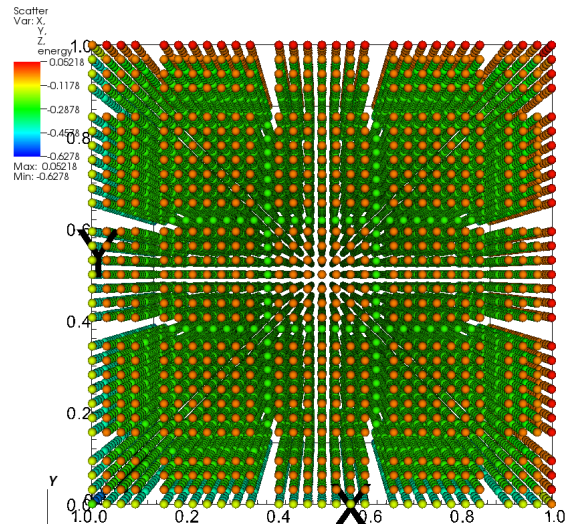
Figure 4.2.6: Finite temperature QC - Lennard Jonnes energy at cluster site at mean state(initial configuration) with $\tau = 0.01$. NiAl system.
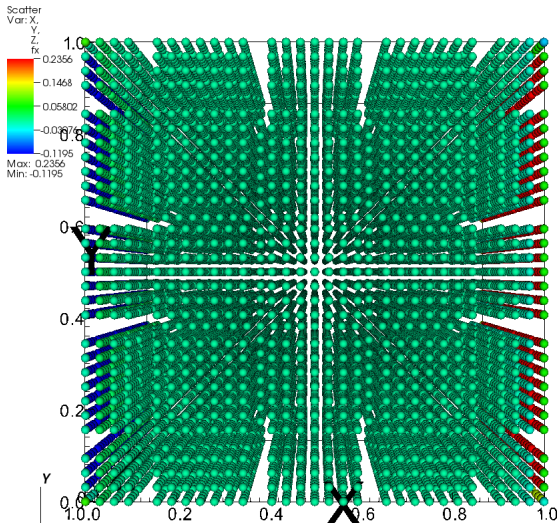
Figure 4.2.7: Zero temperature QC - Lennard Jonnes force $\boldsymbol{f_x}$ at initial configuration. NiAl system.
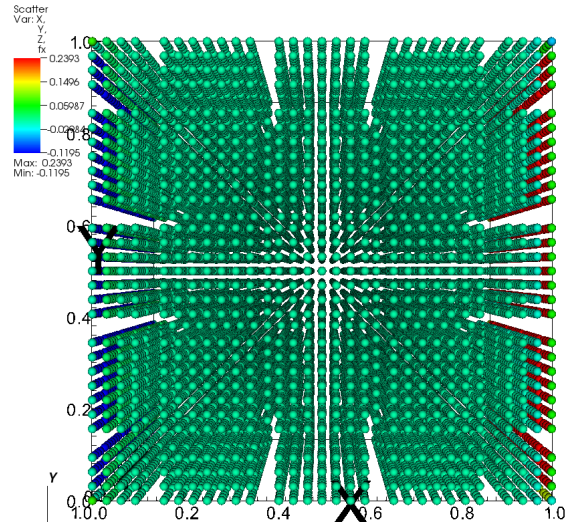
Figure 4.2.8: Finite temperature QC - Lennard Jonnes force $\boldsymbol{f_x}$ at cluster site at mean state(initial configuration) with $\tau = 0.01$. NiAl system.
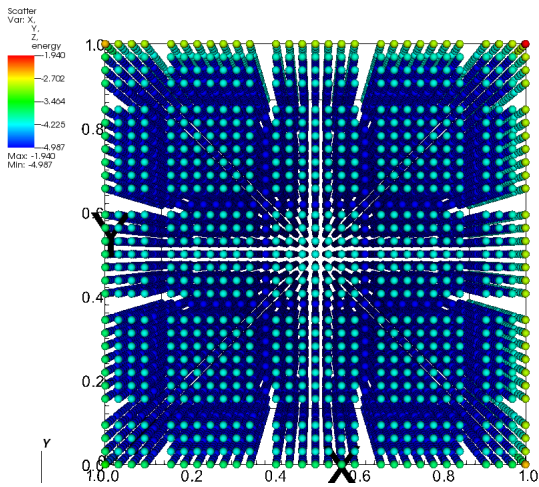
Figure 4.2.9: Zero temperature QC - EAM energy at cluster site at initial configuration. NiAl system.
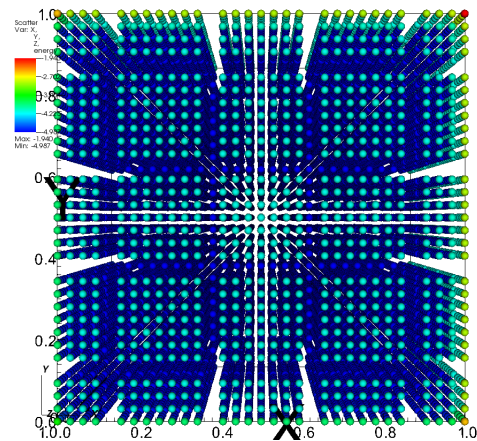
Figure 4.2.10: Finite temperature QC - EAM energy at cluster site at mean state(initial configuration) at $\tau = 0.001$. NiAl system.
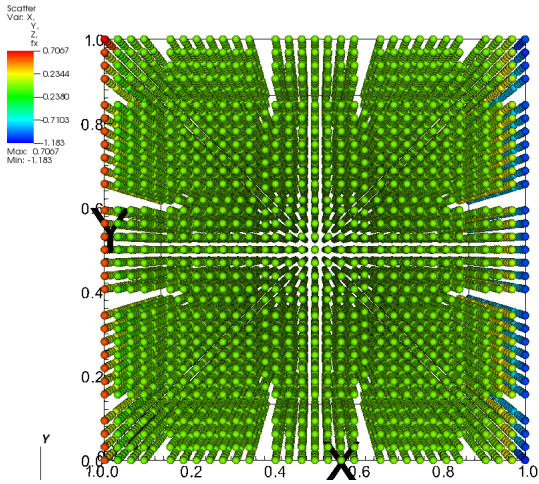
Figure 4.2.11: Zero temperature QC - EAM force $\boldsymbol{f_x}$ at initial configuration. NiAl system.

Figure 4.2.12: Finite temperature QC - EAM force $\boldsymbol{f_x}$ at cluster site at mean state(initial configuration) with $\tau = 0.001$. NiAl system.

Electrostatics

To compare the electrostatics calculation of new code, we assign the artificial charge $+1$ to Ni atoms and -1 to Al atoms. Figure 4.2.13 and Figure 4.2.14 show the energy at nodes and Figure 4.2.15 and Figure 4.2.16 show the force at nodes.

Figure 4.2.13: Zero temperature QC - Electrostatics energy at initial configuration. NiAl system.
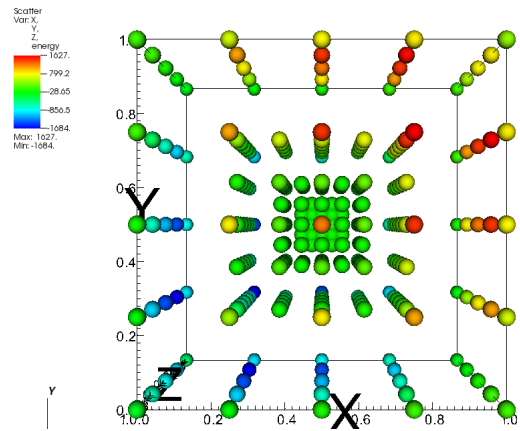
Figure 4.2.14: Finite temperature QC - Electrostatics energy at mean state(initial configuration) with $\tau = 0.001$. NiAl system.

89
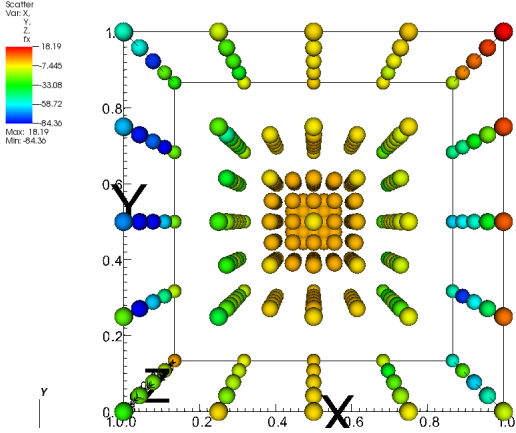
Figure 4.2.15: Zero temperature QC - Electrostatics force $\boldsymbol{f_x}$ at initial configuration. NiAl system.
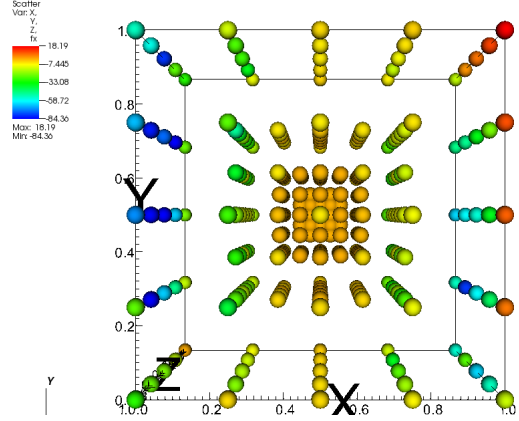
Figure 4.2.16: Finite temperature QC - Electrostatics $\boldsymbol{f_x}$ at mean state(initial configuration) with $\tau = 0.001$. NiAl system.

4.2.2 Gallium Nitride system

We consider 6 lattice core-shell model of Gallium Nitride. See [Zapol et al., 1997] for more details. The details of the system are given in Table 4.2.

Table 4.2: GaN system for force and energy verification of QC code

temperature	300K
system size	24x24x24
k_B, h, and ϵ_0	actual values
atomic mass Ga	69.722999
atomic mass N	14.006700
potential	core-shell 6 lattice

Pairwise

Figure 4.2.17 and Figure 4.2.18 show the energy at nodes for old and new QC code. Figure 4.2.19 and Figure 4.2.20 show the force at nodes for old and new QC code. From figures it is clear that if the standard deviation of position is small, here $\tau = 0.01$, then force and energy from both old and new QC code agree well.

90
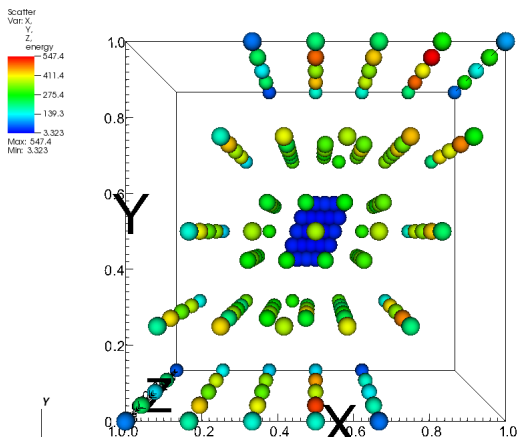
Figure 4.2.17: Zero temperature QC -
Pairwise energy at initial configuration.
GaN system.
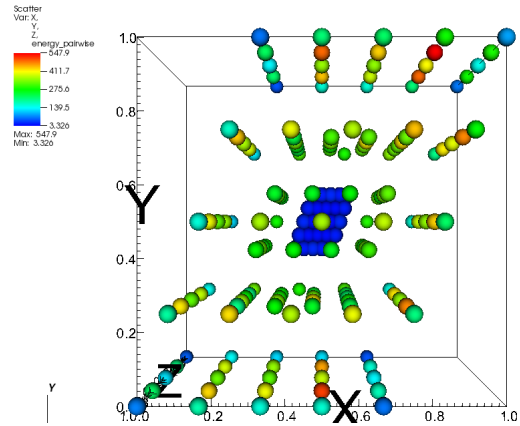
Figure 4.2.18: Finite temperature QC
- Pairwise energy at mean state(initial
configuration) with $\tau = 0.01$. GaN sys-
tem.
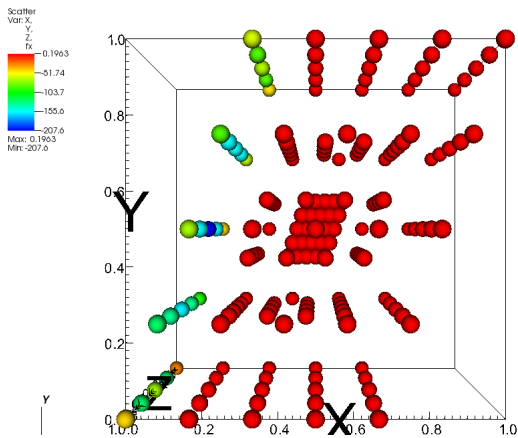
Figure 4.2.19: Zero temperature QC -
Pairwise force $\boldsymbol{f_x}$ at initial configuration
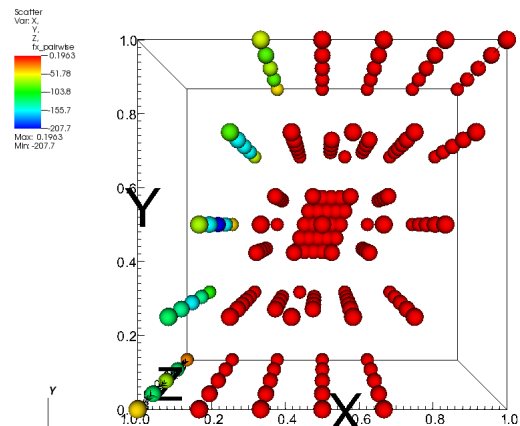
Figure 4.2.20: Finite temperature QC -
Pairwise $\boldsymbol{f_x}$ at mean state(initial config-
uration) with $\tau = 0.01$. GaN system.

Electrostatics

Figure 4.2.21 and Figure 4.2.22 show energy at nodes and Figure 4.2.23 and Figure 4.2.24 show force at nodes. From the figure it is clear that force and energy match well for small τ.
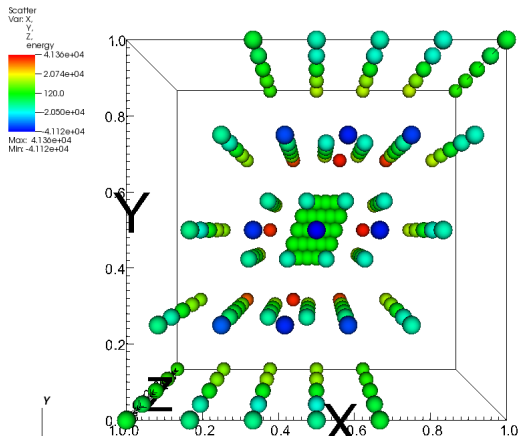
Figure 4.2.21: Zero temperature QC - Electrostatics energy at initial configuration. GaN system.
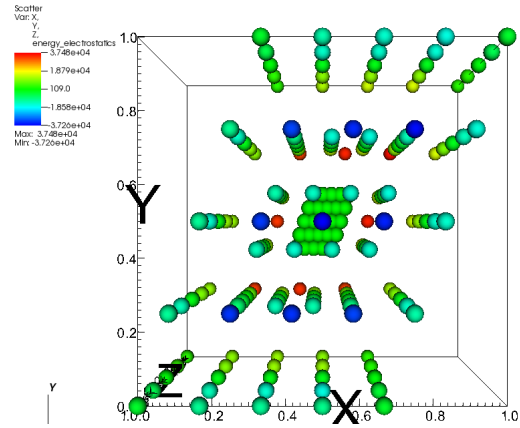
Figure 4.2.22: Finite temperature QC - Electrostatics energy at mean state(initial configuration) with $\tau = 0.01$. GaN system.
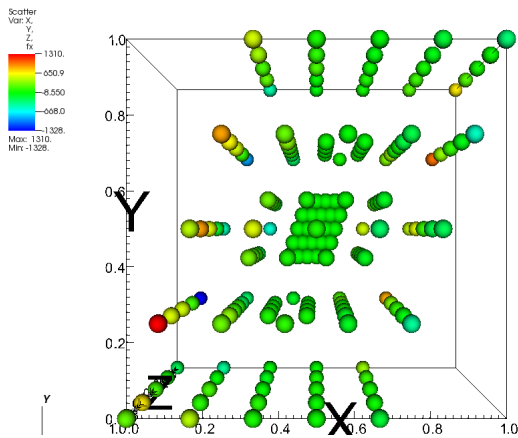
Figure 4.2.23: Zero temperature QC - Electrostatics force $\boldsymbol{f_x}$ at initial configuration. GaN system.
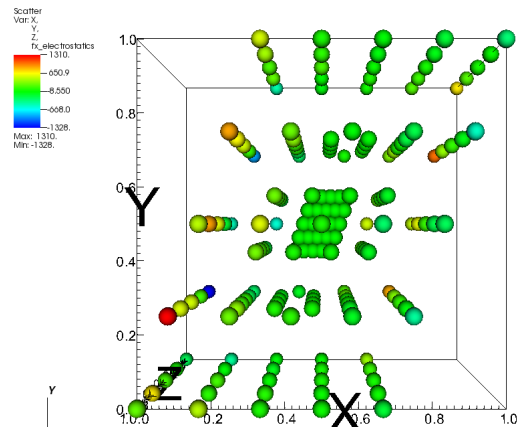
Figure 4.2.24: Finite temperature QC - Electrostatics $\boldsymbol{f_x}$ at mean state(initial configuration) with $\tau = 0.01$. GaN system.

4.3 Frequency minimization

In this section, we will present the results for frequency minimization. We first present the result for the quasi-harmonic approximation. See section 3.6. In the case of quasi-harmonic approximation, we can compute the frequency analytically. Therefore, we can compare the results of the code with the analytical result. We then present the result from our QC code without quasi-harmonic approximation. Meaning, we solve the minimization problem, see Equation 3.3.15, where the free energy is given in Equation 3.3.14.

4.3.1 Argon gas

We consider Ar gas modeled as single lattice simple cubic crystal with Lennard-Jonnes potential. The size of the system is eight atoms in all three directions. We use full atomistic mesh, i.e., we solve for mean frequency of all the atoms. Temperature is $100K$. Parameters are presented in Table 4.3.

Table 4.3: Ar system

lattice constant a	3.6697304
temperature	100K
initial freq	288.2
lj σ_0	3.4
lj ϵ	0.0104
lj cutoff radius	8.5
system	8x8x8 (full atomistic)

Quasi-harmonic result

We fix the position of all atoms in the initial configuration of simple cubic lattice and minimize the energy with respect to frequency. In this case, we consider the quasi-harmonic free energy. Initial frequency of all atoms is 288.2. Figure 4.3.1 shows the frequency which minimizes the free energy(with quasi-harmonic approximation) and Figure 4.3.2 shows the analytical frequency. They both match well. Further, in Figure 4.3.4 we can see the force at the minimum configuration. We compare this with the forces at initial

configuration shown in Figure 4.3.3.
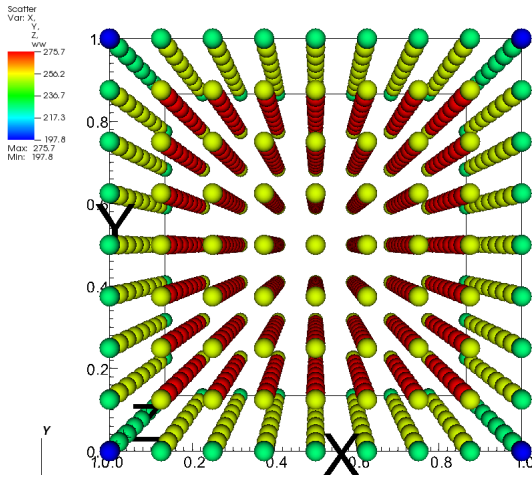
Figure 4.3.1: Ar - Converged freqeuncy from our QC code.

Figure 4.3.2: Ar - Analytical value of freqeuncy for quasi-harmonic approximation.

Figure 4.3.3: Ar - Force f_w at initial configuration.
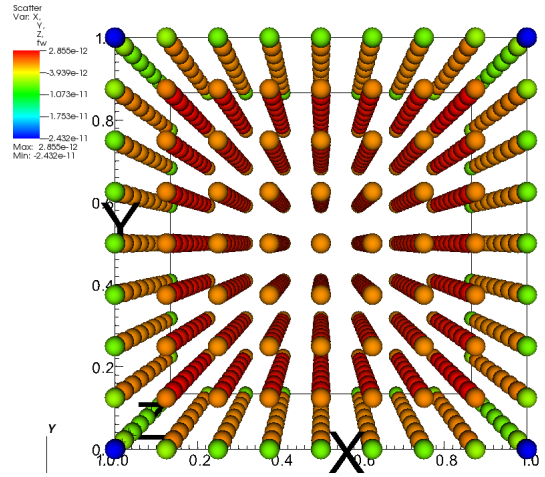
Figure 4.3.4: Ar - Force f_w at converged configuration. We can see that force is very less as expected for state which minimizes the energy.

Freq minimization without quasi-harmonic approximation

We will present the results which show that the QC code is independent of the initial value of frequency when the initial value is within some reasonable range. For Argon, we

94

found that initial frequency should be less than 245.0. We will show results, for different initial frequency, arriving at the same minimum frequency.

The plot of initial frequency is shown only for the first case. Since initial frequency is chosen to be uniform, we will just state the value of initial frequency, and show the minimum frequency we get from the QC code.

Figure 4.3.5 show the initial frequency of each atom. Figure 4.3.6 show the forces at atoms at minimum configuration. Figure 4.3.7, Figure 4.3.8, Figure 4.3.9 and Figure 4.3.10 are the plots of frequency which minimizes the free energy corresponding to initial frequency $\omega = 230.5$, $\omega = 192.1$, $\omega = 144.1$ and $\omega = 115.3$.
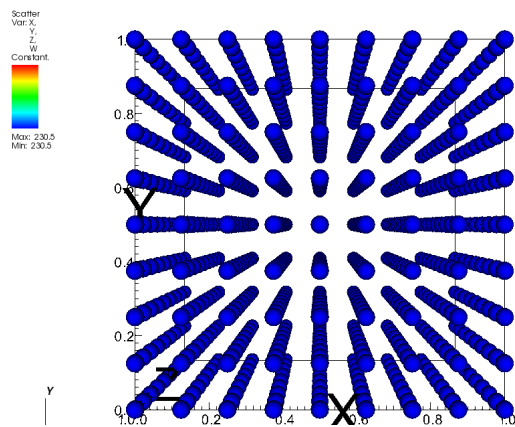
Figure 4.3.5: Ar - Initial frequency plot.
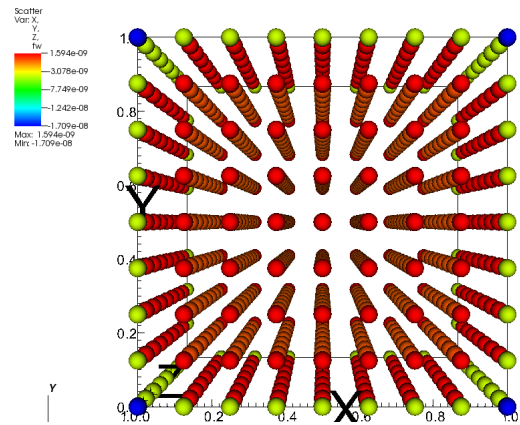
Figure 4.3.6: Ar - f_w at minimizing state. Initial frequency = 230.5.
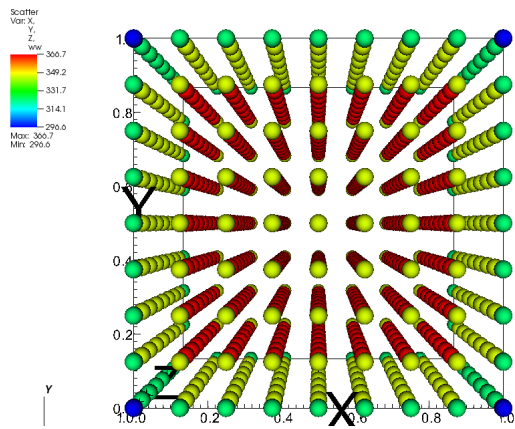
Figure 4.3.7: Ar - Minimizing frequency. Initial frequency = 230.5.
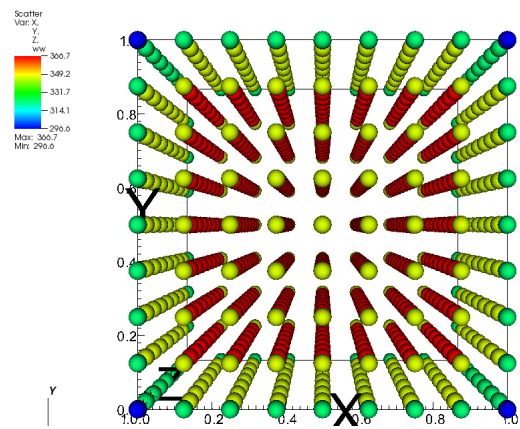
Figure 4.3.8: Ar - Minimizing frequency. Initial frequency = 192.1.
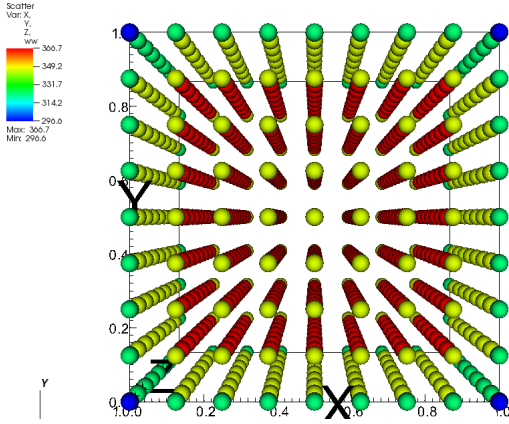
Figure 4.3.9: Ar: Minimizing frequency. Initial frequency = 144.1.
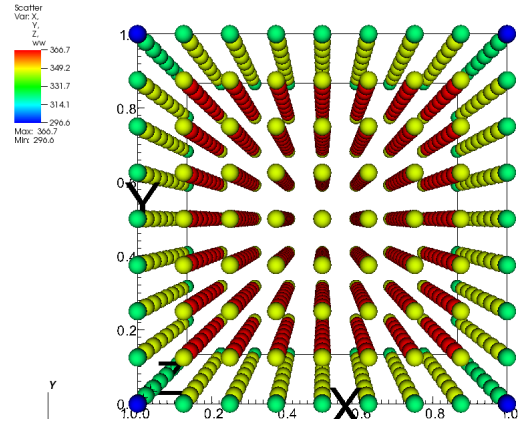
Figure 4.3.10: Ar: Minimizing frequency. Initial frequency = 115.3.

4.3.2 Gallium Nitride

We consider Gallium Nitride with the core-shell model. This consists of 6 lattices. See [Zapol et al., 1997] for more details. See Table 4.4 below for more details about GaN system.

Table 4.4: GaN system

temperature	300K
system size	24x24x24
universal constant k_B, h, and ϵ_0	actual values
atomic mass Ga	69.722999
atomic mass N	14.006700
potential	core-shell 6 lattice

Quasi-harmonic results

We fix the position of all nodes to initial configuration and minimize the quasi-harmonic free energy with respect to the mean frequency. Figure 4.3.11, Figure 4.3.12, Figure 4.3.13 and Figure 4.3.14 show the frequency which minimize quasi-harmonic free energy corresponding to initial frequency $\omega = 659.4$, $\omega = 527.5$, $\omega = 439.6$ and $\omega = 376.8$.

Remark: For the frequency minimization without quasi-harmonic approximation, we tried different values of initial frequency, but the code did not converge.
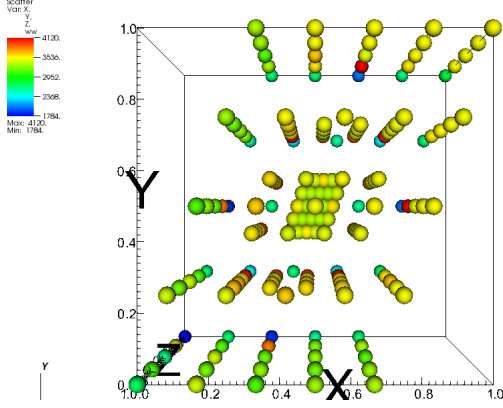
Figure 4.3.11: GaN - Minimizing frequency with quasi-harmonic approximation. Initial frequency is 659.4.
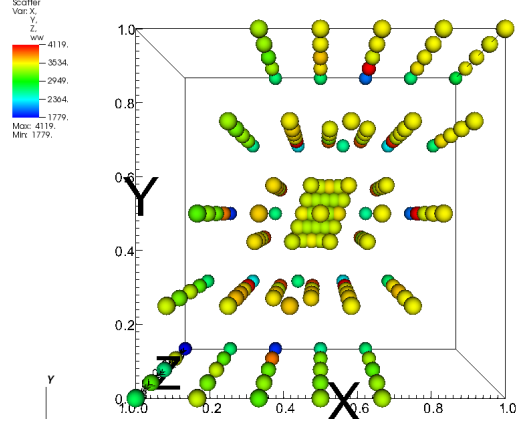
Figure 4.3.12: GaN - Minimizing frequency with quasi-harmonic approximation. Initial frequency is 527.5.
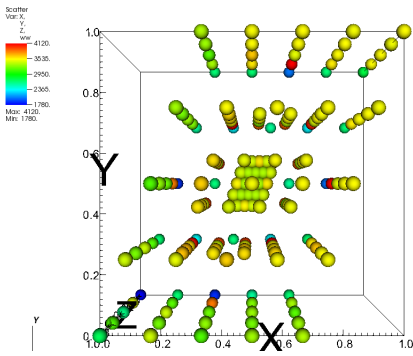
Figure 4.3.13: GaN - Minimizing frequency with quasi-harmonic approximation. Initial frequency is 439.6.
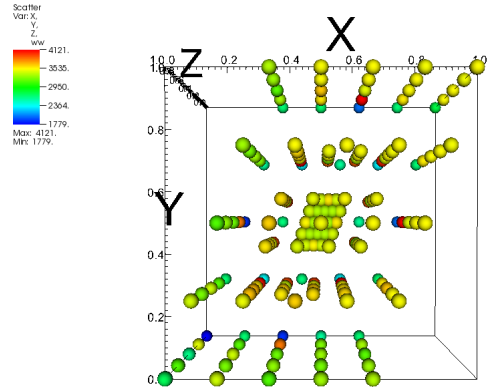
Figure 4.3.14: GaN - Minimizing frequency with quasi-harmonic approximation. Initial frequency is 376.8.

4.3.3 Comments on initial value of frequency

Free energy is a function of mean frequency and mean position. The initial value of mean position can be assumed to be crystal lattice sites. However, for mean frequency, the choice of initial value is not trivial.

In this framework, the standard deviation of momenta of all the atoms is given by $\sigma = \sqrt{2k_B T}$. Therefore, the mean frequency would be inverse of τ, i.e. $w = \dfrac{\sigma}{\tau}$.

As we will see in this section, too less a value of τ (or high value of initial frequency) as the initial value, results in a uniform force, $f_w = \dfrac{\partial E}{\partial w}$, on all sites. Too high a value of

initial τ means we are considering a very large domain, around the mean configuration, to compute the phase average of interatomic potential. In this large domain, there will be many states of the system, for which the significant number of pairs of atoms will be very close. Therefore, we see that the forces on atoms are very large. For example, if we have a Lennard-Jonnes potential $\phi(r)$, with $r = r_0$ as the equilibrium separation of ϕ, then as r goes below r_0 the force increases very rapidly. Therefore, for high value of τ (or low value of mean frequency), we have very large value of forces $\boldsymbol{f_x}$ and f_w. This is also not desirable, as conjugate gradient will either diverge or give results which are not desirable. Therefore, one has to be careful with the initial value of mean frequency.

Also, it is reasonable to expect the code to be independent of the initial value of frequency, provided the initial value remain in some range, for which the forces are neither uniform nor extremely large. We have demonstrated this by considering the different values of initial frequency for which the code converged to the same frequency that minimized the free energy.

Argon gas

We show the force f_w for different values of initial frequency. The details of Ar system are in Table 4.5.

Table 4.5: Ar system to compare the forces on atoms corresponding to low and high initial frequency

lattice constant a	3.6697304
temperature	100K
lj σ_0	3.4
lj ϵ	0.0104
lj cutoff radius	8.5
system	8x8x8 (full atomistic)

We list the magnitude of force f_w due to entropy and interatomic potential for three choices of initial frequency. See Figure 4.3.15 and Figure 4.3.16 for f_w due to the entropy and the interatomic potential when the initial frequency is very high. Figure 4.3.17 and Figure 4.3.18 show f_w when the initial frequency is very low. Figure 4.3.19 and

Figure 4.3.20 show f_w when the initial frequency is optimum for the conjugate gradient to converge to minimum.

Table 4.6: Force comparison for different values of initial frequency

	High frequency	Low frequency	Optimum frequency
	$\omega = 5763.0$	$\omega = 115.3$	$\omega = 230.5$
$f_w^{entropy}$	$4.486e - 06$	0.0002243	0.0001121
$f_w^{interatomic}$	$5.298e - 09$	0.02640	0.0002848
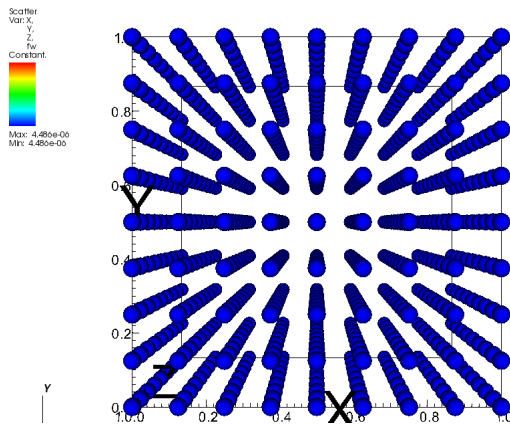
Figure 4.3.15: Ar - f_w due to entropic energy. Initial frequency is 5763.0.
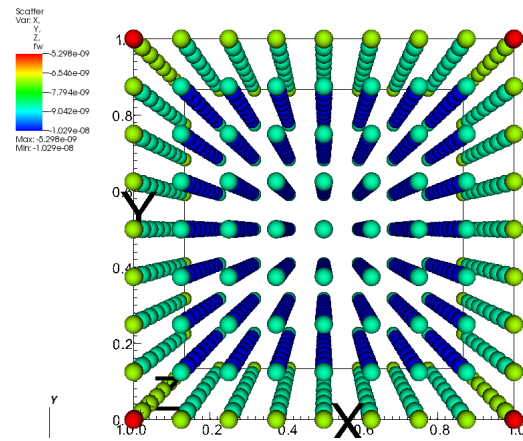
Figure 4.3.16: Ar - f_w due to interatomic potential. Initial frequency is 5763.0.
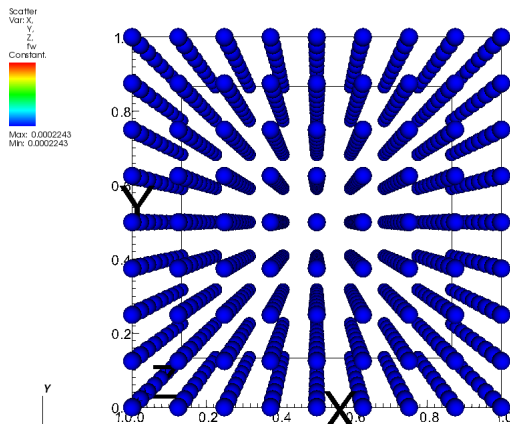
Figure 4.3.17: Ar - f_w due to entropy energy. Initial frequency is 115.3.
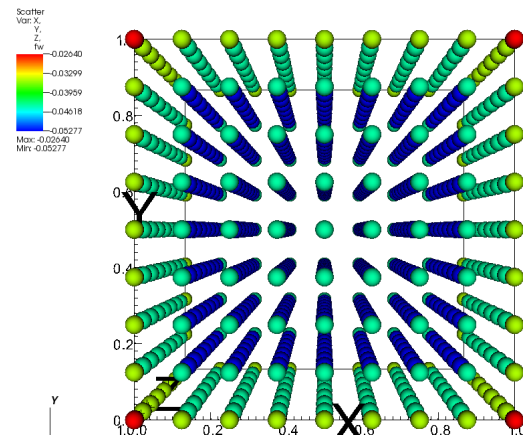
Figure 4.3.18: Ar - f_w due to interatomic potential. Initial frequency is 115.3.
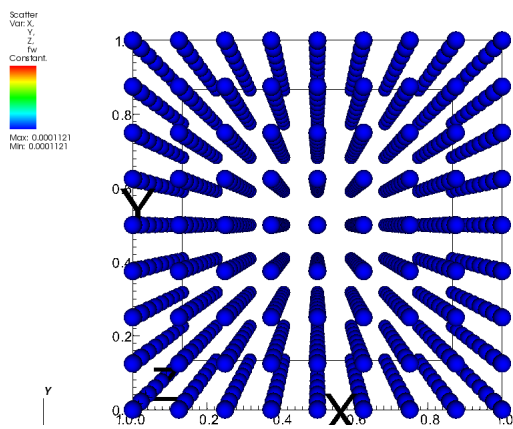
Figure 4.3.19: Ar - f_w due to entropy energy. Initial frequency is 230.5.
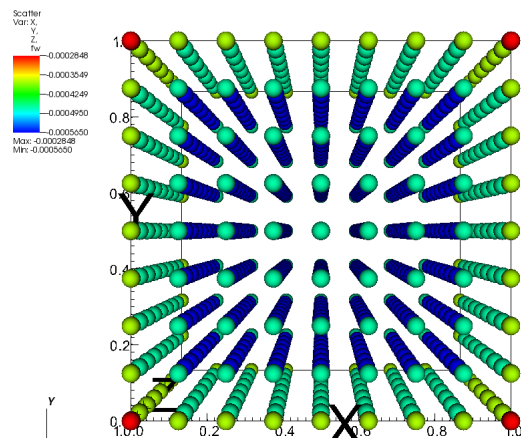
Figure 4.3.20: Ar - f_w due to interatomic potential. Initial frequency is 230.5.

Chapter 5

Discussion and future works

In this chapter, the discussion of the work is presented. We would also like to talk about problems we want to focus on in future. We would like to thank Army Research Office for funding this work. The expenses of first year of Ph.D. was covered by Dean's fellowship at Civil and Environmental Engineering. We are thankful to the department for this fellowship.

5.1   Discussion

One of the goals of this work was to analyze the electrical and magnetic interactions in nanostructures. As we observed from our calculations, the way electrical and/or magnetic interactions take place in the macroscopic material, which is neither like a nanorod or like a thin film, is different from the electrical and/or magnetic interactions happening in the nanostructures. We find this observation interesting. Nanostructures find application in many types of devices like electronic devices, sensing devices, and medical tools. Our continuum limit calculations for nanostructures can be used in the multiscale method for nanostructures.

As we argued in section 2.6, the reason for this contrast observation in the case of nanostructures is the scaling of dipole field kernel $\boldsymbol{K}$. The nonlocal behavior of energy density is due to the dipole field kernel, and as we know it has $1/r^3$ scaling. The scaling of $1/r^3$ makes it fast decaying for the nanostructures and thin film. We explain this in more detail in section 2.6.

We modeled the charge density of atomic system at the finite temperature as a random field. Although we assumed the charge density field to be ergodic and stationary, it is a further generalization of the periodic and the quasi-periodic charge density field. The assumption of ergodicity means, spatial average of the charge density field is equal to the average over large time. For a material which is at equilibrium at finite temperature, this assumption should hold. We also assume the charge density field to be stationary. Stationarity means statistical properties are invariant with respect to the position in space. For example, time average, or expectation of charge density field, would be invariant with respect to the position at which we are computing the average. This assumption will not hold if suppose material has too many impurities or if one part of the material, at the scale of atomic spacing, is statistically different from the other part.

For the random media, we see that, in the continuum limit, the local energy is an expectation of the local energy as a random function. Also, nonlocal energy is independent of ω. The reason for this is, as we tend to continuum limit, the size of the material point ϵ is much greater than the size of atomic spacing. Since nonlocal energy is due to one material point interacting with another material point, the distance between interacting charges is now of the order of ϵ. As charge-charge interaction is linear in nature, and the fact that atomic fluctuations are happening at the scale of atomic spacing l, while non-local energy is the interaction at the scale of ϵ, we do not see the fluctuations in the non-local energy.

As in the case of electric calculations for nanostructures, we extended the method presented in [James and Müller, 1994], to the 1-D case of a straight line and helix. We placed dipole moment along the straight line and on the helix, equally spaced apart, and computed the limit of energy. In the limit, the energy is not long-range. The approach of the discrete system of dipoles and the charge density field is equivalent, as argued in [Xiao, 2004]. Therefore, the results for the system of dipole moments in 1-D rod and helix is not different from the results derived from nanostructures using the charge density field. In [Gioia and James, 1997], the thin film limit of magnetostatics energy is computed. There too the energy is short-range in the limit.

We have used *max-ent* framework developed by Kulkarni ([Kulkarni et al., 2008]), and extended it to the multi lattices. We have developed the QC code for finite temperature

multiscale calculations. QC code is in Object oriented framework.

Our observation shows that the choice of initial frequency is not a trivial task. We found that if the initial frequency is too high, we have a uniform value of f_w, because the contribution from entropy dominates, and if it is too low, the forces are very high because the contribution from interatomic potentials dominates. Recall that the standard deviation of a position of an atom is the inverse of mean frequency for the given temperature. In either case, the conjugate gradient method has difficulty in converging to result. We propose that the initial value of frequency should be such that the contribution from entropy, interatomic potential and also the electrostatics interaction is of the same order.

We also observed that the potentials, which are often developed using molecular dynamics, are not always suitable for the multiscale method. We tried a number of potentials, the core-shell for the Gallium Nitride, Lennard-Jonnes for Argon, Lennard-Jonnes for NiMn, the core-shell potential for $PbTiO_3$, and almost all of these potentials failed to converge or failed to give reasonable results. At this point, it will be unfair to blame the potentials, as it is possible that multiscale model we are using is something which these potentials can not handle, and it can also be possible that we are using wrong tolerance, line search tolerance parameters in conjugate gradient method.

We compared the result of our QC code with zero temperature calculation, and we found that the code gives correct results. We also presented the results for conjugate gradient minimization of free energy with respect to the mean frequency. We have shown that, for the quasi-harmonic approximation, results agree with the analytical value of mean frequency. Further, we show that the frequency minimization is independent of initial value of frequency, given that the initial value of frequency is not too small (high initial forces) or not too large (small initial forces).

We also observed that the electrostatics interactions have zero contribution to mean frequency in quasi-harmonic approximation. We analyzed it and found that the potential of type $\phi(r) = c_1 + c_2/r$, see section 3.6, has zero contribution to the quasi-harmonic approximation. ' Also, Green's function of Partial differential equation $\boldsymbol{\nabla} \cdot \boldsymbol{\nabla} \phi = \delta(\boldsymbol{x})$, is of the type $1/|\boldsymbol{x}|$, and hence energy of all pdes of type $\boldsymbol{\nabla} \cdot \boldsymbol{\nabla} u = f$ will result in zero value of trace of second derivative of energy.

5.2 Future works

Designing the multiscale method for non-equilibrium temperature process is one of the major challenges in the field of multiscale simulations. Many authors, including Ortiz and Knapp, and Tadmor have tried to develop the multiscale method for material at finite temperature. See [Venturini et al., 2014] where they extend the *max-ent* framework to the non-equilibrium problem. See [Dupuy et al., 2005], [Tadmor et al., 2013], and [Kim et al., 2014] for finite temperature QC implementation. One of the main difficulty, as noted by the author in [Tadmor et al., 2013], is to transfer the heat between the atomistic region and the continuum region. The handling of coupling is not yet clear.

We would like to work in the non-equilibrium multiscale method. And, also extend the electrostatics calculations at equilibrium temperature to the non-equilibrium. However, to extend the electrostatics to non-equilibrium process, we would need to find the continuum limit of electrostatics energy. Especially, we need to focus on the nonlocal part of electrostatics energy, as the local part of electrostatics energy is already coupled to interatomic potentials, and hence, it is taken care off with the short-range calculations. For the nonlocal part of the energy, we need to see if the continuum limit calculations we carried out assuming the charge density field to be ergodic and stationary, still holds. The assumption of ergodicity is very critical as it relates the spatial average to the average over time. If charge density field is not ergodic, then computing dipole $\hat{\boldsymbol{p}}(\boldsymbol{x})$, at the material point, is not clear. Assumption of stationarity has more to do with the crystal structure and arrangement of atoms within the material. If we are modeling crystal solid than stationarity condition can still be used in non-equilibrium calculations. We would like to investigate further, and see if we can still assume the charge density field to be ergodic.

Another approach for computing the continuum limit of electrostatics energy is to consider the charge density field to be the sum of two fields: constant random field, which is also the mean, and the random field which is due to thermal fluctuations of atoms. We can assume that the fluctuating part of charge density field is bounded and then compute the limit of energy. The similar idea is used to calculate the continuum limit for short range potentials in [Blanc et al., 2007b].

We can also extend the idea of the random charge density field to the nanostructures, objective structures, and thin film. They will find application in multi-scale methods for nanostructures and thin films. For the case of nanostructures, we can find the critical length of the nanostructure to the size of cross-section ratio, such that above the critical ratio, we can use the continuum limit expression of energy presented in the thesis. We can design the multi-scale method, which is specific to nanostructures.

We can also consider the vibrating thin film such that the mean of the thin film is in XY-plane, YZ-plane, or XZ-plane, i.e., the mean of the thin film has constant normal.

Dealing with interatomic potential is a challenging task. The potentials are developed for the specific purpose, and with the assumption of periodic boundary condition in Molecular Dynamics method. Therefore, it is not always necessary that the potential would work with multiscale method. We would like to investigate further into this aspect and try to find the conditions which cause the potentials to fail. We are interested in developing a method which can critically test the potential.

Appendix A

Phase average calculation

In the QC method, we often need to compute the phase average of interactions. Here we briefly discuss the calculation of phase average. We use [Kulkarni et al., 2008] as a reference.

A.1   Gauss quadrature rule for multiple integrals

We are interested in following n-dimensional integral

$$I[f] = \int_{-\infty}^{\infty} ... \int_{-\infty}^{\infty} f(x_1, ..., x_n) \exp[-x_1^2 - \cdots - x_n^2]dx_1...dx_n \qquad (A.1.1)$$

For M-point quadrature method, we will have

$$I[f] \approx \sum_{k=1}^{M} f(x_1^k, x_2^k, ..., x_n^k)W_k \qquad (A.1.2)$$

where $x^K = (x_1^k, x_2^k, ..., x_n^k)$ is k^{th} quadrature point in n-dimensional space. And W_k is the weight corresponding to k^{th} quadrature point. The vector x^k and weight W_k for 3-point and 5-point quadrature point are given below.

Third degree quadrature: We need $2n$ points to approximate the integral such that it is accurate up to third order polynomial. The points and weights are obtained by requiring that the formula should integrate all monomials of degree ≤ 3 exactly. Following

are the $2n$ points and weights

$$(+_-r, 0, ..., 0), (0, +_-r, ..., 0), ..., (0, ..., 0, +_-r) \tag{A.1.3}$$

$$W_k = \frac{1}{2n}V, \ k = 1, ..., n \tag{A.1.4}$$

$$V = I(1) = pi^{n/2}, \ r^2 = \frac{n}{2} \tag{A.1.5}$$

Fifth degree quadrature: We refer the reader to [Kulkarni et al., 2008] for a list of points and weights. Further, the parameters can also be found on [Krylov and Stroud, 2006].

A.2 Kinetic energy

We can analytically calculate the phase average of K.E. as follows

$$< \frac{1}{2}|\boldsymbol{p}_a^n|^2 > = \frac{1}{2}\left[3(\sigma_a^n)^2 + |\bar{\boldsymbol{p}}_a^n|^2\right] = \frac{3}{2}k_B T_a^n$$

Where we have used the quasi-static condition and also the equipartition of energy. We see that K.E. does not contribute to force.

A.3 Potential energy

Consider the term $< V_a^n(\mathbf{q}(\hat{\mathbf{q}}) >_p$. This is the phase average of atomic interaction energy of atom (n, a). For a given interatomic potential, analytical calculation of integrals is not an easy task, as one has to sample all points in phase space and calculate V_a^n for all such points (or configuration). Instead, we approximate the integration involved in $< V_a^n >_p$. We can use three-point quadrature rule or five-point quadrature rule to get the phase average numerically. In this section, we consider Lennard-Jonnes and EAM potential.

A.3.1 Energy and force due to k-body potential

Let k be the integer and let $\phi_k : \mathbb{R}^{3k} \to \mathbb{R}$ be k-body potential. Then, the calculation of phase average involves integral of the following type

$$I = < \phi_k(\boldsymbol{q}_1, \boldsymbol{q}_2, ..., \boldsymbol{q}_k) >_p$$

$$= \left(\frac{1}{[(QN)!]^{1/2QN} h^{3/2}} \right)^k \int_{\mathbb{R}^{3k}} \phi_k(\boldsymbol{q}_1, \boldsymbol{q}_2, ..., \boldsymbol{q}_k) \Pi_{i=1}^k \frac{\exp[-\alpha_i^2 |\boldsymbol{q}_i - \bar{\boldsymbol{q}}_i|^2]}{(\pi/\alpha_i^2)^{3/2}} d\boldsymbol{q}_i$$

$$\frac{1}{[(QN)!]^{1/2QN} h^{3/2}}$$

where, $\alpha_i = \dfrac{w_i}{\sqrt{2}\sigma_i}$. By change of variable, we have

$$I = \left(\frac{1}{\sqrt{\pi}} \right)^{3k} \int_{\mathbb{R}^{3k}} \phi_k \left(\frac{\boldsymbol{y}_1}{\alpha_1} + \bar{\boldsymbol{q}}_1, \frac{\boldsymbol{y}_2}{\alpha_2} + \bar{\boldsymbol{q}}_2, ..., \frac{\boldsymbol{y}_k}{\alpha_k} + \bar{\boldsymbol{q}}_k \right) \Pi_{i=1}^k \exp[-|\boldsymbol{y}_1|^2] d\boldsymbol{y}_i$$

Above integral is $3k$ dimensional. We approximate the integral using M number of quadrature points in $3k$ dimensional space, as follows

$$I \approx \left(\frac{1}{\sqrt{\pi}} \right)^{3k} \sum_{i=1}^M \phi_k \left(\frac{\eta_1^i}{\alpha_1} + \bar{\boldsymbol{q}}_1, \frac{\eta_2^i}{\alpha_2} + \bar{\boldsymbol{q}}_2, ..., \frac{\eta_k^i}{\alpha_k} + \bar{\boldsymbol{q}}_k \right) W^i$$

where $\eta^i = (\eta_1^i, \eta_2^i, ..., \eta_k^i) \in \mathbb{R}^{3k}, i = 1, 2.., M$ and $W^i, i = 1, 2, .., M$ are M number of quadrature points and weights.

A.3.2 Lennard Jonnes potential

We consider following LJ potential :

$$\phi(r) = 4c_1 \left[\left(\frac{c_2}{r} \right)^{12} - 2 \left(\frac{c_2}{r} \right)^6 \right]$$

Total energy due to this potential is

$$E(\mathbf{q}) = \sum_{(n,a)} E_a^n = \sum_{(n,a)} \left(\frac{1}{2} \sum_{(m,b)} \phi(|\boldsymbol{q}_a^n - \boldsymbol{q}_b^m|) \right)$$

Phase average of energy is

$$< E_a^n > = \frac{1}{2} \sum_{(m,b)} \left(\frac{1}{\sqrt{\pi}} \right)^6$$

$$\int_{\mathbb{R}^6} \phi \left(\left| \frac{\sqrt{2}\sigma_a^n}{w_a^n} \boldsymbol{y}_1 - \frac{\sqrt{2}\sigma_b^m}{w_b^m} \boldsymbol{y}_2 + \bar{\boldsymbol{q}}_a^n - \bar{\boldsymbol{q}}_b^m \right| \right) \exp[-|\boldsymbol{y}_1|^2 - |\boldsymbol{y}_2|^2] d\boldsymbol{y}_1 d\boldsymbol{y}_2$$

Let, for $i = 1, 2, .., M$, $\eta^i = (\eta_1^i, \eta_2^i) \in \mathbb{R}^6$ and W^i are i^{th} quadrature point and weight. Then

$$
\begin{aligned}
\bar{E}_a^n(\bar{\mathbf{q}}, w) &:=< E_a^n > \\
&= \frac{1}{2} \left(\frac{1}{\sqrt{\pi}} \right)^6 \sum_{(m,b)} \left[\sum_{i=1}^{M} \phi \left(\left| \frac{\sqrt{2}\sigma_a^n}{w_a^n} \eta_1^i - \frac{\sqrt{2}\sigma_b^m}{w_b^m} \eta_2^i + \bar{q}_a^n - \bar{q}_b^m \right| \right) W^i \right] \\
&= \frac{1}{2} \left(\frac{1}{\sqrt{\pi}} \right)^6 \sum_{i=1}^{M} \left\{ \sum_{(m,b)} \phi \left(\left| \frac{\sqrt{2}\sigma_a^n}{w_a^n} \eta_1^i - \frac{\sqrt{2}\sigma_b^m}{w_b^m} \eta_2^i + \bar{q}_a^n - \bar{q}_b^m \right| \right) \right\} W^i \quad \text{(A.3.1)}
\end{aligned}
$$

Force due to displacement

The derivative of $\bar{E}_a^n$ w.r.t. $\bar{q}_b^m$ is given by

$$
\boldsymbol{f}_{(n,a),(m,b)}(\bar{\mathbf{q}}, w) = \frac{1}{2} \left(\frac{1}{\sqrt{\pi}} \right)^6 \sum_{i=1}^{M} \left\{ \phi' \left(\left| \frac{\sqrt{2}\sigma_a^n}{w_a^n} \eta_1^i - \frac{\sqrt{2}\sigma_b^m}{w_b^m} \eta_2^i + \bar{q}_a^n - \bar{q}_b^m \right| \right) \right.
$$
$$
\left. \frac{\frac{\sqrt{2}\sigma_b^m}{w_b^m} \eta_1^i - \frac{\sqrt{2}\sigma_a^n}{w_a^n} \eta_2^i + \bar{q}_b^m - \bar{q}_a^n}{\left| \frac{\sqrt{2}\sigma_a^n}{w_a^n} \eta_1^i - \frac{\sqrt{2}\sigma_b^m}{w_b^m} \eta_2^i + \bar{q}_a^n - \bar{q}_b^m \right|} \right\} W^i \quad \text{(A.3.2)}
$$

when $(m, b) \neq (n, a)$. For $(m, b) = (n, a)$, we have

$$
\boldsymbol{f}_{(n,a),(n,a)}(\bar{\mathbf{q}}, w) = \frac{1}{2} \left(\frac{1}{\sqrt{\pi}} \right)^6 \sum_{i=1}^{M} \left\{ \sum_{(m,b)} \phi' \left(\left| \frac{\sqrt{2}\sigma_a^n}{w_a^n} \eta_1^i - \frac{\sqrt{2}\sigma_b^m}{w_b^m} \eta_2^i + \bar{q}_a^n - \bar{q}_b^m \right| \right) \right.
$$
$$
\left. \frac{\frac{\sqrt{2}\sigma_a^n}{w_a^n} \eta_1^i - \frac{\sqrt{2}\sigma_b^m}{w_b^m} \eta_2^i + \bar{q}_a^n - \bar{q}_b^m}{\left| \frac{\sqrt{2}\sigma_a^n}{w_a^n} \eta_1^i - \frac{\sqrt{2}\sigma_b^m}{w_b^m} \eta_2^i + \bar{q}_a^n - \bar{q}_b^m \right|} \right\} W^i
$$

$$
\text{(A.3.3)}
$$

Force due to frequency

Let $\mathcal{W}_{(n,a),(m,b)}$ denote the derivative of energy $\bar{E}_a^n$ w.r.t. frequency of atom (m, b). Then

$$\mathcal{W}_{(n,a),(m,b)}(\bar{\mathbf{q}}, w) = \frac{1}{2}\left(\frac{1}{\sqrt{\pi}}\right)^6 \sum_{i=1}^{M}\left\{\phi'\left(\left|\frac{\sqrt{2}\sigma_a^n}{w_a^n}\eta_1^i - \frac{\sqrt{2}\sigma_b^m}{w_b^m}\eta_2^i + \bar{\mathbf{q}}_a^n - \bar{\mathbf{q}}_b^m\right|\right)\right.$$

$$\left.\frac{\frac{\sqrt{2}\sigma_b^m}{w_b^m}\eta_1^i - \frac{\sqrt{2}\sigma_a^n}{w_a^n}\eta_2^i + \bar{\mathbf{q}}_b^m - \bar{\mathbf{q}}_a^n}{\left|\frac{\sqrt{2}\sigma_a^n}{w_a^n}\eta_1^i - \frac{\sqrt{2}\sigma_b^m}{w_b^m}\eta_2^i + \bar{\mathbf{q}}_a^n - \bar{\mathbf{q}}_b^m\right|}\cdot\left(-\frac{\sqrt{2}\sigma_b^m}{(w_b^m)^2}\right)\eta_2^i\right\}W^i \qquad \text{(A.3.4)}$$

For $(m, b) = (n, a)$, we have

$$\mathcal{W}_{(n,a),(n,a)}(\bar{\mathbf{q}}, w) = \frac{1}{2}\left(\frac{1}{\sqrt{\pi}}\right)^6 \sum_{i=1}^{M}\left\{\sum_{(m,b)}\phi'\left(\left|\frac{\sqrt{2}\sigma_a^n}{w_a^n}\eta_1^i - \frac{\sqrt{2}\sigma_b^m}{w_b^m}\eta_2^i + \bar{\mathbf{q}}_a^n - \bar{\mathbf{q}}_b^m\right|\right)\right.$$

$$\left.\frac{\frac{\sqrt{2}\sigma_a^n}{w_a^n}\eta_1^i - \frac{\sqrt{2}\sigma_b^m}{w_b^m}\eta_2^i + \bar{\mathbf{q}}_a^n - \bar{\mathbf{q}}_b^m}{\left|\frac{\sqrt{2}\sigma_a^n}{w_a^n}\eta_1^i - \frac{\sqrt{2}\sigma_b^m}{w_b^m}\eta_2^i + \bar{\mathbf{q}}_a^n - \bar{\mathbf{q}}_b^m\right|}\cdot\left(-\frac{\sqrt{2}\sigma_a^n}{(w_a^n)^2}\right)\eta_1^i\right\}W^i \qquad \text{(A.3.5)}$$

A.3.3 EAM potential

EAM potential of any atom (n, a) is given by

$$E_a^n(\mathbf{q}, w) = F(\rho_a^n) + \frac{1}{2}\sum_{(m,b)}\phi\left(|\mathbf{q}_a^n - \mathbf{q}_b^m|\right)$$

Where F is an embedding function of charge density field. ρ_a^n is the charge density field at atom (n, a) due to its neighbor. Typically, the energy depends on nearest neighboring atoms. For the single fcc lattice, the charge density field at one atom depends on 13 neighboring atoms.

The second term in energy E_a^n is similar to LJ potential. We have already discussed the calculation of force and energy of LJ potential. Here we only focus on the energy due to embedding function. Let

$$E_a^n(\mathbf{q}, w) = F(\rho_a^n)$$

110

Let us assume that charge density ρ_a^n of any atom (n,a) depends on $\nu_a^n \in \mathbb{N}$ number of neighboring atom, including itself. And let $\mathcal{N}_a^n$ is set of neighboring atoms, and including atom (n,a), on which ρ_a^n depends. Then, phase average of E_a^n is given by

$$
\begin{aligned}
\bar{E}_a^n(\bar{\mathbf{q}}, w) :&=< E_a^n >_p \\
&= \left(\frac{1}{\sqrt{\pi}} \right)^{3\nu_a^n} \int_{\mathbb{R}^{3\nu_a^n}} F\left(\rho_a^n \left(\frac{\sqrt{2}\sigma_{\mathcal{N}_a^n(1)}}{w_{\mathcal{N}_a^n(1)}} \boldsymbol{y}_1 + \bar{\boldsymbol{q}}_{\mathcal{N}_a^n(1)}, \right. \right. \\
&\qquad \left. \left. \frac{\sqrt{2}\sigma_{\mathcal{N}_a^n(2)}}{w_{\mathcal{N}_a^n(2)}} \boldsymbol{y}_2 + \bar{\boldsymbol{q}}_{\mathcal{N}_a^n(2)}, ..., \frac{\sqrt{2}\sigma_{\mathcal{N}_a^n(\nu_a^n)}}{w_{\mathcal{N}_a^n(\nu_a^n)}} \boldsymbol{y}_{\nu_a^n} + \bar{\boldsymbol{q}}_{\mathcal{N}_a^n(\nu_a^n)} \right) \right) \Pi_{i=1}^{\nu_a^n} \exp[-|\boldsymbol{y}_i|^2] d\boldsymbol{y}_i
\end{aligned}
$$

where $\boldsymbol{q}_{\mathcal{N}_a^n(i)}$ is displacement of atom $\mathcal{N}_a^n(i)$. And, $\mathcal{N}_a^n(i)$ gives index of ith neighboring atom, of a atom (n,a).

Approximating above integral using Gauss quadrature points. Since, the dimension of integral, $3\nu_a^n$, depends on the index of the atom, we will have a different number of quadrature points for energy $\bar{E}_a^n$ of different atom. Let us assume M_a^n represent the number of quadrature points for atom (n,a). Then, the expression of energy, using Gauss quadrature approximation is

$$
\begin{aligned}
\bar{E}_a^n(\bar{\mathbf{q}}, w) \approx \left(\frac{1}{\sqrt{\pi}} \right)^{3\nu_a^n} \sum_i^{M_a^n} &\left[F\left(\rho_a^n \left(\frac{\sqrt{2}\sigma_{\mathcal{N}_a^n(1)}}{w_{\mathcal{N}_a^n(1)}} \eta_1^i + \bar{\boldsymbol{q}}_{\mathcal{N}_a^n(1)}, \right. \right. \right. \\
&\left. \left. \left. \frac{\sqrt{2}\sigma_{\mathcal{N}_a^n(2)}}{w_{\mathcal{N}_a^n(2)}} \eta_2^i + \bar{\boldsymbol{q}}_{\mathcal{N}_a^n(2)}, ..., \frac{\sqrt{2}\sigma_{\mathcal{N}_a^n(\nu_a^n)}}{w_{\mathcal{N}_a^n(\nu_a^n)}} \eta_{\nu_a^n}^i + \bar{\boldsymbol{q}}_{\mathcal{N}_a^n(\nu_a^n)} \right) \right) \right] W^i \qquad \text{(A.3.6)}
\end{aligned}
$$

where $\eta^i = (\eta_1^i, \eta_2^i, ..., \eta_{\nu_a^n}^i) \in \mathbb{R}^{3\nu_a^n}$ is i^{th} quadrature point in $\mathbb{R}^{3\nu_a^n}$ dimensional space.

Force due to displacement

Let $\boldsymbol{f}_{(n,a),(m,b)}$ is derivative of E^n. It is given by

$$
\boldsymbol{f}_{(n,a),(m,b)}(\bar{\mathbf{q}}, w) = \begin{cases} \mathbf{0}, & \text{if } \rho_a^n \text{ doesn't depend on } (m,b), \\ \dfrac{\partial}{\partial \bar{\boldsymbol{q}}_b^m} \bar{E}_a^n & \text{otherwise} \end{cases} \qquad \text{(A.3.7)}
$$

Similar to this, we can find the derivative of energy with respect to the mean frequency.

Appendix B

Units of constants and variables in QC Code

We present the list of units of important constants and variables here.

1. mass = grams/mole = $\dfrac{10^3}{N_A}$kg, where N_A is Avagrado's number.

2. distance = = 10^{-10} m

3. time = ps (picoseconds) = 10^{-12}s

4. energy = eV = $1.602176565 \times 10^{-19}$ Joule

5. velocity = $\dfrac{}{\text{ps}}$

6. force = $\dfrac{eV}{}$

7. charge = e, where e is charge of one electron.

8. momenta = $\dfrac{\text{gram}}{\text{mole}}\dfrac{}{\text{ps}}$

9. $\dfrac{\partial}{\partial w}E = \dfrac{\text{gram}}{\text{mole}}\dfrac{1}{\text{ps}}$, where E is energy.

  We list the relevant variables and units used to measure them

1. $\boldsymbol{q}_i, \tau_i =$

2. $\boldsymbol{p}_i, \sigma_i = \dfrac{\text{gram}}{\text{mole}}\dfrac{}{ps}$

3. $m_i = \dfrac{\text{gram}}{\text{mole}}$, where m_i is atomic mass of atom i

4. $w_i \dfrac{sigma_i}{\tau_i} = \dfrac{\text{gram}}{\text{mole}} \dfrac{1}{ps}$

5. entropy $= \dfrac{eV}{K}$

B.0.1 Boltzmann constant

Consider the kinetic energy and temperature relation

$$< \frac{1}{2m_i} |\boldsymbol{p}_i|^2 > = \frac{3}{2} k_B T_i$$

$$\Rightarrow \frac{\sigma_i^2}{m_i} = k_B T_i$$

Thus k_B should be given in unit $\dfrac{\text{gram}}{\text{mole}}^2 \dfrac{1}{\text{ps}^2} \dfrac{1}{K}$.

$$k_B = 1.38064852 \times 10^{-23} kg m^2 K^{-1} s^{-2}$$

$$= 1.38064852 \times 10^{-23} \times 10^3 \times N_A \times 10^{20} \times 10^{-24} \frac{\text{gram}}{\text{mole}}^2 \frac{1}{\text{ps}^2} \frac{1}{K}$$

B.0.2 Max-planck constant

$$\left(\frac{1}{(QN)! h^{3QN}} \right) \int_{\bar{\Gamma}} p d\mathbf{q} d\mathbf{p} = 1$$

$$\Rightarrow \frac{1}{[h]^{3QN}} [p] \left[\frac{\text{gram}}{\text{mole ps}} \right]^{3QN} = [1]$$

We take value of h in unit $\text{grammole} \dfrac{}{\text{ps}}$. Then

$$[p] = [h]^{3QN} \left[\frac{\text{gram}}{\text{mole ps}} \right]^{-3QN}$$

$$= \left[\frac{[h]}{\text{gram/mole/ps}} \right]^{3QN}$$

$$= [1]$$

Value of h is

$$h = 6.626070040 \times 10^{-34} Jouless$$

$$= 6.626070040 \times 10^{-34} kgm^2 s^{-1}$$

$$= 6.626070040 \times 10^{-34} \times 10^3 \times N_A \times 10^{20} \times 10^{-12} \frac{\text{gram}}{\text{mole}} \frac{2}{\text{ps}}$$

Reduced max-planck constant is defined as

$$\hbar = \frac{h}{2\pi}$$

B.0.3 Dielectric constant

Energy of two charge q_i and q_j is

$$E = \frac{q_i q_j}{4\pi\epsilon_0} \frac{1}{|\boldsymbol{x}_i - \boldsymbol{x}_j|}$$

eV unit is used to measure the energy, and e unit, the charge of one electron, to measure the charges. Thus, from the equation above, it is clear that we need to use the value of dielectric constant ϵ_0 in $\frac{e^2}{eVeV}$ unit.

$$\epsilon_0 = 8.854187817 \times 10^{-12} \frac{C^2}{Jm}$$

$$= 8.854187817 \times 10^{-12} \times \frac{1}{10^{10}} \times \frac{1}{6.24150974 \times 10^{18} eV} \left[6.24150913 \times 10^{18} e \right]^2$$

$$= 0.0055263488697 \frac{e^2}{eV}$$

Unit of energy and its derivative are as follows

- energy: eV

- $\dfrac{\partial \text{Energy}}{\partial \boldsymbol{q}_i}$: $\dfrac{\text{eV}}{e}$

- $\dfrac{\partial \text{Energy}}{\partial \boldsymbol{w}_i}$: $\dfrac{\text{eV}}{\frac{\text{gram}}{\text{mole}} \frac{1}{\text{ps}}}$

Kinetic energy K.E. will be in unit $\dfrac{\text{gram}}{\text{mole}}\dfrac{^2}{\text{ps}^2}$. To convert it back to unit eV, we find the factor as follows

$$K.E. = \frac{3}{2}k_B T \qquad \frac{\text{gram}}{\text{mole}}\frac{^2}{\text{ps}^2}$$
$$= factor_{K.E.}\frac{3}{2}k_B T \qquad \text{eV}$$

Where, $factor_{k.E.}$ is given by

$$1\frac{\text{gram}}{\text{mole}}\frac{^2}{\text{ps}^2} = \frac{10^{-3}}{N_A}\frac{10^{-20}}{10^{-24}}\,\text{kg}\frac{m^2}{s^2}$$
$$= \frac{10}{N_A}Joule$$
$$= \frac{6.24150974 \times 10^{19}}{N_A}\text{eV}$$

Thus,

$$factor_{K.E.} = \frac{6.24150974 \times 10^{19}}{N_A}$$

Energy due to entropy: This energy will also be in unit $\dfrac{\text{gram}}{\text{mole}}\dfrac{^2}{\text{ps}^2}$ as $\log\left[\dfrac{\sigma_i^2}{\hbar w_i}\right]$ is dimensionless. Thus, $factor_{entropy} = factor_{K.E.}$.

Potential energy: We use interatomic potential in eV unit.

Electrostatic energy: Our choice of unit for dielectric constant and position is such that the unit of electrostatics energy is eV.

Appendix C

New Algorithm to compute force due to EAM like N-body potential

In this chapter, we discuss our new algorithm for force calculation due to EAM potential. Advantage of this algorithm is that it ensures that numerically expensive quantities, like density, are not computed more than once at any atom for given Gauss quadrature point.

C.1 EAM energy and force

For EAM, force is given by

$$\boldsymbol{f}_i = \sum_j \left[F'(\rho_i)g'(r_{ij}) + F'(\rho_j)g'(r_{ij}) + V'(r_{ij}) \right] \frac{ij}{r_{ij}} \tag{C.1.1}$$

where $ij = \boldsymbol{q}_i - \boldsymbol{q}_j$ and $r_{ij} = |_{ij}|$. EAM energy is given by

$$E = \sum_{i \in \mathcal{L}} \left[F(\rho_i) + \sum_j V(r_{ij}) \right]$$

where, electron density ρ_i at atom i is given by

$$\rho_i = \sum_j g(r_{ij})$$

Let $\mathcal{C}_I^h$ be the set of cluster sites of rep. atom I, and n_I^h be the weight associated to rep. atom I. Then,

$$\boldsymbol{f}_I^h = \sum_{J \in \mathcal{L}^h} n_J^h \left[\sum_{j \in \mathcal{C}_J^h} \boldsymbol{f}_j \Psi_I^h(\boldsymbol{x}_i) \right] \tag{C.1.2}$$

and force $\boldsymbol{f}_j$, at atom j, is given by Equation C.1.1 for EAM potential.

C.1.1 Zero temperature calculation

We note that for zero temperature case, we do not need to compute the phase average. The algorithm of force calculation is as follows

1. Construct neighbor list of each cluster site of each rep. atom. Let us denote neighbor list of cluster site j of rep. atom J as $\boldsymbol{A}[J][j]$.

2. Compute density ρ_k for each neighbor site $k \in \boldsymbol{A}[J][j], \forall J \mathcal{L}^h, \forall j \in \mathcal{C}_J^h$ and store it in some density cache.

3. Compute force at each cluster site of all rep. atoms :

   For rep. atom $I \in \mathcal{L}^h$

       For cluster site $j \in \mathcal{C}_J^h$

           For neighbor site $k \in \boldsymbol{A}[J][j]$

               compute contribution of atom k to $\boldsymbol{f}_j$ using formula for EAM potential

   In the internal loop, we use the density cache to get the density.

C.2 Finite temperature calculation

In the finite temperature case, we have mean displacement and mean frequency of rep. atoms as unknowns. Let $\boldsymbol{q}_I^h$ be mean displacement of rep. atom I, and w_I^h be mean frequency of rep. atom I.

Statement of the problem:

$$\min_{\boldsymbol{q}^h, w^h} E_{total}(\boldsymbol{q}^h, w^h) \tag{C.2.1}$$

We need to solve :

$$\boldsymbol{f}_{q,I}^h = \sum_{J \in \mathcal{L}^h} n_J^h \left[\sum_{j \in \mathcal{C}_J^h} \boldsymbol{f}_{q,j} \Psi_I^h(\boldsymbol{x}_j) \right] \tag{C.2.2}$$

$$f_{w,I}^h = \sum_{J \in \mathcal{L}^h} n_J^h \left[\sum_{j \in \mathcal{C}_J^h} f_{w,j} \Psi_I^h(\boldsymbol{x}_j) \right] \tag{C.2.3}$$

where subscript q in $\boldsymbol{f}_{q,j}$ refers to derivative of total energy with respect to mean displacement of atom j, and subscript w in $f_{w,j}$ refers to derivative of total energy with respect to mean frequency of atom j.

We will only focus on calculation of $\boldsymbol{f}_{q,j}$. Discussions for $\boldsymbol{f}_{q,j}$ also holds for $f_{w,j}$.

C.2.1   Force in finite temperature

In finite temperature, we write total energy as (using EAM as an example)

$$E_{total} = \sum_{i \ in\mathcal{L}} E_i \tag{C.2.4}$$

where

$$E_i = \frac{1}{(N!)h^{3N}} \int_{\mathbb{R}^{3N}} F_i(\rho_i(\boldsymbol{u})) p(\boldsymbol{u}; \boldsymbol{q}) \Pi_{j=1}^N d\boldsymbol{u} \tag{C.2.5}$$

Approximating the phase average   Let, energy E_i, of atom i, depends on N_i number of neighboring atoms, including atom i itself. Then expression of energy E_i will involve integration of $F_i(\rho_i(\boldsymbol{u}))$ in $\mathbb{R}^{3N_i}$. E_i can be written as

$$E_i = \left(\frac{1}{\sqrt{\pi}} \right)^{3N_i} \sum_{k=1}^M F_i(\rho_i(\boldsymbol{x}(\eta^k))) W^k \tag{C.2.6}$$

Then, forces are

$$\boldsymbol{f}_{q,i} = \sum_{\substack{j \in \text{neighbor of i,} \\ j \neq i}} \left[\left(\frac{1}{\sqrt{\pi}} \right)^{3N_i} \left(\sum_{k=1}^{M_i} F_i'(\rho_i(\boldsymbol{x}(\eta^k))) g_i'(r_{ij}(\eta^k)) \frac{ij(\eta^k)}{r_{ij}(\eta^k)} W^k \right) \right. \quad \text{(C.2.7)}$$

$$\left. + \left(\frac{1}{\sqrt{\pi}} \right)^{3N_j} \left(\sum_{k=1}^{M_j} F_j'(\rho_j(\boldsymbol{x}(\eta^k))) g_j'(r_{ij}(\eta^k)) \frac{ij(\eta^k)}{r_{ij}(\eta^k)} W^k \right) \right] \quad \text{(C.2.8)}$$

C.2.2   Numerical strategy

First strategy is the direct extension of zero temperature algortihm. The second strategy is a new strategy that we are using in our QC Code.

Extending zero temperature algortithm: Loop over cluster sites

In this, we loop over cluster sites, and for each cluster site we compute the force.

1. Compute the neighbor list of all cluster sites of all the rep. atoms. Let $A[J][j]$ be the set of neighboring sites for cluster site j of rep. atom J.

2. Loop over the cluster site and compute force

For rep. atoms $J \in \mathcal{L}^h$

For cluster site $j \in \mathcal{J}_J^h$

For neighboring site $l \in$ neighbor sites of J

For quadrature point $k = 1, 2, ..., M_l$

compute contribution from atom l to force at atom j for quad. point k

The last loop over l will require us to compute $F_l(\rho_l(\boldsymbol{x}(\eta^k)))$ M_l number of times, where M_l is the total number of quadrature-points associated to atom l.

If we use third order approximation then $M_l = 3^{3N_l}$.

Disadvantage of above algorithm: Suppose cluster site j and j' both share same atom l as its neighbor. When we will compute the force at cluster site j, we will do EAM

calculation on atom l, and we will do the same calculation again when we will compute force at site j'.

Basically, we will compute the density, M_l number of times, each time atom l appears as a neighbor of cluster site.

In zero temperature, we only need to compute density once, as there is no phase average calculation involved. Thus, we could compute the density of all neighbor sites at the beginning of force calculation, save it in a density cache, and later use it whenever it is required. The same method can not be adopteddused for finite temperature case because for each neighbor site l, we will have to save M_l number of densities in density cache.

New algortihm: Loop over neighbor sites

Consider the following algorithm. We first loop over neighbor site and then loop over cluster sites. This way, we will not be doing same calculation related to any neighbor site.

1. Compute the list of all the neighbor sites, at which force has to be computed. Let all the neighboring sites are stored in C, and let $B[i]$, for $i \in C$, is the set of all cluster sites which have atom i as their neighbor. That is, for given neighbor site i, we can find the cluster sites $B[i]$ that has i as their neighbors.

2. Loop over neighboring sites

$$\text{For neighboring sites } i \in C$$
$$\text{For quadrature point } k \in \{1, 2, ..., M_i\}$$
$$\text{Compute } F_i'(\rho_i) \text{ for quadrature point quad}$$
$$\text{For cluster sites } j \in B[i]$$
$$\text{Compute } g'(r_{ij}) \text{ for quadrature point quad}$$
$$\text{Add } \left[\left(\frac{1}{\sqrt{\pi}} \right)^{3N_i} F_i'(\rho_i) g'(r_{ij}) \frac{ij}{r_{ij}} \right] \text{ to } \boldsymbol{f}_j$$

In this algorithm, for each neighbor sites, we are doing computation only once. For each neighbor site, we first loop over quad points, compute density for the quad point, and then add the contribution to all the cluster sites associated to the neighboring site.

Bibliography

[Aghai and Dayal, 2011] Aghai, A. and Dayal, K. (2011). Symmetry-adapted non-equilibrium molecular dynamics of chiral carbon nanotubes under tensile loading. *J. Appl. Phys.*, 109.

[Aghai et al., 2013] Aghai, A., Dayal, K., and Elliott, R. S. (2013). Symmetry-adapted phonon analysis of nanotubes. *J. Mech. and Phys. of Solids*, 61.

[Alexanderian,] Alexanderian, A. A brief introduction to homogenization in random media.

[Allaire, 1992] Allaire, G. (1992). Homogenization and two-scale convergence. *SIAM J. MATH. ANAL.*, 23. 2.2.2

[Andersen, 1980] Andersen, H. C. (1980). Molecular dynamics simulations at constant pressure and/or temperature. *The Journal of Chemical Physics*, 72. 1.3.1

[Arndt et al., 2009] Arndt, M., Sorkin, V., and Tadmor, E. B. (2009). Efficient algorithms for discrete lattice calculations. *J Computational Physics*, 228.

[Atkinson et al., 2003] Atkinson, D., Allwood, D. A., Xiong, G., Cooke, M. D., Faulkner, C. C., and Cowburn, R. P. (2003). Magnetic domain-wall dynamics in a submicrometre ferromagnetic structure. *Nat Mater*, 2. 1.4

[Balagurusamy, 2008] Balagurusamy, E. (2008). *Object Oriented Programming with C++*. Tata McGraw-Hill, fourth edition.

[Bensoussan et al.,] Bensoussan, A., Lions, J.-L., and Papanicolaou, G. *Asymptotic Analysis For Periodic Structures*. North-Holland Publishing Company.

[Blanc et al., 2002] Blanc, X., Bris, C. L., and Lions, P. L. (2002). From molecular models to continuum mechanics. *Arch. Rational Mech. Anal.*, 164. 1.2

[Blanc et al., 2003] Blanc, X., Bris, C. L., and Lions, P. L. (2003). A definition of the ground state energy for systems composed of infinitely many particles. *COMMUNI-CATIONS IN PARTIAL DIFFERENTIAL EQUATIONS*, 28. 1.2, 2

[Blanc et al., 2007a] Blanc, X., Bris, C. L., and Lions, P. L. (2007a). The energy of some microscopic stochastic lattices. *Arch. Rational Mech. Anal.*, 184. 1.2, 2

[Blanc et al., 2007b] Blanc, X., Bris, C. L., and Lions, P. L. (2007b). Stochastic homogenization and random lattices. *J. Math. Pures Appl.*, 88. 1.2, 2, 5.2

[Blanc et al., 2007c] Blanc, X., Le Bris, C., and Lions, P.-L. (2007c). Atomistic to continuum limits for computational materials science. *ESAIM: Mathematical Modelling and Numerical Analysis*, 41.

[Blanc et al., 20] Blanc, X., Lions, P. L., Legoll, F., and Patz, C. (20). Finite temperature coarse-graining of one-dimensional models : Mathematical analysis and computational approaches. *J Nonlinear Science*, 2010. 2

[Chaikin and Lubensky, 1995] Chaikin, P. M. and Lubensky, T. C. (1995). *Principles of Condensed Matter Physics*. Cambridge University Press. 3.2.4

[Chandler, 1987] Chandler, D. (1987). *Introduction to Modern Statistical Mechanics*. Oxford University Press.

[Cohn, 2010] Cohn, D. L. (2010). *Measure Theory*. Birkhauser.

[Daw and Baskes, 1984] Daw, M. S. and Baskes, M. I. (1984). Embedded-atom method : Derivation and application to impurities, sufaces, and other defects in metals. *Physical Review B*, 29. 1.1

[Dayal and James, 2010] Dayal, K. and James, R. D. (2010). Nonequilibrium molecular dynamics for bulk materials and nanostructures. *J. Mech. and Phys. of Solids*, 58. 2

[Dobson et al., 2007] Dobson, M., Elliott, R. S., Luskin, M., and Tadmor, E. B. (2007). A multiscale quasicontinuum for phase transforming materials : Cascading cauchy born kinematics. *J Computer-Aided Mater Des*, 14. 1.3.1

[Duffy, 2001] Duffy, D. G. (2001). *Green's Functions with Applications*. Chapman Hall/CRC.

[Dumitrica and James, 2007] Dumitrica, T. and James, R. D. (2007). Objective molecular dynamics. *J. Mech. Phys. Solids*, 55. 2

[Dupuy et al., 2005] Dupuy, L. M., Tadmor, E. B., Miller, R. E., and Phillips, R. (2005). Finite-temperature quasicontinuum : Molecular dynamics without all the atoms. *Physical Review Letters*, 95. 1.3.1, 3, 5.2

[Ericksen, 1975] Ericksen, J. L. (1975). Equilbrium of bars. *J. of Elasticity*, 5.

[Ericksen, 2008] Ericksen, J. L. (2008). On the cauchy-born rule. *Mathematics and Mechanics of Solids*, 13.

[Eringen, 1963] Eringen, A. C. (1963). On the foundation of electrostatics. *Int. J. Engng. Sci.*, 1.

[Fan,] Fan, J. *Multiscale Analysis of Deformation and Failure of Materials*. Wiley.

[Folland, 1999] Folland, G. B. (1999). *Real Analysis : Modern Techniques and Their Application*. John Wiley and Sons.

[Geymonat et al., 1993] Geymonat, G., M{ü2

ller, S., and Triantafyllidis, N. (1993). Homogenization of nonlinearly elastic materials, microscopic bifurcation and macroscopic loss of rank-one convexity. *Arch. Rational Mech. Anal.*, 122.

[Gioia and James, 1997] Gioia, G. and James, R. D. (1997). Micromagnetics of very thin films. *Proc. R. Soc. Lond. A*, 453. (document), 2.6, 5.1

[Halmos and Sunder, 1978] Halmos, P. R. and Sunder, V. S. (1978). *Bounded Integral Operators on L2 Spaces*. Ergebnisse der Mathematik und ihrer Grenzgebiete. 2. Folge. Springer, 1 edition.

[Hao et al., 2011] Hao, F., Fang, D., and Xu, Z. (2011). Mechanical and thermal transport properties of graphene with defects. *APPLIED PHYSICS LETTERS*, 99. 1

[James, 2006] James, R. D. (2006). Objective structures. *J. Mech. Phys. Solids*, 54. 2, 2.3.1

[James and Müller, 1994] James, R. D. and Müller, S. (1994). Internal variables and fine-scale oscillations in micromagnetics. *Continuum Mech. Thermodyn.*, 6. 1.2, 2, 2.5, 5.1

[Jaynes, 1957a] Jaynes, E. T. (1957a). Information theory and statistical mechanics. *Physical Review*, 106. 3.2.1

[Jaynes, 1957b] Jaynes, E. T. (1957b). Information theory and statistical mechanics 2. *Physical Review*, 108.

[Jikov et al., 1994] Jikov, V. V., Kozlov, S. M., and Oleinik, O. A. (1994). *Homogenization of Differential Operators and Integral Functions*. Springer-Verlag. 2.4.1, 2.4.1, 2.4.1, 2.4.1, 2.4.4

[Kanwal, 1983] Kanwal, R. P. (1983). *Generalized Functions : Theory and Technique*. Academic Press.

[Kim et al., 2014] Kim, W. K., Luskin, M., Perez, D., Voter, A. F., and Tadmor, E. B. (2014). Hyper-qc : An accelerated finite-temperature quasicontinuum method using hyperdynamics. *J. Mech. and Phys. Solids*, 63. 1.3.1, 3, 5.2

[Knapp and Ortiz, 2001] Knapp, J. and Ortiz, M. (2001). An analysis of the quasicontinuum method. *J. Mech. and Phys. of Solids*, 49. 1.6, 3.4.3, 3.4.3

[Krylov and Stroud, 2006] Krylov, V. I. and Stroud, A. H. (2006). *Approximate calculation of integrals*. Courier Corporation. A.1

[Kulkarni, 2007] Kulkarni, Y. (2007). *Coarse graining of atomistic description at finite temperature*. PhD thesis, California Institute of Technology.

[Kulkarni et al., 2008] Kulkarni, Y., Knapp, J., and Ortiz, M. (2008). A variational approach to coarse graining of equilibrium and non-graining atomistic description at finite temperature. *J. Mech. and Phys. of Solids*, 56. (document), 1.3.1, 3, 3, 5.1, A, A.1

[Landis,] Landis, C. M. A new finite element formulation for electromechanics.

[Low, 1997] Low, F. E. (1997). *Classical Field Theory*, chapter 1. Wiley-VCH.

[Marshall, 2014] Marshall, J. (2014). *Atomistic multiscale modelling with long-range electrostatic interactions*. PhD thesis, Carnegie Mellon University.

[Marshall and Dayal, 2013] Marshall, J. and Dayal, K. (2013). Atomistic to continuum multiscale modelling with long range electrostatic interaction in ionic solids. *J. Mech. and Phys. of Solids*, 1. (document), 1.4.1, 1.6, 2.2.1, 2.2.4, 2.3, 3, 3.5.1, 4.2

[Martin, 2004] Martin, R. M. (2004). *Electronic Structure : Basic theory and practical methods*, chapter 18. Cambridge University Press.

[McMeeking and Landis, 2005] McMeeking, R. M. and Landis, C. M. (2005). Electrostatic forces and stored energy for deformable dielectric materials. *J. Appl. Mech.*, 72.

[McMeeking et al., 2007] McMeeking, R. M., Landis, C. M., and Jimenez, S. M. A. (2007). A principle of virtual work for combined electrostatic and mechanical loading of materials. *Int. J. Non-Linear Mech.*, 42.

[Mielke, 2006] Mielke, A. (2006). *Analysis, Modelling and Simulation of Multiscale Problems*. Springer. 1

[Miller and Tadmor, 2009] Miller, R. E. and Tadmor, E. B. (2009). A unified framework and performance benchmark of foureten multiscale atomistic/continuum coupling methods. *Mod. Sim. Mat. Science and Engg.*, 17. 1.3.1

[Milton, 2004] Milton, G. W. (2004). *The Theory of Composites*. Cambridge University Press. 1

[Mishin et al., 2002] Mishin, Y., Mehl, M., and Papaconstantopoulos, D. (2002). Embedded-atom potential for b 2- nial. *Physical Review B*, 65(22):224114.

[Miu, 1992] Miu, D. K. (1992). *Mechatronics : Electromechanics and Contromechanics.* Springer-Verlag.

[Ostoja-Starzewski, 2008] Ostoja-Starzewski, M. (2008). *Microstructural Randomness and Scaling in Mechanics of Materials.* Champions and Hall/CRC. 2.4.1

[Pathak,] Pathak, R. S. *A Course in Distribution : Theory and Applications.*

[Perez et al., 2009] Perez, D., Uberuaga, B. P., Shim, Y., Amar, J. G., and Voter, A. F. (2009). *Annual Reports in Computational Chemistry*, volume 5, chapter 4. Elsevier. Chapter 4 : Accelerated Molecular Dynamics Method : Introduction and Recent Developments. 1.1.1

[Perez and Voter, 2008] Perez, D. and Voter, A. F. (2008). Introduction to accelerated dynamic methods. Presentation slides. 1.1.1

[Price et al., 1984] Price, S. L., Stone, J., and Alderton, M. (1984). Explicit formulae for the electrostatic energy, forces and torques between a pair of molecules of arbitrary symmetry. *Molecular Physics*, 52.

[Rapaport, 2004] Rapaport, D. C. (2004). *The Art of Molecular Dynamics Simulation.* Cambridge University Press, second edition. 1.1

[Sepliarsky and Cohen, 2002] Sepliarsky, M. and Cohen, R. (2002). Development of a shell model potential for molecular dynamics for pbtio3 by fitting first principles results. 626(1):36–44. 1.1

[Shenoy et al., 1999] Shenoy, V., Shenoy, V., and Phillips, R. (1999). Finite temperature quasicontinuum methods. *Mat. Res. Soc. Symp. Proc.*, 538. 1.3.1

[Shimada et al., 2008] Shimada, T., Wakahara, K., Umeno, Y., and Kitamura, T. (2008). Shell model potential for pbtio3 and its applicability to surfaces and domain walls. *Journal of Physics: Condensed Matter*, 20(32):325225. 1.1, 1.1.1

[Steigmann, 2007a] Steigmann, D. J. (2007a). Asymptotic finite-strain thin-plate theory for elastic solids. *Intl. J. Computers and Mech. with Applications*, 53.

[Steigmann, 2007b] Steigmann, D. J. (2007b). Thin-plate theory for large elastic deformations. *Intl. J. Non Linear Mech.*, 42.

[Stephensor et al., 2016] Stephensor, D., Kermode, J. R., and Lockerby, D. A. (2016). Accelerating a hybrid continuum-atomistic fluidic model with on-the-fly machine learning. *ArXiv e-prints*. 1.1

[Stroustrup, 1997] Stroustrup, B. (1997). *The C++ Programming Language*. Addison-Wesley, third edition.

[Tadmor et al., 2013] Tadmor, E. B., Legoll, F., Kim, W. K., Dupuy, L. M., and Miller, R. E. (2013). Finite-temperature quasi-continuum. *Appl. Mech. Rev.*, 65. 1.3.1, 3, 5.2

[Tadmor and Miller,] Tadmor, E. B. and Miller, R. E. The theory and implementation of the quasicontinuum method. 1.3.1

[Tadmor and Miller, 2011] Tadmor, E. B. and Miller, R. E. (2011). *Modelling Materials : Continuum, Atomistic and Multiscale Techniques*. Cambridge University Press. 1, 1.1, 1.2

[Tadmor et al., 1996] Tadmor, E. B., Ortiz, M., and Phillips, R. (1996). Quasicontinuum analysis of defects in solids. *Philosophical Magazine A*, 73. 1.3.1

[Tadmor et al., 1999] Tadmor, E. B., Smith, G. S., Bernstein, N., and Kaxiras, E. (1999). Mixed finite element and atomistic formulation for complex crystals. *Physical Review B*, 59. 1.3.1

[Tan et al., 2014] Tan, L., Acharya, A., and Dayal, K. (2014). Modelling of slow time-scale behavior of fast molecular dynamic systems. *J. Mech. and Phys. of Solids*, 64.

[Tartar, 2010] Tartar, L. (2010). *The General Theory of Homogenization*. Springer.

[Torquato, 2002] Torquato, S. (2002). *Random heterogeneous materials*. Springer.

[Toupin, 1956] Toupin, R. A. (1956). The elastic dielectric. *J. Rational Mech. Anal.*, 5.

[Truskinovsky, 1996] Truskinovsky, L. (1996). Fracture as a phase transition. *Contemporary Research in the Mechanics and Mathematics of Materials*.

[Venturini et al., 2014] Venturini, G., Wang, K., Romero, I., Ariza, M. P., and Ortiz, M. (2014). Atomistic long-term simulation of heat and mass transport. *J. Mech. and Phys. of Solids*, 73. 1.3.1, 5.2

[Voter, 1997] Voter, A. F. (1997). A method for accelerating the molecular dynamics simulation of infrequent events. *The Journal of Chemical Physics*, 106. 1.1.1

[Voter, 2007] Voter, A. F. (2007). Accelerated molecular dynamic methods. Presentation slides. 1.1.1

[Voter et al., 2002] Voter, A. F., Montalenti, F., and Germann, T. C. (2002). Extending the time scale in atomistic simulation of materials. *Annu. Rev. Mater. Res.*, 46. 1.1.1

[Wan et al., 1986] Wan, C. L., Pan, W., Xu, Q., Qin, Y. X., Wang, J. D., Qu, Z. X., and Fang, M. H. (1986). Effect of point defects on the thermal transport properties of $(La_xGd_{1-x})_2Zr_2O_7$: Experiment and theoretical model. *PHYSICAL REVIEW B*, 74. 1

[Weiner, 2002] Weiner, J. H. (2002). *Statistical mechanics of elasticity*. Dover. 3.3.3

[Xiao, 2004] Xiao, Y. (2004). *The influence of oxygen vacancies on domain patterns in ferroelectric perovskites*. PhD thesis, California Institute of Technology. 2.5, 5.1

[Yang and Dayal, 2011] Yang, L. and Dayal, K. (2011). A completely iterative method for the infinite domain electrostatic problem with nonlinear dielectric media. *Journal of Computational Physics*, 230.

[Zapol et al., 1997] Zapol, P., Pandey, R., and Gale, J. D. (1997). An interatomic potential study of the properties of gallium nitride. *Journal of Physics: Condensed Matter*, 9(44):9517. 4.2.2, 4.3.2